Towards a Structural and Functional Insight into the Human Immunodeficiency Virus (HIV) – 1 Membrane Protein, Vpu.

by

Arpan Deb

A Dissertation Presented in Partial Fulfilment
of the Requirements for the Degree
Doctor of Philosophy

Approved July 2016 by the
Graduate Supervisory Committee

Tsafrir Leket-Mor, Chair
Petra Fromme
Hugh Mason
Valerie Stout

ARIZONA STATE UNIVERSITY

August 2016

ABSTRACT

Viral protein U (Vpu) is a type-III integral membrane protein encoded by the Human Immunodeficiency Virus-1 (HIV- 1). It is expressed in infected host cells and plays vital roles in down-regulation of CD4 receptors in T cells and also in the budding of virions. But, there remain key structure/function questions regarding the mechanisms by which the Vpu protein contributes to HIV-1 pathogenesis and thus, it makes for an attractive target to study the structural attributes of this protein by elucidating a structural model with X-ray crystallography. This study describes a multi-pronged approach of heterologous over-expression of Vpu. The strategies of purification and biophysical/ biochemical characterization of the different versions of the protein to evaluate their potential for crystallization are also detailed. Furthermore, various strategies employed for the crystallization of Vpu by both *in surfo* and *in cubo* techniques, and the challenges faced towards the structural studies of this membrane protein by characterization with solution Nuclear magnetic resonance (NMR) spectroscopy are also described.

ACKNOWLEDGMENTS

I would like to express my deepest gratitude to my mentor Prof. Tsafrir S Mor who gave me the opportunity to pursue this research under his guidance, for his support, expertise, understanding, and advice. I thank my dissertation committee members Prof. Petra Fromme, Dr. Hugh Mason and Dr. Valerie Stout who have been a great helping hand throughout this work. I also thank Dr. Wade van horn and Dr. Wei Liu for their support and guidance in NMR and LCP crystallization studies respectively.

Past and present members of the Mor Lab have made the whole journey extremely memorable with their constant and continued support and friendship. I would like to thank all of them for a wonderful experience in and outside the lab. I would like to thank Dr. Latha Kannan for smooth day to day running of the lab, Dr. Sarah Kessans, Dr. Kathy Larrimore and Dr. Lydia Meador for being the kind of people with whom I could share both the successes and failures of the day.

I would like to give special thanks to Dustin Srinivas, William Johnson, Rika Judd, Randy Watson, Alexander Kline and Boston Scott for their tremendous help and involvement during various stages of the project. I thank Dr. Jose Martin Garcia, Dr. Katerina Dörner, Dr. Ho-Hsien Lee, Dr. Zhen Gong, Dr. James Zook, Dr. Sasha Daskalova, Dr. Debra Hansen and Dr. Brenda Hogue for excellent technical assistance and helpful discussions; Prof Rajeev Misra, and the AIDS Reagent Program (NIAID, NIH) for kind gifts of reagents. I thank Dr. Liqing Chen for helping me set up crystallization screens, Nicholas Sisco for the data collection and analysis of NMR spectroscopy results.

I would like to thank the School of Life Sciences, the Graduate Professional Student Association, and the Center for Membrane Proteins in Infectious Diseases, ASU for financial support. I am grateful for the administrative help provided by Wendi

Simonson, Yvonne Delgado, Mary Wheeler, Paul Hartig, Tina Esquerra and Geronimo Campanile.

Last but not the least, I also would like to acknowledge the contribution of my family and friends in supporting me throughout this endeavor.

TABLE OF CONTENTS

Page

LIST OF TABLES

LIST OF FIGURES

Figure Page

I. The HIV-1 Viral Protein U

Introduction

The Human immunodeficiency virus (HIV) is a member of the genus *Lentivirus*, which is a subgroup of the family *Retroviridae*, that causes a condition of progressive failure of the immune system called the Acquired Immunodeficiency Syndrome (AIDS). Out of the two types of this virus (HIV-1 and HIV-2), HIV-1 has been the cause of the majority of HIV infections globally. The HIV-1 replication, reviewed extensively in Engelman and Cherepanov (2012) and depicted in Figure I-1 starts when the viral envelope (Env) glycoprotein engages host cell surface CD4 and CCR5 receptors. This leads to the fusion of the viral and cellular membranes, entry of the viral particle into the cell, reverse transcription of the viral genetic material and import into the cell nucleus. Viral mRNAs and the genome-length RNA, which are incorporated later into nascent virions, are generated by using host transcription machinery. The viral mRNAs drive the

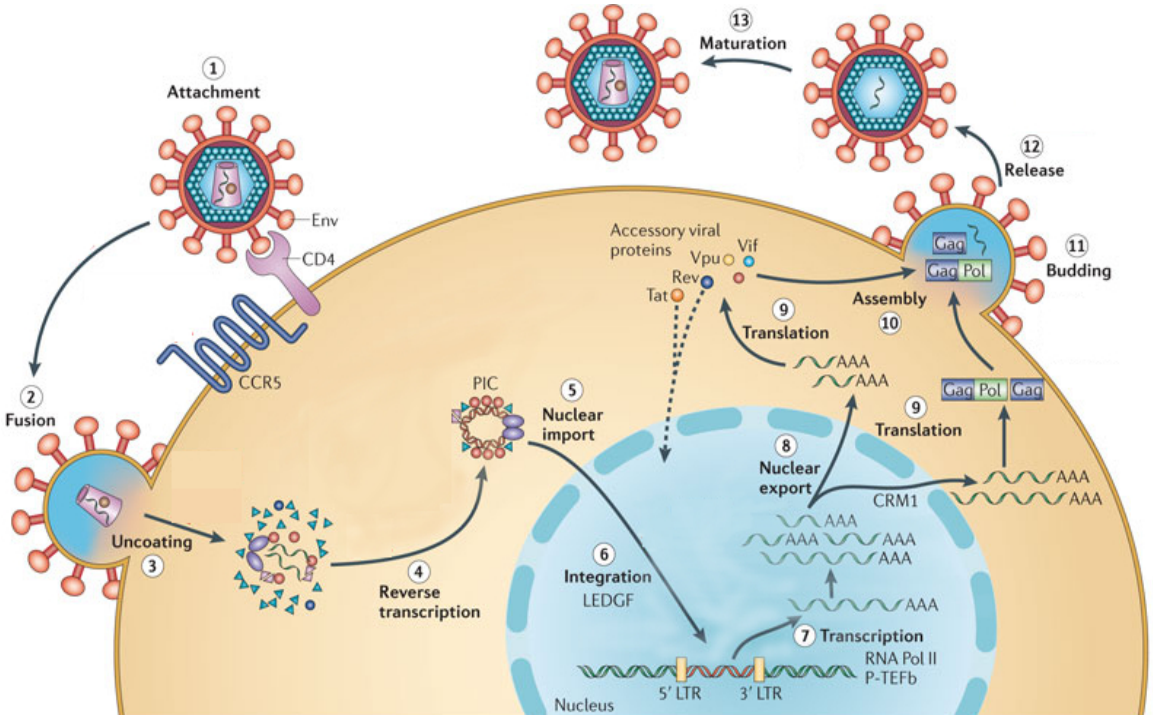

Figure I-1: Life cycle of HIV-1.
Adapted from Engelman and Cherepanov 2012.

production of various viral proteins, which form the protein components of the viral particle. An infectious virion is generated by the subsequent budding and release of the viral particle from the host cell.

In the infected host, the genome of HIV-1 also encodes several proteins whose function initially was deemed inessential for viral replication in various *in vitro* experiments with cell cultures. These proteins, including Nef, Vif, Vpu and Vpr, were therefore dubbed as “accessory”. However, the three decades of HIV-1 research gradually led to the realization that these proteins are directly involved in various aspects of the viral strategy to manipulate host innate and adaptive responses. In fact, we now realize that one cannot exaggerate the importance of the roles that these proteins play in antagonizing host factors that have evolved to safeguard the host cell against retroviral infections (Reviewed in Basmaciogullari and Pizzato (2014), and Guenzel et al. (2014). Here, I present a review of the recent advances in our knowledge about one particular “accessory” protein, Vpu and describe its interactions with various known host cell proteins and its vital contributions to the success of HIV-1 as a human pathogen.

Viral protein U (Vpu) is the product of the *vpu* open reading frame of HIV-1 (Dube et al. , 2010a, Strebel et al. , 1988a). The protein is translated from a bicistronic mRNA which also encodes the envelope glycoprotein (Env) (Schwartz et al. , 1990). The *env* mRNAs of HIV-1 contain the *vpu* start codon followed by the open reading frame (ORF) coding the Env protein (Schwartz et al. , 1992). Env expression is thus a result of leaky scanning of the *vpu* start codon. Interestingly it is found in HIV-1, not in HIV-2 and most simian immunodeficiency viruses (SIVs) except those like SIV_{cpz} (the chimpanzee-specific strain) that lie directly in the evolutionary path leading to HIV-1 (Gao et al. , 1999). It is a type III transmembrane protein of 77-86 amino acids in length depending on the group and subtype of HIV-1. For example, Vpu of strain HXB2 (belonging to group M, subtype

B) is 82 amino acids in length. It has a very short N-terminal domain, a transmembrane domain and a longer cytoplasmic domain which has two predicted α-helical domains separated by a hinge region (Figure 1). The hinge region contains two potential casein kinase II sites (Schubert et al. , 1992b).

Comparisons of Vpu sequences from different geographical isolates have identified some conserved residues, which facilitated in delineating the protein's various independent functions. For example, a tryptophan residue (W23) in the transmembrane domain was found to be invariant across all M group isolates along with L12, V14, I20, V22, I25, and I28, which are fairly conserved in most of them (McCormick-Davis et al. , 2000).

Two models describing potential interactions of one or both cytoplasmic helical domains with the surface of the plasma membrane have been suggested (Figure I-2). These two models need not be mutually exclusive as NMR characterization of the cytoplasmic domain of Vpu indicated that there is a great deal of structural flexibility in the cytoplasmic domain (Wittlich et al. , 2009a). A recently published full-length NMR structure of the denatured-renatured protein (Zhang et al. , 2015) indicates that the relative mobility of the cytoplasmic helices was dependent on the membrane mimetic environments used. In 1,2-dimyristoyl-*sn*-glycero-3-phosphocholine (DMPC) proteoliposomes, the helices were flexible and could be either arranged in a linear or in a U -shaped orientation whereas in 1,2-Dihexanoyl-sn-Glycero-3-Phosphocholine (DHPC)

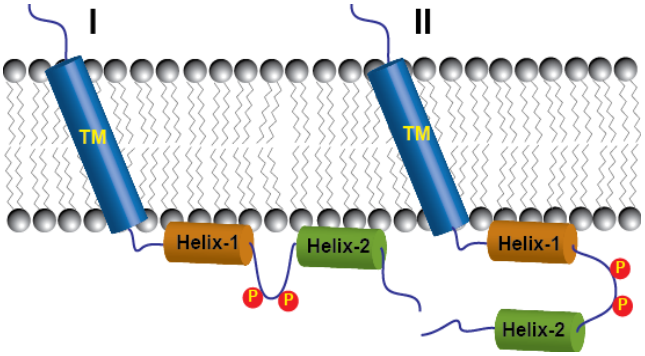

Figure I-2: Structural models of Vpu based on NMR and modeling data.
(Andrew and Strebel, 2010)

micelles, where the backbone dynamics were more restricted and the cytoplasmic helices adopted well-defined U-shaped loop region between them.

Vpu and its interactions with the CD4 receptor.

The T-cell CD4 receptors serve as the primary receptors for HIV-1 allowing it to gain entry to naïve uninfected cells. In infected host cells, HIV-1 effectively down-regulates CD4. This serves the virus by effectively reducing multiplicity of infection on the one hand while efficient dissemination of virus progeny is ensured by minimizing recapture. HIV-1 evolved several independent and partially redundant mechanisms that down-regulate CD4 carried out by two the viral accessory proteins, Nef (Garcia and Miller, 1991) and Vpu (Willey et al. , 1992a). Nef is found in all mammalian lentiviruses that were described thus far. Vpu, however, is unique to HIV-1 and SIV_{cpz} and is not found in HIV-2 and many other SIV strains (Sauter et al. , 2009a). While Vpu is not essential for viral propagation in cell cultures, it is important for

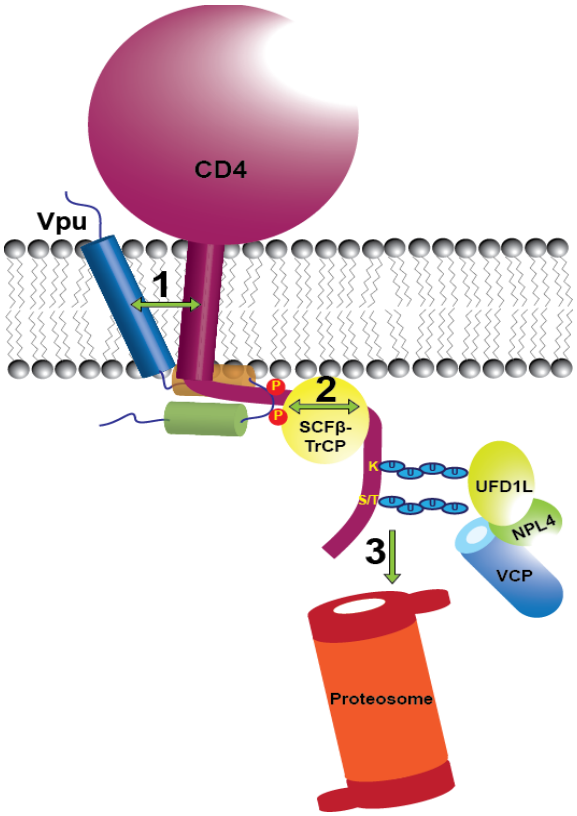

Figure I-3: A model of the interactions between Vpu and CD4 at the ER membrane and the cytosol.
Downregulation of CD4 is the result of multiple mechanisms. At least three such mechanisms may involve Vpu. (1) Direct interactions between Vpu and CD4 through their transmembrane domains leads to ER retention of the latter. (2) ER retention is also the result of indirect interactions between the two proteins via their cytosolic domains through interactions with "third party" cytosolic proteins (such as SCFβ-TrCP complex depicted here) (3) ER-retained CD4 is marked for degradation by ubiquitination mediated by conventional ERAD components (e.g. the VCP-UFD1L-NPL4 complex) and specific interactions with proteins like the cytosolic SCFβ-TrCP complex recruited by the cytoplasmic domain of Vpu (Magadan and Bonifacino, 2012, Magadan et al. , 2010).

virus infection *in vivo*. It is conceivable that Vpu was a major factor in the rapid evolution of HIV-1 from a relatively ineffective zoonotic pathogen to the successful pandemic-causing agent as we know it today (Sauter, Schindler, 2009a).

The involvement of Vpu with downregulation of CD4 receptors is multifaceted. Vpu binds CD4 and thereby causes it to be retained in the endoplasmic reticulum (ER). Vpu further induces CD4 degradation by exploiting a variant of the ER-associated protein degradation (ERAD) pathway (Magadan, Perez-Victoria, 2010). Both the transmembrane and cytoplasmic domains of Vpu were implicated for CD4 binding and degradation (Tiganos et al. , 1998). Without diminishing the importance of other structural and functional attributes of this small protein, it is clear that Vpu interferes with plasma-membrane presentation of CD4 through the interactions of their respective transmembrane domains (Magadan and Bonifacino, 2012). For example, substituting the conserved tryptophan residue (Trp22 in NL4-3 strain Vpu sequence) in the transmembrane domain of Vpu results in a non-functional protein that is incapable of targeting CD4 for degradation through ERAD. On the other hand, Val20 and Ser23 have also been identified as playing roles in CD4 retention in the ER (Magadan and Bonifacino, 2012). Apart from this, the first membrane proximal α-helix in the cytoplasmic domain of Vpu has also been shown to interact with CD4 and the preservation its secondary structure has been shown to be important for binding and degradation of CD4 (Tiganos et al. , 1997). The cytosolic domain of Vpu recruits the ubiquitination factors which ubiquitinate the cytoplasmic domain of CD4 at multiple lysine and serine/threonine residues to mark CD4 for proteasomal degradation and also further contribute in retention of CD4 in the ER (Magadan, Perez-Victoria, 2010).

The interaction and the subsequent down-regulation of CD4 by Vpu also contributes significantly towards the maturation of the HIV-1 *env* gene product gp160 into

gp120 and gp41. The precursor gp160 protein is known to form complexes with CD4 at the ER (Bour et al. , 1991, Crise et al. , 1990, Jabbar and Nayak, 1990). This not only decreases the surface expression of mature CD4 but, also significantly reduces the proteolytic cleavage of gp160 into gp41 and gp120 (Jabbar and Nayak, 1990). Enhancement of intra-cellular processing of gp160 has been observed in the presence of Vpu where it is hypothesized that Vpu may facilitate the release of gp160 from the ER by destabilizing the CD4-gp160 complex (Kimura et al. , 1994, Willey et al. , 1992b).

Vpu and BST-2 / tetherin.

The transmembrane domain of Vpu is involved in its association with tetherin or BST2, an integral membrane protein serving as an anti-viral innate immune system component, whose importance is only starting to be appreciated (Douglas, Gustin, 2010b, Evans et al. , 2010a, Neil, 2013). Tetherin functions to limit the escape of newly formed virions from cells infected by a variety of enveloped viruses like Ebola and HIV-1 (Douglas, Gustin, 2010b, Evans, Serra-Moreno, 2010a). It consists of a short N-terminal cytoplasmic tail, a transmembrane domain and an extra-cellular domain which is anchored to the membrane through a glycosyl-phosphatidylinositol (GPI) moiety (Kupzig et al. , 2003). They localize primarily in the cholesterol rich lipid raft regions of the plasma membrane as well as in the trans-Golgi network and the recycling endosomes (Kupzig, Korolchuk, 2003, Masuyama et al. , 2009). A fraction of the protein is normally targetted for lysosomal degradation through the Endosomal Sorting Complexes Required for Transport (ESCRT)-mediated pathway (Masuyama, Kuronita, 2009, Rollason et al. , 2007).

Vpu mediated degradation of BST-2 has been shown to occur either by the lysosome (Douglas et al. , 2009, Iwabu et al. , 2009, Mitchell et al. , 2009) and/or by the proteasome (Goffinet et al. , 2009, Mangeat et al. , 2009). For either pathway, β-TrCP is indispensable for Vpu aided viral release pointing to a multi-modal mechanism of tetherin

antagonism by Vpu (Tervo et al. , 2011). Vpu counteracts tetherin by its sequestration within the endomembrane system and interference with the normal intracellular trafficking of tetherin, leading to reduced levels of tetherin at the plasma membrane. This involves hijacking host machineries involved in the trafficking and turnover of tetherin (Mitchell, Katsura, 2009). Tetherin is then degraded by a ubiquitin-dependent mechanism in which phosphorylated Vpu recruits a $SCF^{\beta\text{-}TrCP}$ E3 ligase complex to ubiquitinate the cytoplasmic tail of tetherin at multiple residues and eventually targeting it for degradation (Douglas, Viswanathan, 2009, Goffinet, Allespach, 2009, Mangeat, Gers-Huber, 2009, Mitchell, Katsura, 2009, Tokarev and Guatelli, 2011). To target cell surface BST-2 to lysosomal degradation, Vpu interacts with the transmembrane domain of BST-2 (Iwabu, Fujita, 2009). This direct

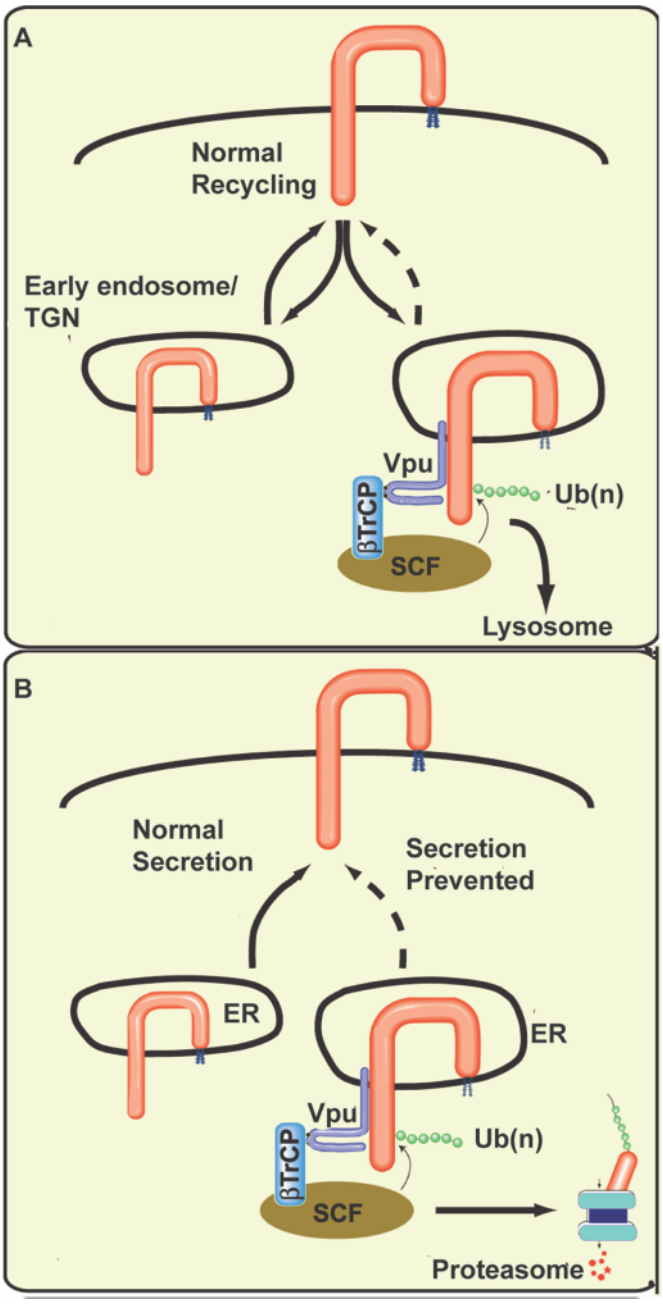

Figure I-4: Antagonism of BST-2 by Vpu.
Schematic representation of Vpu mediated antagonism of BST-2 by the lysosomal degradation pathway (A) and the proteasomal degradation pathway (B). Adapted from (Douglas et al. , 2010b)

interaction is significant since Vpu fails to antagonize BST-2 derived from African green monkeys as well as chimeric human BST-2 containing a modified transmembrane domain (McNatt et al. , 2009, Rong et al. , 2009). A “dileucine” like motif in the second α-helix in the cytoplasmic domain of Vpu (McNatt et al. , 2013a) has been identified to be responsible for efficiently counteracting tetherin which potentially functions by displacing tetherin from the sites of viral assembly (Kueck and Neil, 2012a). In addition, NMR spectroscopy has also revealed a possible role of the C-terminal tryptophan in Vpu in displacing BST-2 from the sites of viral assembly in the plasma membrane by specifically interacting with membrane lipids (Lewinski et al. , 2015). Towards this view, it has indeed been shown that in T cells and primary macrophages, Vpu enhanced viral release is independent of intra-cellular depletion and surface down-modulation of of tetherin (Miyagi et al. , 2009).

Disarming the Natural killer cells.

Vpu has also been implicated in the down-modulation of Natural Killer (NK), T- cell, B-cell antigen (NTB-A) on infected T cells (Richard and Cohen, 2010, Shah et al. , 2010) as an evasion strategy against HIV-1 infected cell lysis by NK cells. NTB-A is found on NK, T and B cells and is a co-factor that regulates NK cell activation (Bottino et al. , 2001) in presence of an infection by homophilic interactions with the receptor on the target cell (Flaig et al. , 2004). In a mechanism completely different from the way in which Vpu down-modulates CD4 and tetherin, Vpu brings about the retention of NTB-A in the Golgi apparatus by altering the glycosylation pattern in nascent NTB-A. This function has been traced to the second α-helical region of Vpu in its cytoplasmic domain (Bolduan et al. , 2013a). Studies also show a role of the transmembrane domain of Vpu in this down-modulation (Shah, Sowrirajan, 2010).

Vpu as a viroporin.

In addition, based on similarities with other viral transmembrane proteins, Vpu has also been shown to possess monovalent cation selective ion-channel activity (Ewart et al. , 1996a, Schubert et al. , 1996), for example, potassium transport in *Saccharomyces cerevisiae* (Herrero et al. , 2013a) which, could potentially make the host membrane protein more permeable and aid in budding and release of nascent virions and thus has been categorized into a viroporin (Gonzalez and Carrasco, 2003). This activity was found to be strongly dependent on the sequence of amino acids in the transmembrane domain where a scrambled sequence of amino acids in the transmembrane domain of Vpu has been shown to complete abrogate the transport of ions (Schubert, Ferrer-Montiel, 1996). The ion-channel activity has also been recently demonstrated *in vivo* in potassium transport deficient bacteria (Taube et al. , 2014). In spite of these conclusive evidences, the functional significance of the role of Vpu as a viroporin in HIV life cycle has not been established (Strebel, 2014).

A common feature of Vpu's interaction with an array of host proteins is the fact the hydrophobic transmembrane domain serves an important functional role in this protein, apart from the soluble cytoplasmic domain. The dependence of the interactions of the transmembrane domain of Vpu with its binding partners on the positions of certain amino acids in the membrane spanning segment underlines the presence of an important structure-function relationship in the protein. Given the important role Vpu plays in the viral life-cycle, the study of these interactions could be exploited in designing efficient anti-viral drugs against HIV-1. An example of targeting the function of Vpu and sensitizing HIV-1 to BST-2 mediated host restriction was demonstrated recently where, 2-thio-6-azauridine was shown to restore cell surface expression of BST-2 in the presence of Vpu by limiting BST-2 ubiquitination (Zhang et al. , 2016). Similarly, amiloride derivatives like 5-(*N,N*-

hexamethylene)amiloride and 5-(*N,N*-dimethyl)amiloride have been shown to block ion transport across the Vpu ion-channel and inhibit budding of HIV-1 virus like particles from HeLa cells (Ewart et al. , 2002). Drugs could also be designed to selectively target the binding of Vpu to host restriction factors. The reliability of such studies depends on the presence of reliable structural models of the protein. Even though a full length NMR structure of Vpu was recently published, further details of the structure with respect to its interactions with host cell factors are yet to be elucidated. Besides, although it is known that Vpu does exist in oligomeric states *in vitro* (Hussain et al. , 2007, Lu et al. , 2010, Maldarelli et al. , 1993), the physiological effects of this phenomena remains unknown.

Aims and review of the dissertation.

The challenges posed in solving the full-length structural model of Vpu, especially in terms of a high-resolution model using X-ray crystallography, due to the presence of the hydrophobic transmembrane domain has led to a somewhat “divide and conquer” approach amongst structural biologists. Taking into account the structural and functional significance of the transmembrane domain, as highlighted earlier, and its effect on the conformation and function of the cytoplasmic domain of this protein, the overall goal of this research was to solve a high-resolution structure of full-length Vpu using X-ray crystallography. Towards this, I intend to propose a suitable strategy to over-express Vpu heterologously. I would develop effective procedures to isolate the recombinant protein in a highly purified form and also subject it to various biophysical/ biochemical and functional characterizations to elucidate its suitability towards crystallization.

Towards my overall goal, multiple strategies of heterologous over-expression of Vpu in bacterial expression system were employed. Expression, purification characterization of Vpu in fusion with bacterial proteins are discussed in Chapter II. Vpu could also be expressed in bacteria as a type I membrane protein, as discussed in Chapter

III. Furthermore, it was also shown that I was able to isolate satisfactory amounts of highly purified, functionally active, mono- disperse samples of the protein. Chapter IV describes my efforts to crystallize Vpu by extensive screening with a wide variety of crystallization conditions. Both *in surfo* and *in cubo* methods of crystallization were employed to this regard. Lastly, Vpu was also characterized in solution by Nuclear Magnetic Resonance (NMR) spectroscopy in the presence on different membrane mimetic environments, which are described in Chapter V.

II. Expression, purification and characterization of HIV -1 Vpu with N- terminal fusion proteins.

Abstract

Structural analysis of membrane proteins has traditionally been bottlenecked by the lack of sufficiently large amounts of pure, folded and functional membrane proteins. Hence multi-pronged protein expression approaches are necessary while attempting to produce membrane proteins for structural studies like X-ray crystallography. Vpu is a type III membrane protein of the HIV-1 which is expressed in host cells and is involved in virus release and propagation. It does so by interacting with an array of cellular factors by involving its transmembrane and cytoplasmic domain. Thus, there is exists an interesting structure-function relationship that is yet to elucidated. In this chapter, I describe my efforts to express Vpu in fusion with various fusion partners like the *Bacilus subtilis* Mistic and the *Escherichia coli* maltose binding protein (MBP). Expression of Vpu in fusion with these proteins posed significant challenges with regards to expression yield, purity, stability and mono-dispersity as discussed in the following sections.

Introduction

Genes encoding membrane proteins make up around 20-30% of the genome for both prokaryotes and eukaryotes. (Wallin and von Heijne, 1998). Many of these membrane proteins are drug targets and play key roles in diseases. But, given their low natural abundance, obtaining required quantities of membrane proteins for structural studies has been a challenge. Although prokaryotic expression systems are relatively robust and cost-effective than most eukaryotic systems, the successful over-expression of eukaryotic membrane proteins in gram-negative bacteria like *Escherichia coli*, has remained limited (Tate, 2001).

Heterologous over-expression of membrane proteins can be inefficient due to various reasons, such as, altered synthesis, targeting, insertion and folding characteristics of the over-expression host (Bowie, 2005, Goder et al. , 2004, Valent et al. , 1997). Some proteins could be dependent on specific chaperones to fold them in their functional conformation (Kota and Ljungdahl, 2005, Matsumoto et al. , 1987, Nagamori et al. , 2004), which may be absent in the chosen expression system. A vast number of eukaryotic membrane proteins rely on post-translational modifications like glycosylation for proper folding, stability and function (Helenius and Aebi, 2004).

Viral protein U (Vpu) (Cohen et al. , 1988b, Strebel et al. , 1988b), is expressed by HIV-1 and its closest simian relative SIV_{cpz} and is not found in most of the other known primate lentiviruses (e.g. HIV-2 and most SIVs) (Strebel, 2014, Yang et al. , 2010). Vpu is required for efficient virus propagation *in vivo* and may have been a factor in the rapid evolution of HIV-1 from a relatively ineffective zoonotic pathogen to the successful pandemic-causing agent that we know today (Andrew and Strebel, 2010, McCarthy and Johnson, 2014, Sauter et al. , 2009b, Yang, Lopez, 2010).

Vpu is a 16-kDa type III transmembrane protein of 77-86 amino acids in length depending on the HIV-1 subtype. Vpu has a very short N-terminal extracellular domain, a transmembrane domain (TMD) and a longer cytoplasmic domain (CTD) which has two predicted α-helical regions separated by a hinge (Figure I-2). The hinge region contains two phosphorylation sites (Schubert et al. , 1992a) and is partially responsible for the flexibility of the CTD (Wittlich et al. , 2009b).

Vpu plays a number of roles in promoting virion assembly and release (Dube et al. , 2010b, Roy et al. , 2014, Strebel, 2014). Vpu largely functions through protein-protein interactions to down-regulate key host-cell proteins (Andrew and Strebel, 2010). For example, Vpu interacts with the CD4 surface receptor through their respective

transmembrane domains, causing the retention of the receptor in the endoplasmic reticulum (Magadan and Bonifacino, 2012, Magadan, Perez-Victoria, 2010). Subsequently, the C-terminal domain of Vpu recruits ubiquitination factors that mark CD4 for proteosomal degradation (Magadan and Bonifacino, 2012, Magadan, Perez-Victoria, 2010). Similar mechanisms are also involved for the roles that the Vpu transmembrane domain and cytoplasmic domain play in the downregulation of tetherin or BST-2, an integral membrane protein that limits the escape of newly formed virions from cells infected by HIV-1 and other enveloped viruses (Douglas et al. , 2010a, Evans et al. , 2010b, Kluge et al. , 2013, Kueck and Neil, 2012a). The C-terminal domain of Vpu directly functions to displace tetherin away from the sites of viral assembly in the host cell membrane (McNatt et al. , 2013b). In addition, Vpu belongs to a diverse group of small transmembrane viral proteins called viroporins that form homo-oligomeric ion channels. While Vpu's channel activity has been well demonstrated (Ewart et al. , 1996b, Herrero, Monroy, 2013a), its physiological role is less clear (Strebel, 2014).

The importance of Vpu for efficient assembly and egress of HIV-1 (Giese and Marsh, 2014, Jafari et al. , 2014, Pickering et al. , 2014) makes it a promising, but so far underexplored, therapeutic target. Developing its therapeutic utility requires establishing reliable structural information, which is the main focus of this thesis. The determination of a full-length structure is very important as the transmembrane domain influences the conformation, structure and dynamics of the C-terminal domain and *vice versa*.

Given the challenges in obtaining a pure, folded, functional membrane protein samples discussed above, I wanted to explore alternative strategies of recombinantly expressing Vpu in bacteria which could supplement our efforts and provide a multi-pronged approach towards crystallization and further structural studies on this protein.

Specifically, I explored the feasibility of over-expressing Vpu in the presence of cleavable fusion partners which could ultimately present us with a protein without any affinity tags.

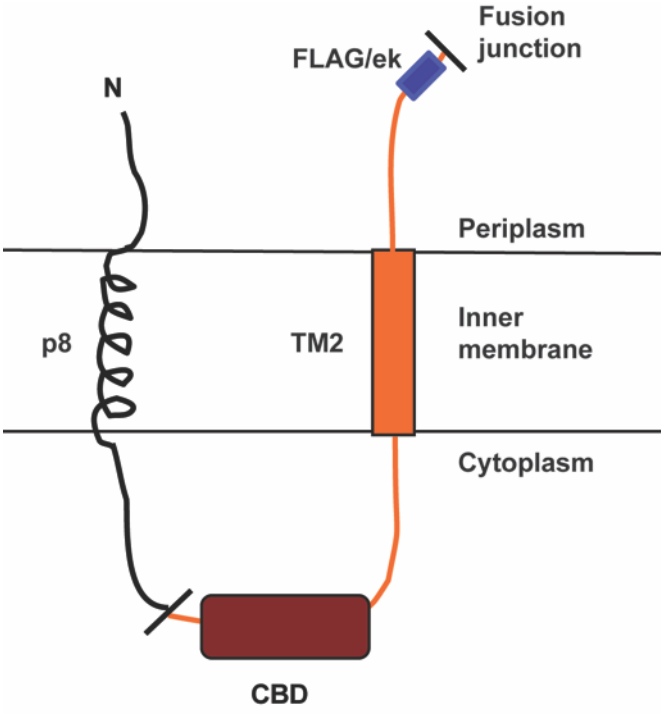

Figure II-1: A schematic representation of the p8CBDek system and its membrane orientation. The P8 transmembrane segment brings about efficient membrane insertion via the SRP pathway. The chitin binding domain (CBD) can serve as an affinity tag. The protein of interest, fused downstream can be proteolytically cleaved using enterokinase. (Adapted from Luo et al., 2009).

Certain fusion strategies were specifically designed to improve bacterial over-expression and correct folding of membrane proteins. Early during the project I was contacted by scientists working for the biotechnology company New England Biolabs to test a prototype they have developed for over-expression of membrane protein they developed for *E. coli.* The expression plasmid consists of a N-terminal wild-type M13 phage major coat protein (P8), with the hydrophobic residues in its transmembrane domain being an ideal target for the Signal recognition particle (SRP). The P8 open reading frame (ORF) was extended by the *E. coli* Signal peptidase which provides for a second transmembrane domain (TM2) to localize the fusion junction in the periplasmic space of the bacteria. The chitin binding domain located in the cytoplasmic loop, between the two transmembrane segments, provided for an affinity and/or detection tag. The Enterokinase (ek) protease cleavage site was engineered at the fusion junction to cleave the protein of interest from the rest of the fusion (Luo et al. , 2009). Apart from that, it also utilizes efficient charge distribution to ensure a predictable

topology of the membrane protein of interest in the bacterial inner membranes (Figure II-1).

The membrane-integrating sequence for translation of integral membrane protein constructs (Mistic) (Roosild et al. , 2005) is a 110 KDa protein fragment derived from *Bacillus subtilis* which has been shown to yield high levels of properly folded integral membrane proteins in the *E. coli* membranes (Dvir and Choe, 2009, Kefala et al. , 2007, Lee et al. , 2008, Liu et al. , 2008, Roosild et al. , 2006, Xu et al. , 2013). Although it is fairly hydrophilic with acidic residues making up most of the surface area of the four-helix bundle protein, it has been shown to associate tightly with the membranes when recombinantly expressed in *E. coli*. Intriguing is also the fact that none of the four helices are predicted to be transmembrane segments and yet it aggregates in an aqueous environment without the presence of detergents (Dvir et al. , 2009).

The maltose binding protein (MBP) from *E. coli* has been used as a fusion partner to increase the solubility of target proteins and also to promote their proper folding (Kapust and Waugh, 1999, Korepanova et al. , 2007, Maina et al. , 1988, Nallamsetty et al. , 2005, Nallamsetty and Waugh, 2007). The 40-kDa maltose-binding protein (MBP) is encoded by the mal E gene of *E. coli* K12 strain (Duplay and Hofnung, 1988). Because MBP is exported across the inner bacterial membrane to the periplasmic space (Bassford, 1990, Bedouelle et al. , 1980), by fusing its C-terminus to a membrane protein, MBP it could facilitate the efficient insertion of the cargo protein into the *E. coli* membrane. Vectors that facilitate the expression and purification of foreign peptides in *E. coli* by fusion to MPB were first described in 1988 (di Guana et al. , 1988). MBP also allows for an additional affinity tag for purification by virtue of its affinity to amylose (Kellermann and Ferenci, 1982), which when used in combination with other affinity tags, such as poly-histidine, provide flexibility in designing purification strategies. Moreover, it has also served as an

excellent crystallization partner which has resulted in over 100 structures of MBP with various proteins so far (Waugh, 2016).

In this chapter, I describe my efforts in expression, purification and characterization of Vpu in fusion with Mistic and MBP. Attempts to express Vpu as a C-terminal fusion of P8CBDek was unsuccessful since I could not obtain any levels of protein expression using that strategy.

Materials and Methods

Target selection and gene optimization.

The sequence of HIV- 1 group M subtype B strain HXB2 Vpu was used. Unfavorable codons for each 82 amino acids in length were replaced using the *E. coli* codon usage table (Sharp and Li, 1987). The vpu gene optimized for expression in *E. coli* was synthesized by overlap extension PCR. Overlapping oligonucleotides, oTMs 638 – 645 (Table II-1) of sizes ranging from 30-40 bases were ordered from Integrated DNA Technologies. The first round of PCR (Roche High Fidelity PCR Kit; cat# 11732641001) to assemble to the gene was done for 25 cycles (initial denaturation: 94 ºC for 2 min; denaturation: 94 ºC for 15 s; annealing: 55 ºC for 30 s; elongation 72 ºC for 30 s; final elongation: 72 ºC for 7 min) and was followed by a second round of PCR with external primers oTMs 646 and 647 for 40 cycles for amplification (initial denaturation: 94 ºC for 2 min; denaturation: 94 ºC for 15 s; annealing: 58 ºC for 30 s; elongation 72 ºC for 30 s; final elongation: 72 ºC for 7 min). The PCR product was first cloned into a TOPO-TA intermediate cloning vector (Invitrogen; cat# 450641).

Cloning of E. coli optimized vpu into various expression vectors.

The *vpu* gene sequence of HIV-1 group M subtype B strain HXB2 Vpu, which was optimized for expression in *E. co*li, as detailed above, was first engineered to have flanking TEV protease cleavage sites by performing a PCR (initial denaturation: 94 ºC for 2 min;

Table II-1: DNA primers used towards the creation of E. coli optimized vpu gene and pTMs 794, 869 and 975.

Primer	Sequence (5' → 3')
oTM 638	ggtaccatgcagccgatcccgatcgttgctatcgtagcactggttgtagctatcatc
oTM 639	atgataacgatggaccatacaacgattgcgatgatagctacaaccagtgctacgatagcaac
oTM 640	atcgcaatcgttgtatggtccatcgttatcatcgaataccgtaaaatcctgcgtcagcgtaaa
oTM 641	cgatcagacgatcgatcagacggtcgattttacgctgacgcaggatttttacggtattcg
oTM 642	atcgaccgtctgatcgatcgtctgatcgaacgtgcagaagactctggcaacgaatc
oTM 643	catttcaaccagtgcagagatttcaccttcggattcgttgccagagtcttctgcacgtt
oTM 644	cgaaggtgaaatctctgcactggttgaaatgggtgttgaaatgggtcaccacgctcc
oTM 645	gtcgaccagatcgtcaacgtcccacggagcgtggtgacccatttcaacacc
oTM 646	ggtaccatgcagccgatcccg
oTM 647	gtcgaccagatcgtcaacgtccc
oTM 657	gaaaacttgtactttcaaggcatgcagccgatcccgatcgttgctatcgtagc
oTM 658	gccctgaaaataaagattctccagatcgtcaacgtcccacggagcgtgg
oTM 662	atgcagccgatcccgatcg
oTM 663	cagatcgtcaacgtcccacgg
oTM 856	atgaaatacctgctgccgaccgctgc
oTM 857	cccattcgccaatccggatatagttcctcc
oTM 903	ccatggatgcagccgatcccgatcg
oTM 905	ctcgagttacagatcgtcaacgtcccacgg

denaturation: 94 ºC for 15 s; annealing: 60 ºC for 30 s; elongation 72 ºC for 30 s; final elongation: 72 ºC for 7 min) with oTMs 657 and 658 (Table II-1) for 30 cycles of amplification and then ligated to a Gateway compatible TOPO TA vector (ThermoFisher Scientific, cat# K250020SC) to generate a Gateway donor vector. The vpu gene was then cloned into an expression vector by LR recombination reaction, following product protocol, and transformed into DH5α electro-competent cells. The resulting bacterial colonies were screened using colony screen PCR using gene specific primers oTMs 662 and 663, which would result in a fusion of Vpu with Mistic (pTM794, Figure II-2), which was also confirmed by DNA sequencing with oTMs 662 and 663.

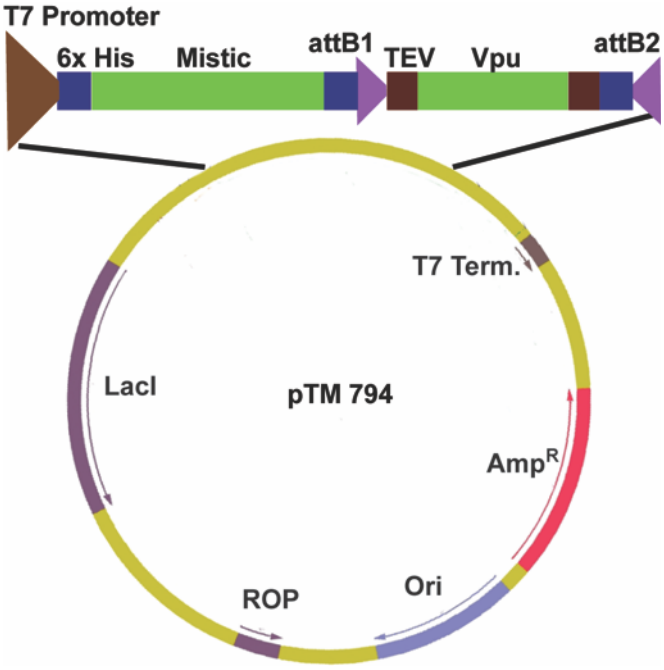

Figure II-2: The pTM794 expression vector. Expression of the Mistic-Vpu fusion is driven by the T7 promoter. The fusion contains TEV protease cleavage sites to isolate Vpu from Mistic and purification tags.

For the creation of a cleavable fusion of MBP and Vpu, a TEV protease cleavage site was engineered at the 5' end of the vpu gene by performing PCR (initial denaturation: 94 ºC for 2 min; denaturation: 94 ºC for 15 s; annealing: 55 ºC for 30 s; elongation 72 ºC for 30 s; final elongation: 72 ºC for 7 min) with primers oTMs 657 and 663 for 30 cycles of amplification. The PCR product was ligated to a Gateway compatible TOPO TA vector as mentioned above and then the gene was recombinantly transferred to an expression vector, and transformed into DH5α electro-competent cells. The resulting bacterial

colonies were screened using colony screen PCR using gene specific primers oTMs 662 and 663 to generate a MBP$_{-TEV-}$Vpu expression vector (pTM869, Figure II-3), which was also confirmed by DNA sequencing with oTMs 662 and 663.

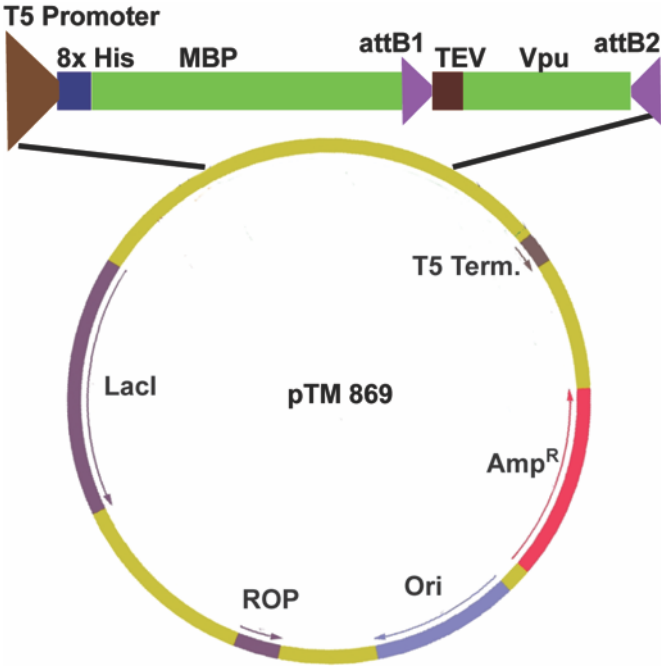

Figure II-3: The pTM869 expression vector. Expression of the MBP$_{-TEV-}$Vpu fusion is driven by the T5 promoter. The fusion contains TEV protease cleavage sites to isolate Vpu from MBP and extra amino acids translated from the Gateway recombination sequences.

Towards manufacturing a variant of a cleavable fusion of MBP and Vpu, with a shorter linker between the two proteins, a PreScission protease cleavage site (PPCS) was engineered at the 5'end of the vpu gene by performing a PCR (initial denaturation: 94 ºC for 2 min; denaturation: 94 ºC for 15 s; annealing: 58 ºC for 30 s; elongation 72 ºC for 30 s; final elongation: 72 ºC for 7 min) with primers oTMs 903 and 905 for 30 cycles of amplification. These primers were also responsible for adding flanking NcoI and XhoI sites on the PCR product. The PCR product was first cloned into a TOPO-TA intermediate cloning vector (Invitrogen; cat# 450641). was excised from this intermediate vector by digestion with NcoI and XhoI restriction enzymes (NEB; cat# R0585S). The same pair of restriction enzymes were also used to linearize the pET26(b) vector containing the *mbp* gene preceding the pelB signal sequence. The restriction digestion reactions were analyzed by agarose gel electrophoresis and the desired DNA bands were excised and purified using a QIAquick gel extraction kit (Qiagen; cat# 28704). The gene was ligated to the backbone by

performing a T4 DNA ligase reaction (Promega; cat# M1801) and transformed into DH5α electro-competent cells. The resulting bacterial colonies were screened using colony screen PCR using gene specific primers oTMs 662 and 663 and plasmid specific primers, oTMs 856 and 857. DNA sequencing using oTMs 856 and 857 was used to verify the final expression clone, pTM975 (Figure II-4).

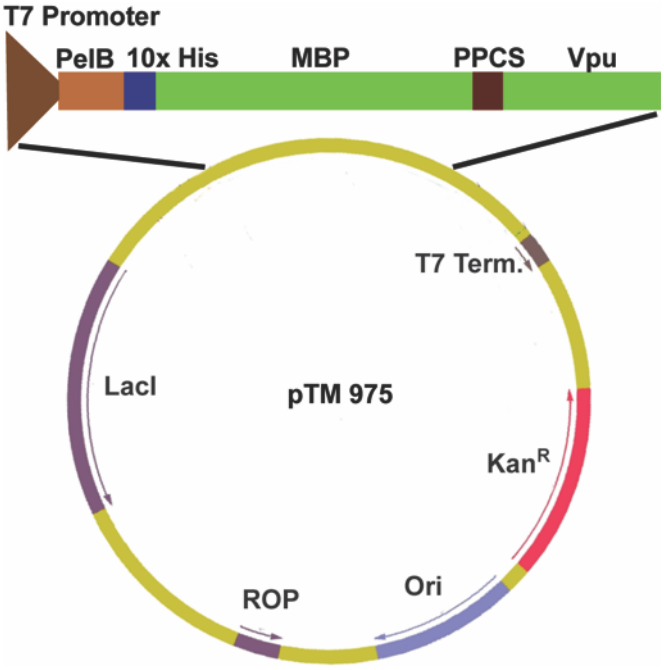

Figure II-4: The pTM975 expression vector. Expression of the MBP-$_{PPCS}$-Vpu fusion is driven by the T7 promoter. The fusion contains PreScission protease cleavage sites to isolate Vpu from MBP.

Expression of Vpu with its fusion partners.

The expression of the Mistic-Vpu and MBP-$_{PPCS}$-Vpu fusion along with the metal affinity tags was driven by a T7 promoter and MBP-$_{TEV}$-Vpu was driven by a T5 promoter. The expression vectors were electroporated into BL21(DE) cells. For protein expression, overnight cultures of BL21(DE) cells containing the respective expression vectors were grown in LB media supplemented with 100 µg/mL ampicillin for pTMs 794 and 869 and 100 µg/mL kanamycin for pTM975 and was used to inoculate a fresh LB media with 100 µg/mL ampicillin for pTMs 794 and 869 and 50 µg/mL kanamycin for pTM975 in a 1:100 dilution. The cultures for expression were shaken at 180 rpm at 37 ºC till an OD_{600} of approximately 0.4. BL21- pTMs 794 and 869 cultures were then moved to 15 ºC and were incubated for 30 min with 180 rpm shaking. Finally, the cultures were induced for expression with 0.1 mM IPTG. In case of BL21- pTM975 cultures, expression was induced

at 30 ºC at an OD_{600} of approximately 0.5 with 0.2 mM IPTG. For standardization of expression conditions, 5 mL of culture were collected at various time points after IPTG induction and pelleted by centrifugation at 4000 ×*g*, 4 ºC for 5 min. For detergent extraction screens and purifications, cultures were pelleted at 4 hr post induction for BL21- pTMs 794 and 869 at 5000 ×*g*, 4 ºC for 15 min. In case of BL21-pTM975, the cultures were pelleted after 16 hr post-induction, allowing for over-night expression of the recombinant protein. All cell pellets were stored at -80 ºC until further use.

Membrane isolation

Cell pellets from 4 L worth of culture (approximately 12 g) were resuspended in 100 mL of ice-cold phosphate buffer saline (PBS; 137 mM NaCl, 2.7 mM KCl, 10 mM Na_2HPO_4, 1.8 mM KH_2PO_4, pH 7.4) supplemented with EDTA-Free SIGMA*FAST*™ Protease Inhibitor Cocktail tablets, to prevent protein degradation. The cells were lysed by passing twice through a microfluidizer (Microfluidics Microfluidizer). The lysate was collected and centrifuged at 36,000 ×*g* for 30 min. The insoluble fraction was washed once by repeated resuspension (30 mL of ice-cold PBS with protease inhibitor cocktail) and centrifugation. If not immediately used, the pellet was frozen at -80 ºC.

Detergent extraction

Aqueous and non-aqueous fractions from 500 mL cultures were prepared as described above, induced for expression and cells were harvested as pellets as mentioned previously. The pellet containing the non-aqueous proteins was re-suspended in 25 mL of PBS-PI buffer. Samples (4 mL) were then subjected to detergent extraction by addition of the following detergents to final concentration of 1% (w/v): n-dodecyl-β-D-maltoside (βDDM, Glycon Biotech; cat# D97002C), n-decyl-β-D-maltoside (βDM, Anatrace; cat# D322), 3-[(3-Cholamidopropyl)dimethylammonio]-1-propanesulfonate (CHAPS, Mclab; cat# DCPS101), n-octyl β-D-glucopyranoside (OG, Glycon Biotech; cat# D97001C), n-

dodecylphosphocholine (DPC, Anatrace; cat# F308S) and n-dodecyl-N,N-dimethylamine-N-oxide (LDAO, Anatrace; cat# D360). The samples were left overnight at 4 ºC with agitation at 200 rpm and centrifuged at 36,000 ×*g* for 30 min at 4 ºC on the following day and the supernatant was collected as the detergent soluble fraction. The fractions were analyzed by SDS-PAGE followed by Coomassie staining and western blot.

For large-scale extractions from 4 L cultures, the pellet, containing the membrane fraction, was fully re-suspended in 200 mL PBS supplemented with EDTA-Free SIGMAFAST™ Protease Inhibitor Cocktail tablets. βDDM was used for solubilization at a final concentration of 1% (w/v). The protein was extracted and at 4 ºC overnight with agitation at 200 rpm. The detergent soluble fraction was obtained by collecting the supernatant after centrifugation at 36,000 ×*g* for 30 min at 4 ºC.

Purification

A gravity driven column (Biorad Econo-column) containing 25 mL bed volume of TALON metal affinity resin (Clontech laboratories Ltd; cat# 635503) was equilibrated with binding buffer (PBS_{500} (8.1 mM Na_2HPO_4, 1.8 mM KH_2PO_4, 2.7 mM KCl, 500 mM NaCl, pH 7.5) supplemented with 0.05% βDDM). Detergent (βDDM)-soluble fraction containing the Mistic-Vpu or $MBP_{\text{-TEV-}}$Vpu fusion protein were loaded onto the Talon resin and passed twice. Column was washed with 10 bed volumes of buffers such as twice with PBS_{500} (WI and WII), once with PBS + 0.05% βDDM (WIII) and once with PBS, 0.05% βDDM, and 5mM Imidazole (WIV). Elution was done with three column volumes of PBS, 0.05% βDDM, supplemented with 250 mM Imidazole.

The eluted sample was concentrated by 30 kDa molecular weight cutoff (MWCO) concentrators (Millipore; cat# UFC903008) to approximately $1/15^{th}$ its original volume. Concentrated samples were further purified by size exclusion chromatography (GE Life sciences, Superdex 200 10/300 GL; column volume: 24 mL; fluid phase: 8 mL) using a

fast pressure liquid chromatography instrument (FPLC, Pharmacia, Äkta Explorer). The running buffer contained 20 mM HEPES pH 7.5, 100 mM NaCl and 0.05% βDDM in case of Mistic-Vpu and PBS pH 7.4, 5% glycerol and 0.05% βDDM in case of MBP_{-TEV-}Vpu. For preparatory separations, a 1 mL sample of concentrated Vpu was loaded onto the S column and chromatography was performed at a flow rate of 0.5 mL/min. The protein elution was detected by absorption at 280 nm.

To purify MBP_{-PPCS-}Vpu, a gravity driven column (Biorad Econo-column) containing 30 mL bed volume of TALON metal affinity resin was equilibrated with binding buffer (20 mM HEPES pH 7.5, 500 mM NaCl, 0.02% βDDM, 5 mM imidazole). The sample was then loaded onto the column, and passed twice. The column was washed with ten bed volumes of wash buffers containing various combinations of salt and imidazole, for example, 20 mM HEPES, pH 7.5 with 500 mM NaCl (Wash I), 500 mM NaCl, 0.02% βDDM (Wash II), 250 mM NaCl, 0.02% βDDM (Wash III) and 250 mM NaCl, 0.02% βDDM, 5% glycerol, 10 mM imidazole (Wash IV) to remove weakly bound proteins. Tightly bound proteins were eluted by application of 3 bed volumes of elution buffer (20mM HEPES pH 7.5, 250 mM NaCl, 0.02% βDDM, 5% glycerol, 300 mM imidazole).

The eluted sample was concentrated by 100 kDa molecular weight cutoff (MWCO) concentrators (Millipore; cat# UFC910024) to approximately 20 times its original volume. Concentrated samples were further purified by size exclusion chromatography (GE Life sciences, Superdex 200 10/300 GL; column volume: 24 mL; fluid phase: 8 mL) using a fast pressure liquid chromatography instrument (FPLC, Pharmacia, Äkta Explorer). The running buffer contained 20 mM HEPES pH 7.5, 250 mM NaCl, 0.02% βDDM and 5% glycerol.

Protease digestion.

The heterologous Tobacco Etch Virus (TEV) protease was expressed from the pRK793 (Addgene, cat# 8827) plasmid, expressing a highly stable mutant of the protease (S219V, (Kapust et al. , 2002, Kapust et al. , 2001). The plasmid was electroporated in BL21(DE) cells and was expressed a self-cleaving fusion with the maltose binding protein by inducing a mid-logarithmic phase culture with 1 mM IPTG at 20 ºC. The cultures were harvested after 4 hr post- induction and lysed as mentioned above. Recombinant TEV protease was purified over a Talon metal affinity resin by first, equilibrating the resin with the binding buffer (20 mM TRIS pH 8, 500 mM NaCl and 5 mM Imidazole). The cell lysate was passed twice and washed with 30 column volumes of the binding buffer and was eluted in two column volumes of the same buffer, with 300 mM imidazole. The purified protease was stored at a concentration of 1 mg/mL in a buffer consisting 50 mM TRIS pH 7.5, 1 mM EDTA, 5 mM DTT, 50% glycerol and 0.1% Triton X-100 at -20 ºC. For cleavage, the protease was used up to an amount of 1 mg per the amount of target fusion protein obtained per 1L of culture.

PreScission Protease (GE Healthcare, cat# 27-0843-01) was used up to amounts of 100 U per the amount of fusion protein obtained per 1L of culture.

Gel electrophoresis, staining and western blots

SDS-PAGE using TRIS - based buffers (25 mM TRIS, 200 mM glycine and 3.5 mM SDS) was performed in a Biorad Mini-PROTEAN Tetra Cell. Following electrophoresis, gels were stained by coomassie brilliant blue, subjected to silver staining, or processed for immuno-blotting. For immuno-blotting, the acrylamide gel was first rinsed with water and equilibrated in a non-denaturing buffer (25 mM TRIS base and 200 mM glycine). The nitrocellulose membrane (Biorad; cat# 162-0112) was also equilibrated in the non-denaturing buffer. The gel and the membrane were sandwiched between extra-thick blot filter papers (VWR; cat# 28298-014) soaked in the non-denaturing buffer and

proteins were electro- blotted for 15 min at 15 V using a Biorad Transfer-blot SD Semi-dry Transfer Cell. Following an hour long blocking in PBSTM (PBS, 0.05% Tween 20 and 5% dry milk), the nitrocellulose membrane was further incubated in the presence of the appropriate primary antibody. The membrane was then washed 3×15 min in PBST (PBS and 0.05% Tween 20) prior to a one-hour incubation with the appropriate secondary antibody conjugated to horseradish peroxidase. Following additional 3x 15 min washes, the nitrocellulose membrane was then soaked in Immunocruz western blotting luminol reagent (Santa Cruz Biotechnology; cat# sc-2048), exposed to a chemiluminescence sensitive film (GE Heathcare; cat# 28906838) for the optimum time of exposure and the film was developed with a Konica SRX-101A system. Anti- Vpu polyclonal antibody, raised in rabbits, was kindly provided by the NIH's AIDS Reagent Program and was used at a dilution of 1: 30,000. Monoclonal antibodies against the poly-histidine tag (Sigma, cat# H-1029), raised in mouse, was used at a dilution of 1: 5,000. Goat anti-rabbit IgG - HRP (Santa Cruz Biotechnology; cat# sc-2923) and rabbit anti-mouse IgG-HRP (Sigma A-9044) were used at a dilution of 1:10,000 in PBSTM.

Dynamic light scattering

Dynamic light-scattering (DLS) measurements were performed using a NaBiTec GmbH setup comprising a SpectroSize 302 (Molecular Dimensions) in combination with an S6D microscope (Leica). The purified protein sample was concentrated to 10 mg/mL as described earlier was illuminated in a 2 µL hanging drop using a 24-well crystallization plate (VDX Greased Plate, Hampton Research) covered with siliconized-glass circular cover slides (22 mm; Hampton Research). The well itself was filled with 400 µL S running buffer. Prior to the measurement, the protein solution was centrifuged at 18000 ×*g*, 30 min, 4 ºC to remove possible dust and other suspended particles. All measurements were done at 20 ºC. Ten consecutive measurements, each with an integration time of 20 s, were

averaged. Hydrodynamic size of the particles was estimated with the instrument software using the following parameters: refractive index 1.33, viscosity 1.006, shape factor 1.0 and hydrated shell 0.2 nm.

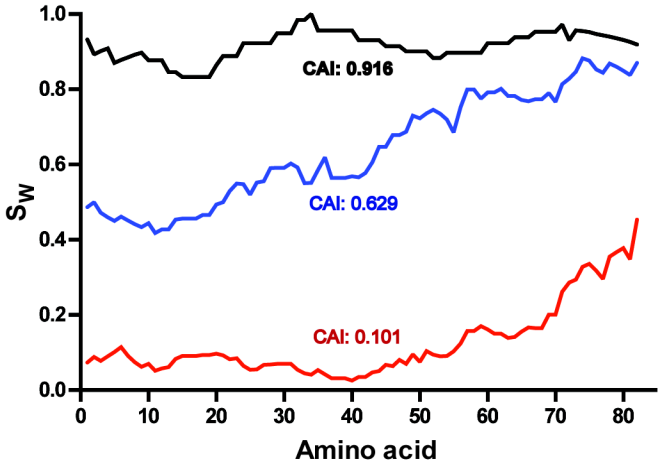

Figure II-5: Codon Usage analysis of Vpu. Codon usage analysis of the native HIV-1 *vpu* gene in *E. coli* (red) and *H. sapiens* (blue). The *vpu* gene optimized for expression in *E. coli* (black).

Results and Discussion

Gene Optimization.

Vpu is an important accessory protein involved in HIV – 1 pathogenesis. Furthermore, the presence of a transmembrane domain with an intriguing structure – function relationship makes it an attractive target for structural studies. In this study, unfavorable codons from the native Vpu gene from subtype B HIV – 1 were removed and were replaced by codons widely used in the *E. coli* expression system (Figure II-5). Codon optimization to increase yield and stability of the target recombinant protein has been successfully used in the laboratory for the expression of human butyrylcholineesterase (Geyer et al. , 2010) and HIV-1 Gag/dgp41 virus like particles (Kessans et al. , 2013) in *Nicotiana benthamiana*. Codon optimization of the *vpu* gene has been shown to improve its mRNA stability and magnitude of expression in HeLa cells when transcribed under the control of a CMV promoter (Nguyen et al. , 2004). Upon analysis, it was seen that the native *vpu* gene is composed of significantly unfavorable codons with respect to the *E. coli* codon usage patterns with a codon adaptation index (CAI) of 0.101. Removal of these unfavorable codons and replacing them with codons more suited to the *E. coli* codon usage patterns resulted in an increase of the CAI to 0.916. In the human genome, there is a weak positive correlation between frequency of optimal

codons and levels of gene expression (Lavner and Kotlar, Urrutia and Hurst, 2003). It is interesting to observe that the frequency of non-optimal codons is significantly higher at the region of the native gene encoding the N – terminal part of the protein. There is evidence to suggest that usage of low frequency codons within a coding sequence could be indicative of a genetic instruction that regulates the rate of protein synthesis. This phenomena could facilitate the formation of some secondary and/or tertiary structure in the nascent polypeptide (Marin, 2008, Purvis et al. , 1987). But, the idea of the action of codon usage bias to improve translational efficiency remains unconfirmed in mammals (Kanaya et al. , 2001). On the other hand, in unicellular organisms like *E. coli*, there is a strong correlation between the most frequently used codons and the abundance of tRNAs (Ikemura, 1981, 1982).Thus, the codon usage pattern can greatly influence the rate and efficiency of translation in *E. coli* (Robinson et al. , 1984, Sorensen et al. , 1989), leading to enhanced expression levels of the recombinant membrane protein. This *E. coli* optimized gene was cloned into the expression vectors discussed in this chapter.

Expression in E. coli.

Bacterial cells harboring pTMs 794, 869 and 975 were grown till mid logarithmic phase and induced with IPTG for protein expression. Expression conditions were optimized in regard to host strain, culture growth temperature and shaking during induction, length of induction period. A test for induction period length is shown in Figure II-6 in regard to the fusion of Vpu with MBP and Mistic. Best expression was obtained using the strain BL21(DE3) while other expression strains such as C41, C43, C41PlyS and C43PlyS were erratic in their expression patterns and were not reproducible over time. Expression at 15 ºC for Mistic-Vpu and MBP_{-TEV-}Vpu resulted in negligible leaky expression from all these constructs as seen when expression is analyzed at various time

points by SDS-PAGE followed by immunoblotting with anti-Vpu rabbit antiserum (Figure II-6). All the constructs produced useful quantities of Vpu with its fusion partners. Higher amounts of expression were observed in case of Mistic-Vpu than the fusion of Vpu with MBP. This could be due to the fact that MBP is a larger protein than Mistic and thus imposed a larger metabolic cost on the bacterial cells.

Detergent extraction screen.

Since the transmembrane domain of Vpu, which otherwise targets the protein into host cell membranes in natural conditions, is unable to target the protein effectively in bacterial cells (Ma et al. , 2002), I relied on its fusion partners to efficiently target and integrate the protein into the bacterial inner membranes. To have a sense of the localization of the protein in the cells and to select the optimal detergent

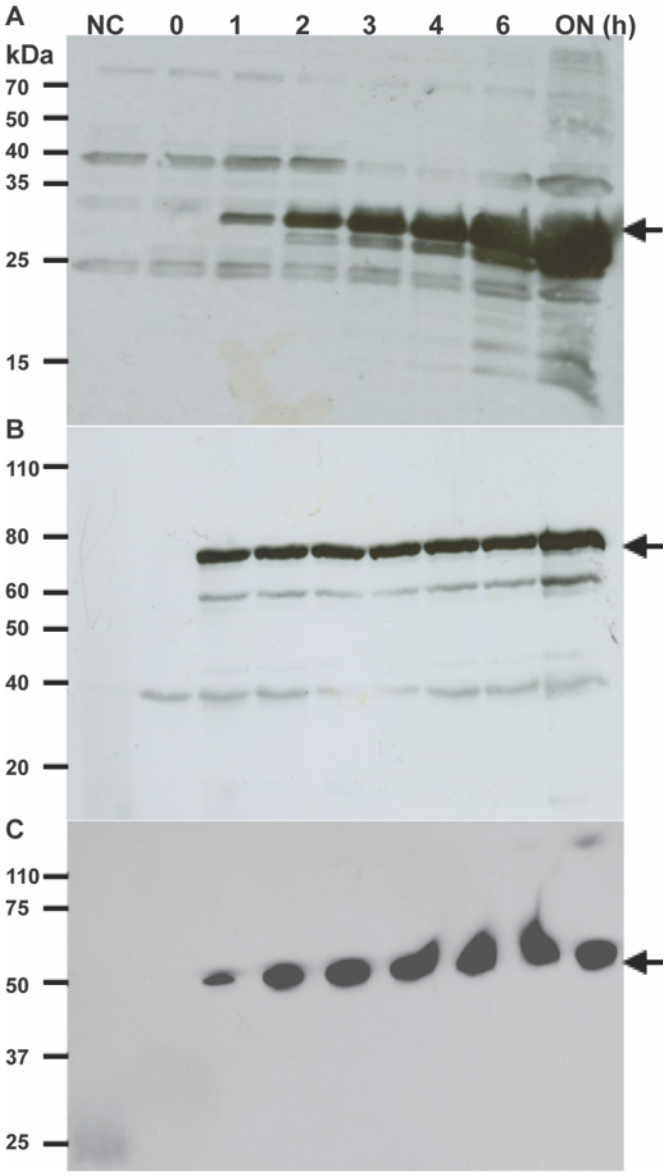

Figure II-6: Expression time-course of Vpu with Mistic and MBP.
Expression of Mistic-Vpu (A) MBP_{-TEV-}Vpu (B) and MBP_{-PPCS-}Vpu (C) fusion in BL-21 cells as a function of induction time. Samples from control cells (BL21, NC) and cells harboring respective plasmids were induced by IPTG and harvested at the indicated time points (in hr post induction, ON, overnight or ~12 hr) and lysed in SDS sample buffer. Proteins in samples were resolved by SDS/PAGE and subjected to immunoblot analysis, probed with anti-Vpu. The arrows indicate the position of bands corresponding to the protein of interest in each case.

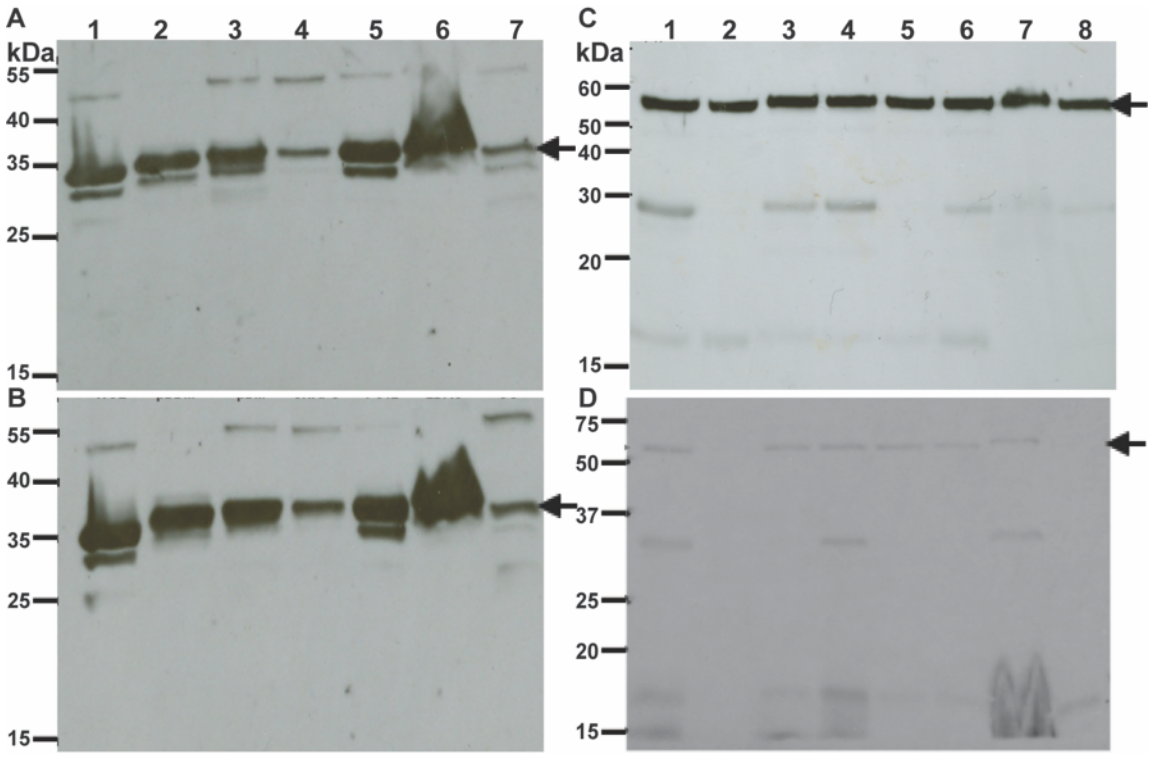

Figure II-7: Detergent extraction screen of Vpu with Mistic and MBP.
Detergent extraction screen for Mistic-Vpu at 4 ºC (A) and 25 ºC (B). Cells were lysed by passage through a microfluidizer, the homogenate was centrifuged to separate water-soluble proteins from the insoluble fraction (Lane 1). The pellet was resuspended in buffer containing the indicated detergents βDDM (Lane 2), βDM (Lane 2), CHAPS (Lane 4), DPC (Lane 5), LDAO (Lane 6) and OG (Lane 7) at 1% w/v. Supernatant was collected following centrifugation and proteins were resolved by SDS-PAGE followed by immunoblot analysis, probed with anti-Vpu.
Similar procedure was followed for detergent extraction screen for MBP_{-TEV-}Vpu (C) and MBP_{-PPCS-}Vpu (D). Cells were lysed by passage through a microfluidizer, the homogenate was centrifuged to separate water-insoluble (lane 1) proteins from the soluble fraction (lane 2). The pellet was resuspended in buffer containing the indicated detergents βDM (Lane 3), βDDM (Lane 4), CHAPS (Lane 5), OG (Lane 6), LDAO (Lane 7) and DPC (Lane 8) at 1% w/v. Supernatant was collected following centrifugation and proteins were resolved by SDS-PAGE followed by immunoblot analysis, probed with anti-Vpu. Black arrows indicate the protein of interest.

extraction conditions I conducted a small-scale detergent extraction screen for all the fusion proteins with mild maltoside detergent βDDM and βDM, zwitterionic detergents like DPC and LDAO and shorter chained detergents such as OG and CHAPS. The extraction was done at the indicated temperature (Figure II-7). The Mistic-Vpu fusion was found in the non-aqueous fraction and was efficiently extractable by both of the maltosides and

zwitterionic detergents (Figure II-7 A and B). The short-chained detergents, with relatively inflexible hydrophobic tails, like OG and CHAPS were relatively weak in extracting Mistic-Vpu from bacterial membranes and temperature seemed to have no drastic effect in helping the cause.

The MBP-Vpu fusion expressed from BL21-pTM 869 (MBP_{-TEV-}Vpu) was targeted by its native signal peptide at the N-terminal region, which targets MBP to the periplasmic space of the bacteria (Bedouelle, Bassford, 1980). I observed that the fusion protein fractionated evenly into both the aqueous and the non-aqueous fractions (Figure II-7C). Why would a fusion protein containing a hydrophobic alpha helical domain be found in the aqueous fraction? A possible explanation could be that the translocon-facilitated insertion of the over-expressed membrane protein into the membrane is constrained either by the finite membrane surface area (Drew et al. , 2003), or by the capacity of the translocation machinery to keep up with the translation process. Either way the fusion protein ends up accumulating in the cytoplasm. The bacteria often accumulate such proteins in the form of dense, insoluble aggregates (inclusion bodies). However, MBP is known to prevent the aggregation of its fused cargo and maintain it in solution even at high concentrations. In fact, this is one of the main reason why MBP is considered to be such a successful fusion partner. It is therefore conceivable that MBP prevents aggregation of MBP_{-TEV-}Vpu as inclusion bodies. Since a membrane protein in an aqueous environment is not likely to maintain its functional conformation, I proceeded to extract the protein in the non-aqueous fraction with detergents. In this case, it is observed that the protein is extractable by the whole panel of detergents. In view of the compatibility with the down-stream processes, βDDM was the detergent of choice.

On the other hand, the MBP-Vpu fusion protein obtained from BL21-pTM 975 (MBP_{-PPCS-}Vpu), which is targeted by the PelB signal peptide is exclusively found in the

non-aqueous fraction (Figure II-7D). This protein was extractable with a wide range of detergents, except OG which, performed poorly. Again, taking in to consideration the suitability of the detergents towards subsequent experiments, βDDM was used for all future purposes.

Large-scale extraction purification of Mistic-Vpu.

Cells harboring pTM 794 were induced for 3 h post-induction with 0.1 mM IPTG, lyzed by passage through a microfluidizer, centrifuged to remove water-soluble proteins and the pellet was subjected to 1% βDDM extraction at 4 ºC overnight and centrifuged to separate βDDM-soluble (supernatant fluid) and insoluble (pellet) fractions. The detergent-soluble protein fraction was subjected to metal affinity chromatography purification (Figure II-8). I observed that the fusion protein was efficiently bound to the affinity resin with little or no loss of protein in the flow-through and the washes. The presence of multiple histidine

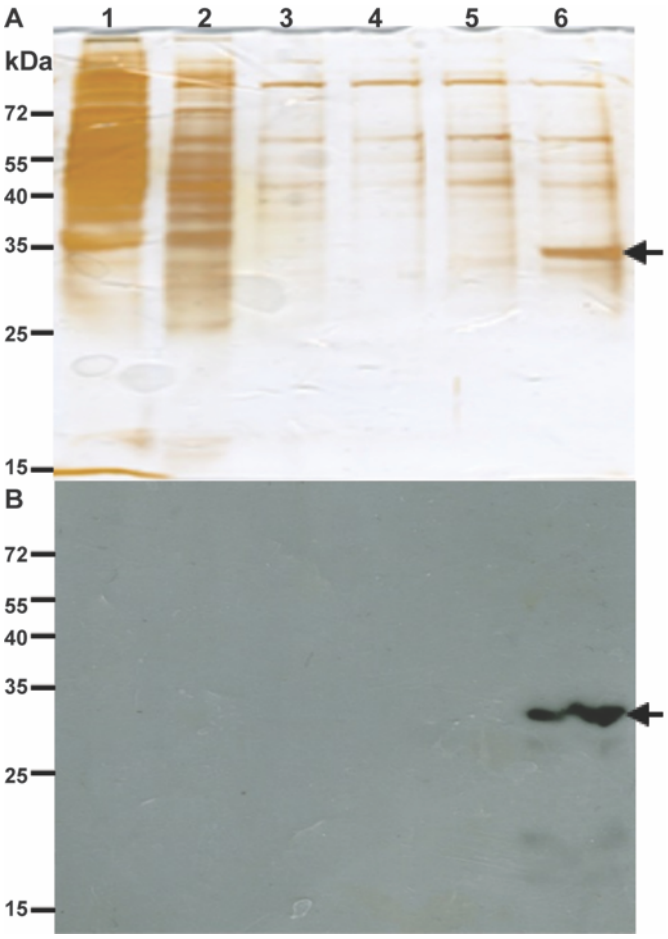

Figure II-8: Talon metal affinity chromatography purification of Mistic-Vpu.
Detergent (βDDM)-soluble fraction containing the Mistic-Vpu fusion protein were loaded onto a Talon resin pre-equilibrated with PBS_{500} (8.1 mM Na_2HPO_4, 1.8 mM KH_2PO_4, 2.7 mM KCl, 500 mM NaCl, pH 7.5) supplemented with 0.05% βDDM (lane1, flow through). Column was washed twice with PBS_{500} (W1, lane 2 and W2, lane 3), once with PBS + 0.05% βDDM (W3, lane 4) and once with PBS, 0.05% βDDM, and 5mM Imidazole (W4, lane 5). Elution was done with PBS, 0.05% βDDM, 250 mM Imidazole (E, lane 6). Protein fractions were subjected to SDS-PAGE followed by silver staining (A) and immunoblot analysis, probed with anti-Vpu (B). Black arrow indicates Mistic-Vpu.

tags in the construct probably was instrumental to achieve such excellent binding. The desired protein, eluting with high concentrations of imidazole, was seen to be containing some higher molecular weight contaminants.

Because the Mistic protein largely resisted attempts to crystallize it, was mostly characterized by NMR spectroscopy (Dvir, Lundberg, 2009, Roosild, Greenwald, 2005), I anticipate that the Mistic-Vpu fusion protein would not be an ideal candidate for crystallization. My intention was therefore to cleave the protein from Vpu by complete digestion with TEV protease and subject the cleaved products to a second round of metal affinity purification. The contaminants co-eluting with the Mistic-Vpu fusion is predicted to elute with the Mistic protein containing the poly-histidine tag in this second round of affinity purification whereas relatively pure Vpu should be found in the flow-through and washes.

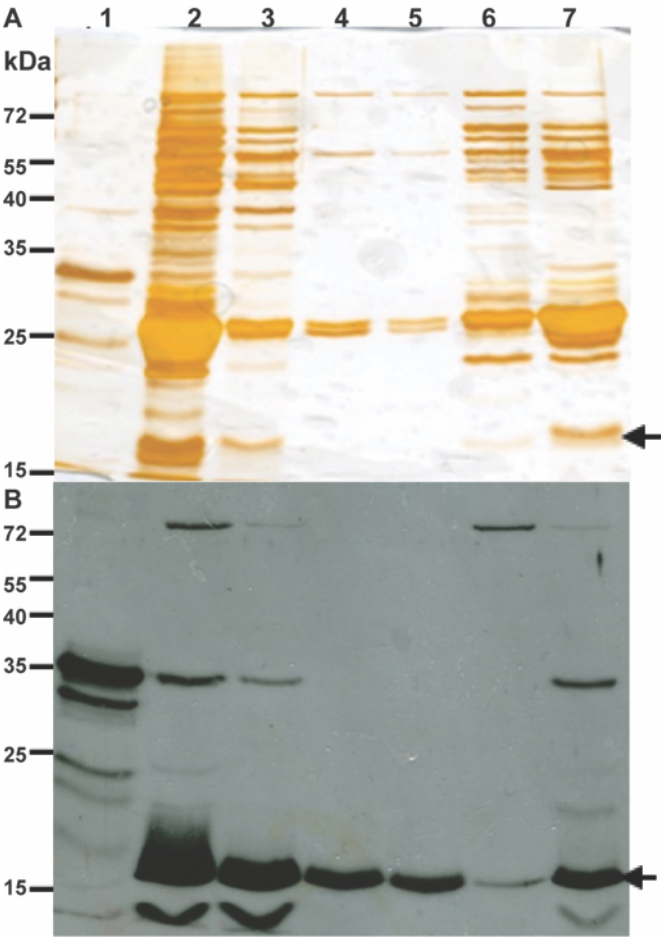

Figure II-9: Site specific proteolytic cleavage of Mistic-Vpu.
Affinity-purified Mistic-Vpu (lane 1) was subjected to digest with TEV protease (lane 2) followed by a second-round of metal-affinity chromatography. Unbound proteins were collected (lane 3), and the column was washed with 10 CV of wash buffer thrice (lanes 4-6). Tightly bound proteins were eluted with a higher concentration of imidazole (lane 7). Protein fractions were subjected to SDS-PAGE followed by silver staining (A) and immunoblot analysis, probed with anti-Vpu (B). Black arrow indicates cleaved Vpu.

The TEV protease is a site-specific protease that has a seven-amino-acid recognition site; E-X-X-Y-X-Q-S. Cleavage occurs between the conserved glutamine and serine (Dougherty et al. , 1989) where, X can be various amino acid residues but not all are tolerated. The optimal sequence for cleavage is E-N-L-Y-F-Q-S (Carrington and Dougherty, 1988, Dougherty et al. , 1988) was used in between the fusion proteins involving Vpu. Its high specificity, its activity on a variety of substrates, and the efficient cleavage at low temperature were the major reasons why I chose to use the TEV protease to removing the Mistic tag from our fusion protein (Parks et al. , 1994). The efficiency of cleavage depends on both the tag and the protein fused to the carboxyl terminus of the TEV cleavage site and is difficult to predict a priori and has to be determined experimentally.

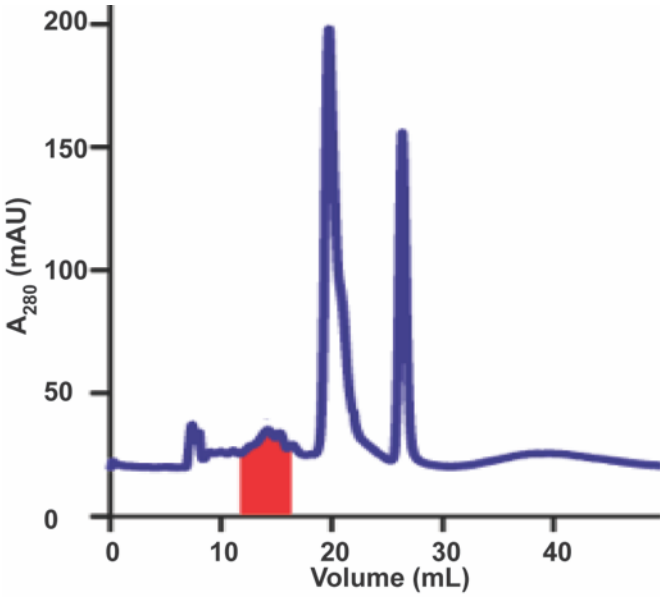

Figure II-10: Size-exclusion chromatography of the FT fraction from Figure II-9.
SEC resin: Superdex 200 10/300 GL; Flow-rate: 0.5 mL/min, Running buffer: 20 mM HEPES, 100 mM NaCl, 0.05% βDDM. Fraction highlighted in red contained the majority of Vpu.

Thus, following the affinity chromatography step, the eluate was concentrated and then subjected to digestion with the TEV protease (Figure II-9). The fusion protein was difficult to cleave to completion. In fact, even in the presence of high concentrations of TEV protease only little digestion was observed. As expected, cleaved Vpu remains without affinity tags and is precluded from binding to a talon metal affinity resin when the preparation is applied to a second affinity chromatography column (Figure II-9). Due to incomplete digestion, Vpu with C- terminal histidine tag is also found in the elution. But,

the amount of contaminants co-eluting with Vpu in the flow-through made the purification very challenging. The problem was compounded by the fact that the Mistic-Vpu protein was found to be very unstable over time, causing extensive aggregation and degradation, and also the use of a large quantity of histidine-tagged TEV protease which saturated the metal affinity resin.

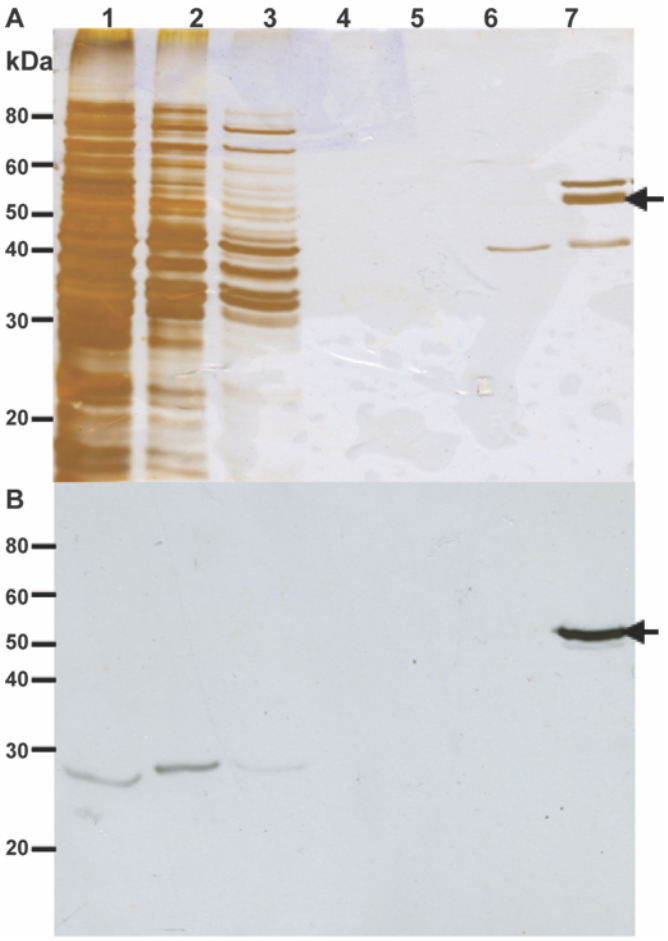

Figure II-11: Talon metal affinity chromatography purification of MBP-Vpu.
Detergent (βDDM)-soluble fraction containing the MBP-Vpu fusion protein (lane 1) was loaded onto Talon resin pre-equilibrated with PBS_{500} supplemented with 0.05% βDDM (lane2, flow through). Column was washed twice with PBS_{500} (lane 3 and lane 4), once with PBS + 0.05% βDDM (lane 5) and once with PBS, 0.05% βDDM, and 5mM Imidazole (lane 6). Elution was done with PBS, 0.05% βDDM, 250 mM Imidazole (lane 7). Protein fractions were subjected to SDS-PAGE followed by silver staining (A) and immunoblot analysis, probed with anti-Vpu (B).
Black arrow indicates $MBP_{-TEV-}Vpu$.

Nevertheless, in an attempt to purify Vpu in the flow through fraction from Figure II-9, the sample was subjected to size exclusion chromatography (SEC) and the elution profile is shown in Figure II-10. Vpu in βDDM micelles was detected in fractions highlighted in red in Figure II-10. The bleak possibility of obtaining pure, working amounts of Vpu is evident from the chromatogram. The presence of multiple peaks co-eluting with each other made the task of purification extremely difficult. Thus, also considering the low yield of the product, as

visualized in the small peak heights in the chromatogram, the strategy of expression and purification of Vpu with the Mistic protein was discarded.

Large-scale extraction and purification of MBP$_{-TEV-}$Vpu.

Towards the effort to isolate His-tagged MBP$_{-TEV-}$Vpu from the rest of the cellular proteins, the βDDM solubilized proteins from the non-aqueous fraction of BL21 cells containing pTM869, which were lyzed after 4 hr post-induction with 0.1 mM IPTG, was subjected to TALON metal affinity purification (Figure II-11). The protein eluted in a relatively pure form, but, in presence of a contaminant which resolved very closely on a denaturing gel. This was also observed by resolving the concentrated elute from metal affinity chromatography by size exclusion chromatography. MBP-TEV-Vpu in βDDM micelles was detected in fractions indicated by the area highlighted in red in Figure II-12. These fractions contained a high amount of contaminant which could not be separated by SEC. As with the Mistic-Vpu fusion, our goal was to cleave the MBP from Vpu by using TEV protease and obtain Vpu in a purified form with a second round of metal affinity chromatography. The longer linker produced by the Gateway recombination sequence was predicted to facilitate efficient cleavage.

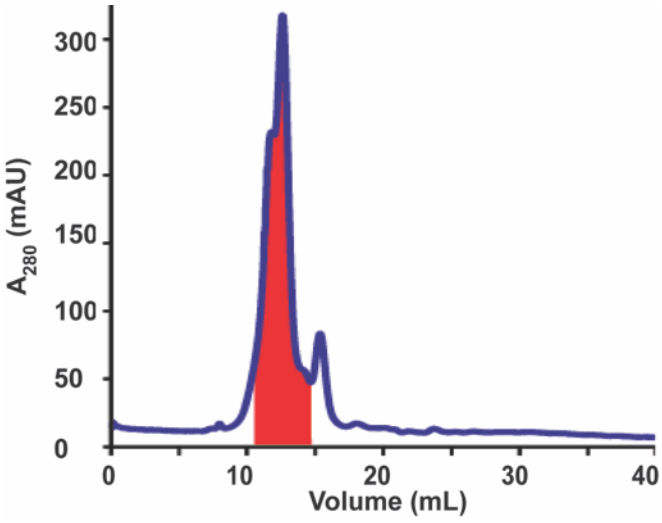

Figure II-12: Size-exclusion chromatography of concentrated metal-affinity chromatography eluate from Figure II-11.
SEC resin: Superdex 200 10/300 GL; Flow-rate: 0.5 mL/min, Running buffer: PBS, 5% glycerol and 0.05% βDDM. Fraction highlighted in red contained the majority of MBP$_{-TEV-}$Vpu.

Cleaved Vpu should remain without the affinity tag. However extensive experimentation with different incubation conditions did not yield appreciable digest. For example, the

protease seemed to have no effect on the fusion protein irrespective of the temperature and the incubation times (Figure II-13).

Large-scale extraction and purification of MBP$_{-PPCS-}$Vpu.

The recurring challenges that were faced by the strategy of expression and purification of Vpu in fusion with other soluble proteins has been the fact that the fusion proteins were difficult to purify to a satisfactory level and were also difficult to cleave by *in vitro* protease digestion. Both of the fusion proteins so far were also unusable for crystallization as they stand because of the fact that crystallization trials with Mistic have so far been unsuccessful and MBP$_{-TEV-}$Vpu contains a very unfavorable linker towards any structural studies. Hence, I experimented with a shorter cleavable linker between MBP and Vpu, which not only could be utilized to get rid of the fusion partner but also, would provide the option of proceeding with the whole fusion. Metal affinity purification was again utilized as the first method to separate the protein of interest from

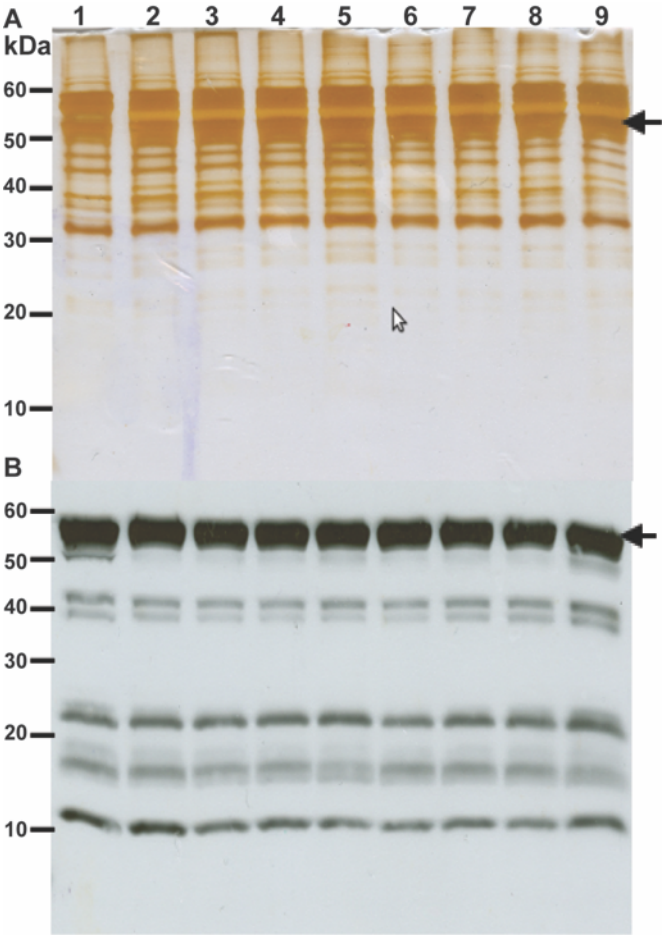

Figure II-13: Proteolytic cleavage of MBP$_{-TEV-}$Vpu. MBP$_{-TEV-}$Vpu fusion protein is resistant to site-directed digestion with the TEV protease. Concentrated eluate (Lane 1) from the talon affinity chromatography step was incubated at 4 ºC (Lanes 2-5) and 25 ºC (Lanes 6-9) for 1 hr (Lanes 2,6), 2 hr (Lanes 3,7), 3 hr (Lanes 4,8) and ON (Lanes 5,9). Protein samples were subjected to SDS-PAGE followed by silver staining (A) and immunoblot analysis, probed with anti-Vpu (B). The uncleaved fusion if denoted by a black arrow.

other cellular impurities. MBP_{-PPCS-}Vpu was found to co-elute with another protein, which was similar in size as per SDS-PAGE followed by silver staining (Figure II-14). This impurity could not be eluted prior to the high imidazole (300 mM) wash by varying the ionic strengths of the buffer and did not react with antibodies against Vpu. When a concentrated eluate of the metal affinity purification was resolved on a size exclusion column, the chromatogram was found to be somewhat similar as in MBP_{-TEV-}Vpu (Figure II-15).

This construct was designed with a cleavable PreScission protease site. Unlike the case of digestion with TEV protease, analytical amounts of MBP_{-PPCS-}Vpu could be cleaved to obtain Vpu without any purification and fusion tags. Complete digestion was only obtained when the fusion protein

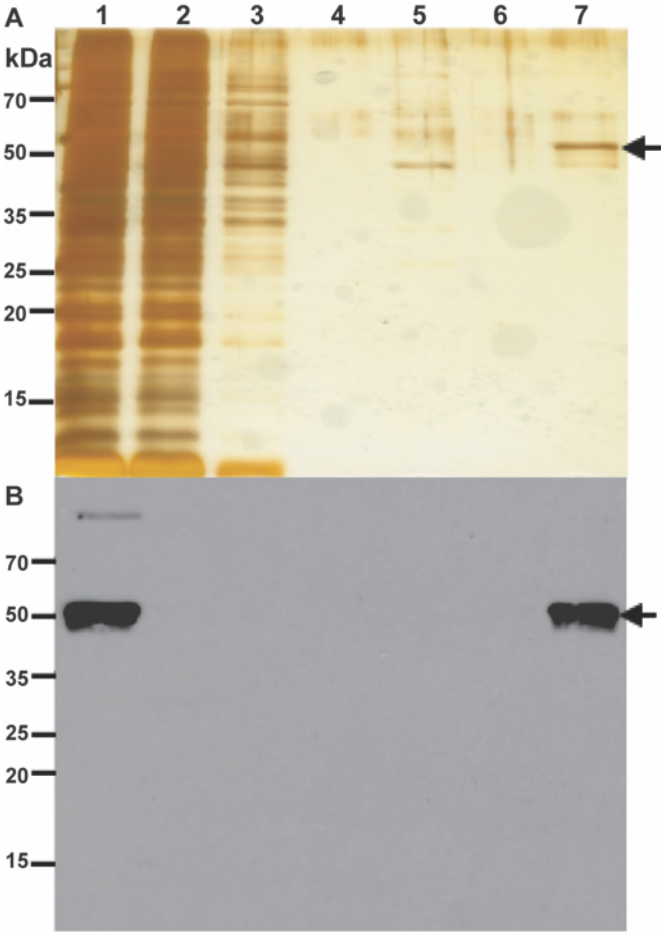

Figure II-14: Talon metal affinity chromatography purification of MBP_{-PPCS-}Vpu.
Detergent (βDDM)-soluble fraction containing MBP_{-PPCS-}Vpu (Lane 1) was loaded onto a column containing Talon resin that was pre-equilibrated with 20 mM HEPES, pH 7.5, supplemented with 500 mM NaCl, 5 mM imidazole, and 0.02% βDDM. Unbound proteins in the flow through were collected (Lane 2) and the column was washed consecutively with four different buffer solutions (20 mM HEPES, pH 7.5): W1 (Lane 3, buffer plus 500 mM NaCl), W2 (Lane 4, buffer plus 500 mM NaCl and 0.02% βDDM), W3 (Lane 5, buffer plus 250 mM NaCl and 0.02% βDDM), and W4 (Lane 6, buffer plus 250 mM NaCl, 0.02% βDDM and 10 mM imidazole). Pure Vpu (Lane 7) was eluted with W4 buffer supplemented with 300 mM imidazole. Protein fractions were subjected to SDS-PAGE followed by silver staining (A) and immublot analysis, probed with anti-Vpu (B). Black arrow indicates MBP_{-PPCS-}Vpu.

was incubated overnight at 25 ºC with high amounts of protease (Figure II-16). This protocol turned out to be non-replicable when scaled up to the amounts of fusion protein obtained from 4L bacterial cultures. The fusion protein, in a concentrated form, was found to be unstable at 25 ºC and formed insoluble precipitates. The consistent trend of Vpu being resistant to protease digestion could reflect a scenario where the protease cleavage site is inaccessible to the protease due to the bulky detergent micelles. Apart from the size, the charge characteristics of the detergent micelles could also play a role in the significantly reduced affinity of the proteases performing site-specific cleavage.

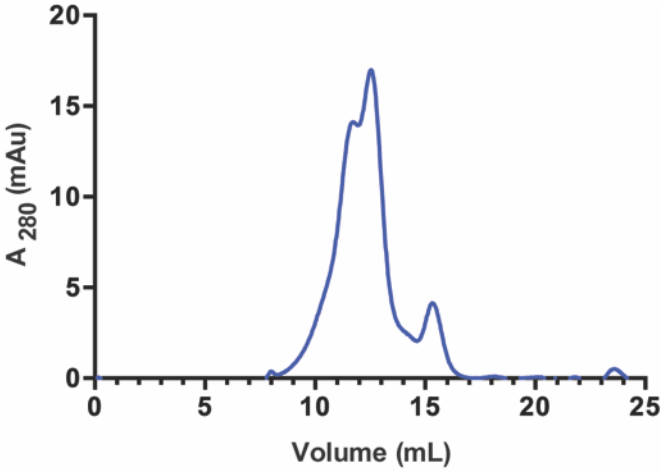

Figure II-15: Size-exclusion chromatography of concentrated metal-affinity chromatography-purified MBP$_{-PPCS-}$Vpu.
Eluate from the metal affinity chromatography purification was subjected to SEC-FPLC. Sec resin: Superdex 200 10/300 GL; Flow-rate: 0.5 mL/min, Running buffer: 20 mM HEPES, pH 7.5, 250 mM NaCl, 5% glycerol and 0.02% βDDM. The presence of MBP$_{-PPCS-}$Vpu was detected in the two highest peaks contained within 10-14 mL column volume.

Moving away from the strategy of separating the fusion partner from Vpu, I decided to subject MBP$_{-PPCS-}$Vpu to a second round of affinity purification, utilizing the affinity of MBP to bind to amylose (di Guana, Lib, 1988, Maina, Riggs, 1988, Riggs, 2001). A substantial loss of binding was observed when I detected the protein in flow-through and washes (Figure II-17). Although this purification strategy has been relatively successful, there have been previous instances on the challenges encountered in this process by the lack of substantial binding between MBP and amylose (Lo-Man et al. , 1993, Rhyum et al.

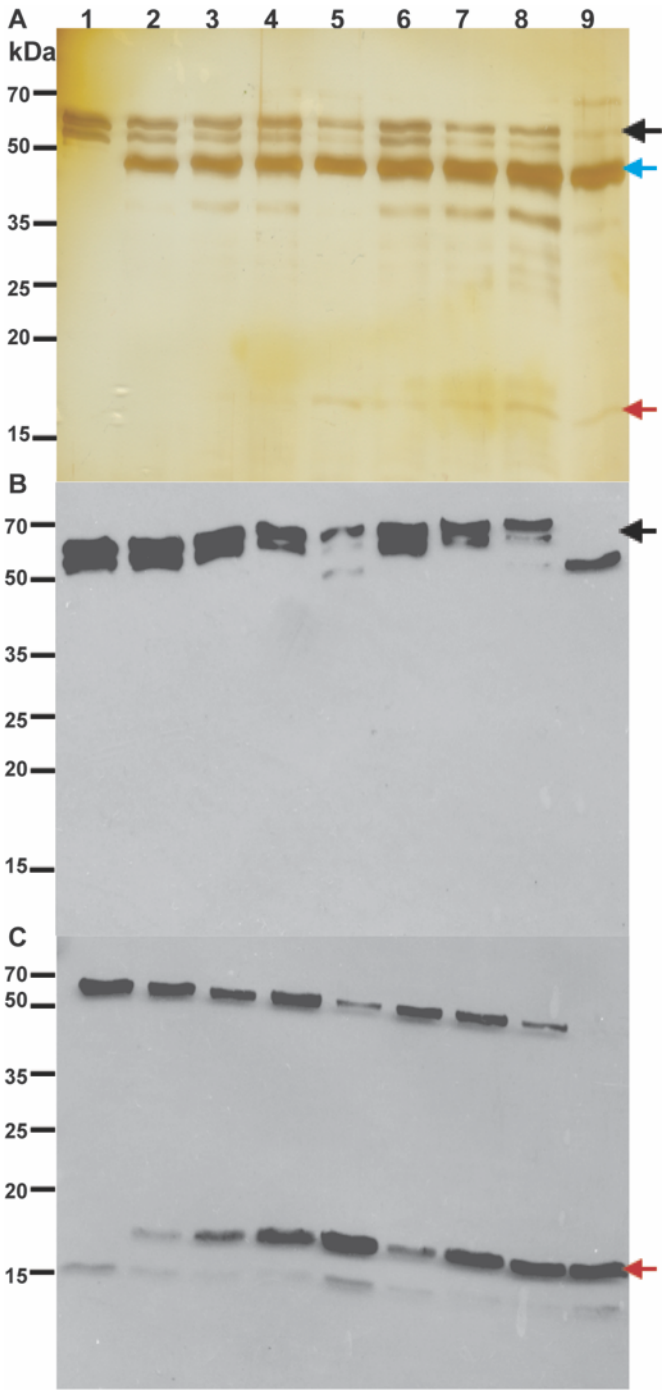

Figure II-16: Small scale digestion of $MBP_{-PPCS-}Vpu$ with PreScission protease.
Size exclusion fractions containing $MBP_{-PPCS-}Vpu$ (lane 1) was was incubated at 4 ºC (Lanes 2-5) and 25 ºC (Lanes 6-9) for 1 hr (Lanes 2,6), 2 hr (Lanes 3,7), 4 hr (Lanes 4,8) and ON (Lanes 5,9). Protein samples were subjected to SDS-PAGE followed by silver staining (A) and immunoblot analysis with antibodies against the poly-histidine tag (B) and Vpu (C). Complete digestion was only achieved when $MBP_{-PPCS-}Vpu$ was incubated with molar excess of protease (indicated on A with a blue arrow) at 25 ºC. Undigested MBP is indicated by a black arrow and cleaved Vpu is indicated by a red arrow.

, 1994). The binding of the MBP to amylose is strictly dependent on the correct biological activity and thus, proper folding of the MBP. Structural disturbances of the fusion partner, Vpu, in the present case, can also compromise the biologically active folding of MBP with respect to its amylose binding affinity (Park et al. , 1998). Interestingly, the doublet of bands was also observed when the protein bound to the amylose resin was eluted with 10

mM maltose, thereby hampering the prospects of this protein to crystallize successfully. Characterization of the concentrated version of this elution by dynamic light scattering confirmed the presence of multiple species in solution, as evident from the lack of a narrow red beam on the heat map image (Figure II-18).

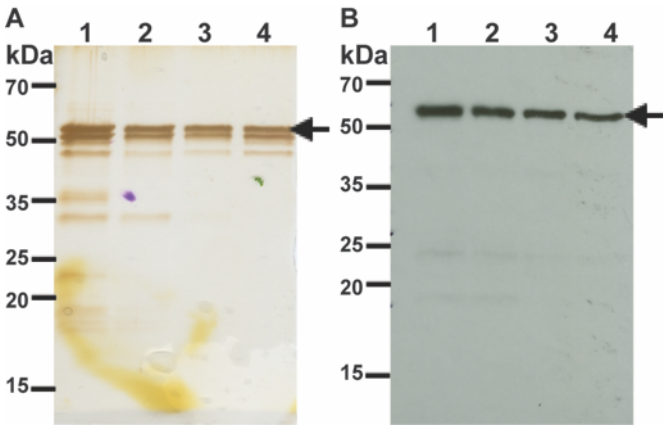

Figure II-17: Amylose column purification of MBP-$_{PPCS}$-Vpu.
Elution from Figure II-14 (lane 1) was passed through an amylose column prequilibrated with 20 mM HEPES pH 7.5, 250 mM NaCl, 0.5 mM EDTA and 0.02% βDDM. Unbound proteins were collected (lane 2) and the column was washed with 10 column volumes of the equilibration buffer (lane 3) and elution was done by supplementing the wash buffer with 10 mM maltose (lane 4). Protein samples were subjected to SDS-PAGE followed by silver staining (A) and immunoblot analysis (B). MBP-$_{PPCS}$-Vpu is indicated with a black arrow.

Conclusions

The strategy of expression of Vpu in fusion with proteins like the *B. subtilis* Mistic and the *E. coli* maltose binding protein (MBP) were successful in producing decent amounts of recombinant fusion protein. Even though relatively pure forms of protein were obtained after the first rounds of purification, the stability of the fusion proteins, especially the Mistic-Vpu fusion, was found to be very poor. The down-stream, polishing-step purification techniques such as size exclusion chromatography did not go a long way in improving the sample quality. The problem was further compounded by the fact that all of the cleavable fusion protein were resistant towards proteolytic digestion, especially in preparatory scales. I hypothesize that this could be due to the short extra-membrane N-terminus of the protein. In this case, the bulky detergent molecules would obscure the cleavage site and combined with the charge characteristics of the detergent, could play a role in substancially reducing the activity of

the protease. To this regard, further proteolytic digestion experiments with the proteins in smaller detergent micelles could be a future prospect.

Hence, towards our goal of exploring various strategies of expression of Vpu for crystallization, I conclude that the expression of Vpu in fusion with other helper proteins provides for samples that are not amiable for the rigorous standards required for structural studies and thus, other innovative strategies should be explored.

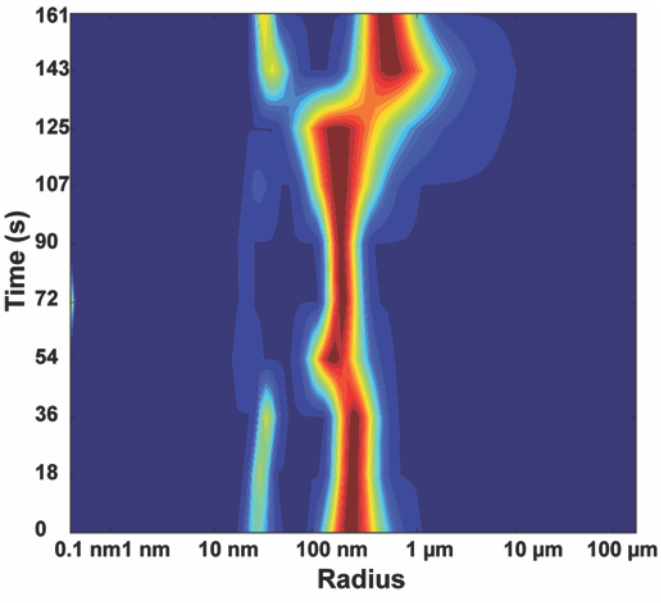

Figure II-18: Dynamic light scattering analysis of $MBP_{-PPCS-}Vpu$.
Amylose affinity purified $MBP_{-PPCS-}Vpu$ was concentrated to 10 mg/mL and was analyzed for dispersity. The sample was polydisperse as shown in the above heat map.

III. Expression, purification and characterization of HIV-1 Viral protein U using PelB signal peptide.

Abstract

Viral protein U (Vpu) is a type-III integral membrane protein encoded by Human Immunodeficiency Virus-1 (HIV- 1). It is expressed in infected host cells and plays several roles in viral progeny escape from infected cells, including down-regulation of CD4 receptors. But key structure/function questions remain regarding the mechanisms by which the Vpu protein contributes to HIV-1 pathogenesis. Here I describe expression of Vpu in bacteria, its purification and characterization. I report successful expression of Vpu in the *Escherichia coli* using the leader peptide pectate lyase B (PelB) of *Erwinia carotovora*. The protein was detergent extractable and could be isolated in a very pure form. I demonstrate that the PelB signal peptide successfully targets Vpu to the cell membranes and inserts it as a type I membrane protein. Vpu was biophysically characterized by circular dichroism and dynamic light scattering experiments and was shown to be an excellent candidate for elucidating structural models.

Introduction

Structural analysis of membrane proteins has traditionally been bottlenecked by the lack of sufficiently large amounts of pure, properly folded and functional membrane proteins. The issue is particular important considering the fact that membrane proteins constitute a significant proportion of clinical drug targets.

The Viral protein U (Vpu) was identified as product of the *vpu* open reading frame from the Human Immunodeficiency Virus-1 (HIV-1) which runs as a 16 kDa protein on a SDS-polyacrylamide gel (Strebel, Klimkait, 1988a). It is a type III trans-membrane protein 77-86 amino acids in length depending on the group and subtype of HIV-1. Vpu is not expressed by HIV-2 but is present in some simian immunodeficiency viruses (SIVs)

(Cohen et al. , 1988a). It has a very short N-terminal domain; a trans-membrane domain and a longer cytoplasmic domain, which has two predicted α-helical domains, separated by a hinge region. The hinge region contains two potential casein kinase II sites (Schubert, Schneider, 1992b). NMR characterization of the cytoplasmic domain of Vpu indicates that there is a great deal of structural flexibility in the cytoplasmic domain (Wittlich, Koenig, 2009a).

Down-regulation of CD4 receptors in the infected host cells is of prime importance for the virus and it accomplishes this through the Nef and Vpu proteins. Vpu not only retains CD4 in the endoplasmic reticulum but also induces CD4 degradation by employing a variant pathway of the ERAD machinery (Magadán et al. , 2010). Vpu retains CD4 in the ER by virtue of their interactions at the trans-membrane domain. The conserved tryptophan residue (Trp22 in NL4-3 strain Vpu sequence) in the trans-membrane domain of Vpu plays a role in inhibiting the dislocation of the CD4 from ER membrane to the cytosol for degradation. Val20 and Ser23 have also been identified to play a role in CD4 retention in the ER (Magadán and Bonifacino, 2012). The cytosolic domain of Vpu recruits the ubiquitination factors which ubiquitinate the cytoplasmic domain of CD4 at multiple lysine and serine/threonine residues to mark CD4 for proteasomal degradation and also further contribute in retention of CD4 in the ER (Magadán, Pérez-Victoria, 2010).

The trans-membrane domain of Vpu is involved in its association with tetherin. This lead to reduced levels of tetherin at the plasma membrane of the cells and thereby prevents the incorporation of tetherin into nascent virions. Tetherin is then degraded by an ubiquitin dependent mechanism in which phosphorylated Vpu recruits a SCG TRCP1/2 E3 ligase complex to ubiquitinate the cytoplasmic tail of tetherin at multiple residues. A motif in the second α-helix in the cytoplasmic domain of Vpu has been identified responsible for efficient counteraction of tetherin has been found (Kueck and Neil, 2012b).

Vpu has also been implicated in retention of NK, T-cell, B-cell antigen (NTB-A) in the Golgi apparatus by altering the glycosylation pattern in nascent NTM-A. This is a part of a strategy to prevent HIV-1 infected cells to be lysed by NK cells. This function has been traced to the second α-helical region of Vpu in its cytoplasmic domain (Bolduan et al. , 2013b). In addition, based on similarities with other viral trans-membrane proteins, Vpu has also been studied for possessing an ion-channel activity, which could potentially make the host membrane protein more permeable and aid in budding and release of nascent virions. Vpu has been shown to mediate potassium transport when expressed recombinantly in *Saccharomyces cerevisiae* (Herrero et al. , 2013b).

The 22 amino acid PelB signal sequence was first described in the identification and characterization of *Erwinia carotovora* pectate lyase B gene and its protein product (Lei et al. , 1987). The expression of the mature form of the protein in *Escherichia coli* was indicative of the fact that *E. coli* contains peptidases to cleave the signal peptide in its periplasmic space. Since then a wide variety of recombinant soluble proteins have been efficiently targeted to the *E. coli* periplasm and also to the extracellular media using this signal peptide like the ligand binding domains of glutamate binding receptor B and D subunits (Arvola and Keinänen, 1996) variable regions of light and heavy chains of antibodies (Fecker et al. , 1996, Power et al. , 1992), phospholipase D (Iwasaki et al. , 1995), and the C terminal domain of OMP C (Walsh et al. , 2003). The PelB signal peptide was also used to express a pentameric ion channel ELIC with a N-terminal fusion of maltose binding protein, which also led to the successful crystallization and x-ray structure determination of ELIC (Hilf and Dutzler, 2008). It was also used to targeting of a fusion of the B subunit of cholera toxin (CTB) and the membrane proximal region (MPR) of HIV-1 GP41, which, interacts with the membrane on the periplasmic side of the *E. coli* cells (Lee et al. , 2014, Matoba et al. , 2008, Matoba et al. , 2004).

In this study I report the successful expression of a eukaryotic type III membrane protein, Vpu, in *E. coli* by expressing it as a type I membrane protein in the presence of the PelB signal sequence. I also describe the purification and characterization of the target protein towards its suitability for structure determination by X-ray crystallography.

Materials and Methods

Target selection, gene optimization and cloning.

The sequence of HIV- 1 group M subtype B strain HXB2 Vpu was used. Unfavorable codons for each 82 amino acids in length were replaced using the *E. coli* codon usage table (Sharp and Li, 1987). The *vpu* gene optimized for expression in *E. coli* was synthesized as described in Chapter II. The *vpu* gene was sub-cloned into a TOPO-TA vector with flanking NcoI and BlpI sites and a C-terminus hexa- histidine tag using oTMs 787 and 788 (Table III-1) and was excised from this intermediate vector by digestion with NcoI (NEB; cat# R3193S) and BlpI restriction enzymes (NEB; cat# R0585S). The same pair of restriction enzymes were also used to linearize the pET26(b) vector by Novagen.

Table III-1: DNA primers used towards the creation of pTM875

Primer	Sequence (5' → 3')
oTM 662	atgcagccgatcccgatcg
oTM 663	cagatcgtcaacgtcccacgg
oTM 787	ccatgggcatgcagccgatcccgatcgttgc
oTM 788	gctcagcttaatggtgatggtgatggtgcagatcgtcaacgtcccacggagcg
oTM 856	atgaaatacctgctgccgaccgctgc
oTM 857	cccattcgccaatccggatatagttcctcc

The restriction digestion reactions were analyzed by agarose gel electrophoresis and the desired DNA bands were excised and purified using a QIAquick gel extraction kit (Qiagen; cat# 28704). The gene was ligated to the pET26(b) vector by performing a T4 DNA ligase reaction (Promega; cat# M1801) and transformed into DH5α electro-competent cells. The resulting bacterial colonies were screened using colony screen PCR using gene specific primers oTMs 662 and 663 and plasmid specific primers, oTMs 856 and 857. DNA sequencing using oTMs 856 and 857 was used to verify the final expression clone, pTM875.

Expression

The expression of Vpu with the N terminal PelB signal peptide, along with the C terminal metal affinity tag was driven by a T7 promoter. *E. coli* BL21 DE cells were transformed with the expression vector, pTM875 by electroporation. For protein expression, an overnight culture of BL21 DE cells containing the expression vector was grown in LB media supplemented with 100 µg/mL kanamycin (Phytotechnology lab; cat# K378) and was used to inoculate a fresh LB media with 50 µg/mL kanamycin in a 1:100 dilution. The cultures for expression were shaken at 200 rpm at 37 ºC to mid-logarithmic phase (OD_{600} ≈ 0.4). The cultures were then moved to 15 ºC and incubated for additional 30 min with 200 rpm shaking. Finally, the cultures were induced for expression with 0.1 mM Isopropyl-β-D-thiogalactoside (IPTG, Roche; cat# 11411446001). For standardization of expression conditions, 5 mL of culture were collected at various time points after IPTG induction and pelleted by centrifugation at 5000 ×*g*, 4 ºC for 15 min. For detergent extraction screens and subsequent purifications, cells were harvested at 6 h post induction by centrifugation at 5000 ×*g*, 4 ºC for 15 min. Cell pellets were stored at -80 ºC until further use.

Separation of water-soluble and insoluble fractions

Cell pellets from 4 L worth of culture (approximately 12 g) were re-suspended in 100 mL of ice-cold PBS-PI buffer (phosphate buffer saline, PBS, supplemented with EDTA-Free SIGMAFAST™ Protease Inhibitor Cocktail tablets, Sigma; cat# S8830). The cells were lysed by double passage through a microfluidizer (Microfluidics Microfluidizer). The lysate was collected and centrifuged at 36,000 ×*g* for 30 min at 4 ºC. The insoluble fraction, containing the inner and outer membranes among other insoluble materials like protein inclusion bodies, was washed once by repeated re-suspension (50 mL of ice-cold PBS with protease inhibitor cocktail) and centrifugation. The pellet was frozen at -80 ºC until further use.

Detergent extraction

Aqueous and non-aqueous fractions from 500 mL cultures were prepared as described above, induced for expression and cells were harvested as pellets as mentioned previously. The pellet containing the non-aqueous proteins was re-suspended in 25 mL of PBS-PI buffer. Samples (4 mL) were then subjected to detergent extraction by addition of the following detergents to final concentration of 1% (w/v): n-dodecyl-β-D-maltoside (βDDM, Glycon Biotech; cat# D97002C), n-decyl-β-D-maltoside (βDM, Anatrace; cat# D322), 3-[(3-Cholamidopropyl) dimethylammonio]-1-propanesulfonate (CHAPS, Mclab; cat# DCPS101), n-octyl β-D-glucopyranoside (OG, Glycon Biotech; cat# D97001C), n-dodecylphosphocholine (DPC, Anatrace; cat# F308S) and n-dodecyl-N,N-dimethylamine-N-oxide (LDAO, Anatrace; cat# D360). The samples were left overnight at 4 ºC with agitation at 200 rpm and centrifuged at 36,000 ×*g* for 30 min at 4 ºC on the following day and the supernatant was collected as the detergent soluble fraction. The fractions were analyzed by SDS-PAGE followed by Coomassie staining and western blot.

For large-scale extractions from 4 L cultures, the pellet, containing the membrane fraction, was fully re-suspended in 200 mL PBS supplemented with EDTA-Free

SIGMAFAST™ Protease Inhibitor Cocktail tablets. βDDM was used for solubilization at a final concentration of 1% (w/v). The protein was extracted and at 4 ºC overnight with agitation at 200 rpm. The detergent soluble fraction was obtained by collecting the supernatant after centrifugation at 36,000 ×*g* for 30 min at 4 ºC.

Purification

A gravity driven column (Biorad Econo-column) containing 60 mL bed volume of TALON metal affinity resin (Clontech laboratories Ltd; Cat# 635503) was equilibrated with binding buffer (20 mM HEPES pH 7.5, 500 mM NaCl, 0.02% βDDM, 5 mM imidazole). The sample was then loaded onto the column, and passed twice. The column was washed with ten bed volumes of wash buffers containing various combinations of salt and imidazole, for example, 20 mM HEPES, pH 7.5 with 500 mM NaCl (Wash I), 500 mM NaCl, 0.02% βDDM (Wash II), 250 mM NaCl, 0.02% βDDM (Wash III) and 250 mM NaCl, 0.02% βDDM, 5% glycerol, 10 mM imidazole (Wash IV) to remove weakly bound proteins. Tightly bound proteins were eluted by application of 3 bed volumes of elution buffer (20mM HEPES pH 7.5, 250 mM NaCl, 0.02% βDDM, 5% glycerol, 300 mM imidazole).

The eluted sample was concentrated by 100 kDa molecular weight cutoff (MWCO) concentrators (Millipore; cat# UFC910024) to approximately 1/20th its original volume. Concentrated samples were further purified by size exclusion chromatography (GE Life sciences, Superdex 200 10/300 GL; column volume: 24 mL; fluid phase: 8 mL) using a fast pressure liquid chromatography instrument (FPLC, Pharmacia, Äkta Explorer). The running buffer contained 20 mM HEPES pH 7.5, 250 mM NaCl, 0.02% βDDM, and 5% glycerol. For preparatory separations, a 1 mL sample of concentrated Vpu was loaded onto the SEC column and chromatography was performed at a flow rate of 0.5 mL/min. The protein elution was detected by absorption at 280 nm. The concentration of protein in the desired peak was determined spectrophotometrically (A_{280}) based on the primary

sequence of Vpu; Σ_{280} was calculated with ProtParam web application (http://web.expasy.org/protparam/).

Determination of Vpu orientation in the E. coli inner membranes

A 500 mL LB media, supplemented with 50 µg/mL kanamycin, was inoculated with an overnight culture of BL21 – pTM875 at a dilution of 1:100. The culture was grown and induced with 0.1 mM IPTG as mentioned above. The culture was allowed to shake at 180 RPM for 3 hr at 15 ºC post-induction after which the cells were harvested by centrifugation at 5000 ×*g* for 15 min at 4 ºC. The cells were gently and thoroughly re-suspended in 10 mL of 200 mM TRIS, 500 mM sucrose and 0.1 mM EDTA and were distributed into 1 mL aliquots. Lysozyme was added at a final concentration of 2 mg/mL and mixed 3 times with gentle inversion and incubated on ice for 20 min. Calcium chloride was added at a final concentration of 30 mM and chymotrypsin at 1:1000, 1:100 and 1:50 v/v ratio was added to the appropriate tubes from a stock of 1 mg/mL. Triton X-100 was added at a final concentration of 2% for controls performed with fully lysed cells. The digestion was done at 25 ºC for 1 hr, with gentle mixing every 15 min. Finally, the cells were lysed by the addition of SDS sample buffer and heating at 100 ºC before analyzing the results by SDS gel electrophoresis followed by immuno blot and coomassie staining.

Co-immunoprecipitation with CD4

A deconstructed version of human CD4 containing the transmembrane and the cytoplasmic domains with an N- terminal fusion of maltose binding protein was expressed in BL21 cells. The protein was extracted and solubilized in buffer containing 0.02% βDDM and purified by metal affinity followed by size exclusion chromatography. MBP was expressed with an N-terminal histidine tag in BL21 strain of *E. coli* cells and similarly purified by metal affinity and size exclusion chromatography. 25 µM of the MBP-CD4 fusion was incubated with 50 µM Vpu for 45 min at 4 ºC. The reaction was incubated with

antibodies against MBP at a dilution of 1:200 for 1 hr followed by 20 µL of Protein A/G PLUS- Agarose immunoprecipitation reagent (Santa Cruz Biotechnology; cat # sc-2003) overnight at 4 ºC. The agarose beads were pelleted by centrifugation at 500 ×*g* for 5 min at 4 ºC. The beads were washed 4 times with 1 mL of 20 mM HEPES pH 7.5, 250 mM NaCl, 0.02% βDDM and centrifuged for 500 ×*g* for 5 min at 4 ºC. Finally, the beads were resuspended in 1× SDS sample buffer and were analyzed by SDS-PAGE followed by immuno-blot analysis using antibodies against Vpu.

Gel electrophoresis, staining and western blots

SDS-PAGE using TRIS - based buffers (25 mM TRIS, 200 mM glycine and 3.5 mM SDS) was performed in a Biorad Mini-PROTEAN Tetra Cell. Following electrophoresis, gels were stained by coomassie brilliant blue, subjected to silver staining, or processed for immuno-blotting. For immuno-blotting, the acrylamide gel was first rinsed with water and equilibrated in a non-denaturing buffer (25 mM TRIS base and 200 mM glycine). The nitrocellulose membrane (Biorad; cat# 162-0112) was also equilibrated in the non-denaturing buffer. The gel and the membrane were sandwiched between extra-thick blot filter papers (VWR; cat# 28298-014) soaked in the non-denaturing buffer and proteins were electro- blotted for 15 min at 15 V using a Biorad Transfer-blot SD Semi-Dry Transfer Cell. Following an hour long blocking in PBSTM (PBS, 0.05% Tween 20 and 5% dry milk), the nitrocellulose membrane was further incubated in the presence of the appropriate primary antibody. The membrane was then washed 3×15 min in PBST (PBS and 0.05% Tween 20) prior to a one-hr incubation with the appropriate secondary antibody conjugated to horseradish peroxidase. Following additional 3× 15 min washes, the nitrocellulose membrane was then soaked in Immunocruz western blotting luminol reagent (Santa Cruz Biotechnology; cat# sc-2048), exposed to a chemiluminescence sensitive film (GE Heathcare; cat# 28906838) for the optimum time of exposure and the film was

developed with a Konica SRX-101A system. Anti- Vpu polyclonal antibody, raised in rabbits, was kindly provided by the NIH's AIDS Reagent Program and was used at a dilution of 1: 30,000. Antibodies against AcrA and GroEL, raised in rabbits, were kind gifts from the lab of Professor Rajeev Misra. Goat anti-rabbit IgG - HRP (Santa Cruz Biotechnology; cat# sc-2923) and rabbit anti-mouse IgG-HRP (Sigma A-9044) were used at a dilution of 1: 10,000 in PBSTM.

Mass spectrometry

I used matrix-assisted laser desorption/ionization-time of flight (MALDI-TOF) Mass spectrometry (MS) to accurately measure the molecular weight of the purified Vpu protein. Purified Vpu (1 µL of 10 mg/mL) was added to 4 µL of sinapinic acid matrix solution (67:33 water:acetonitrile (v/v) containing 0.4% trifluoroacetic acid in the total volume, saturated with sinapinic acid). The protein/ matrix mixture (1 µL) was added onto a steel target plate and allowed to dry in air. An external calibration spot prepared in a similar manner was placed near the Vpu protein spot. The plate was then placed into a Bruker microflex MALDI-TOF mass spectrometer, and spectra were collected in a positive linear mode over a mass range from 1 to 30 kDa. The final results represented the average of 10 separate spectra.

Circular dichroism.

A JASCO J-710 CD spectro-polarimeter was used for measuring the Circular dichroism (CD) spectra of the purified sample at various salt and temperature conditions. The SEC-purified Vpu (eluted in 20 mM HEPES pH 7.5, 250 mM NaCl, 0.02% βDDM, and 5% glycerol) was concentrated to 10 mg/mL by a 100-kDa concentrator and CD measurement was done on samples containing a final protein concentration of 0.5 mg/mL. A baseline CD spectrum was obtained for the buffer and these values were subtracted from the CD measurement of Vpu. CD spectra for the protein were recorded from 190 to

260 nm using a 0.1 cm quartz cuvette. To obtain readings for the protein at different salt concentrations, a temperature of 20 °C was maintained throughout. Parameters were set at 1 nm data pitch, continuous scanning mode, a scanning speed of 50 nm/min, a response of 4 s, and a spectral bandwidth of 1 nm. Output spectra were generated based on an accumulation of five scans. The molar ellipticity (θ) in deg.·cm^2/dmol was calculated as described by (Greenfield, 2006).

Dynamic light scattering

Dynamic light-scattering (DLS) measurements were performed using a NaBiTec GmbH setup comprising a SpectroSize 302 (Molecular Dimensions) in combination with an S6D microscope (Leica). The purified protein sample was concentrated to 10 mg/mL as described earlier was illuminated in a 2 µL hanging drop using a 24-well crystallization plate (VDX Greased Plate, Hampton Research) covered with siliconized-glass circular cover slides (22 mm; Hampton Research). The well itself was filled with 400 µL SEC running buffer. Prior to the measurement, the protein solution was centrifuged at 18000 ×*g*, 30 min, 4^{o}C to remove possible dust and other suspended particles. All measurements were done at 20 ºC. Ten consecutive measurements, each with an integration time of 20 s, were averaged. Hydrodynamic size of the particles was estimated with the instrument software using the following parameters: refractive index 1.33, viscosity 1.006, shape factor 1.0 and hydrated shell 0.2 nm.

Results and Discussion.

Gene Optimization, Cloning and Expression of Vpu.

Vpu is an important accessory protein involved in HIV-1 pathogenesis. Furthermore, the presence of a transmembrane domain with an intriguing structure-function relationship makes it an attractive target for structural studies. Previous attempts to express this protein were either unsuccessful, as with P8CBD expression vector

described in Luo, Choulet (2009) and in Chapter II , or resulted in proteins with unsatisfactory purity and stability to pursue them further for crystallization as was observed with an expression construct with a N-terminal fusion of *Bacillus subtilis* protein Mistic (see Kefala et al. , 2007, Chapter II). In this study, unfavorable codons from the native Vpu gene from subtype B HIV-1 were removed and were replaced by codons widely used in the *E. coli* expression system (Figure II-5). This *E. coli* optimized gene was cloned into the expression vector to obtain pTM875 (Figure III-1) with the addition of a C-terminal hexameric histidine tag.

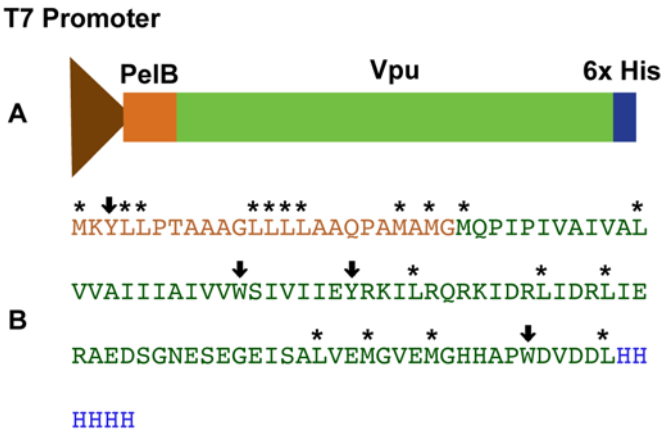

Figure III-1: Organization of the expression cassette on pTM875.
Expression was driven by a T7 promoter as shown in (A). The Vpu gene is flanked by the pelB signal peptide at the N-terminus which, directs the protein to the periplasmic space of the bacteria and thereby helping it integrate into the inner membranes, and a 6x- histidine tag at the C- terminus to aid in purification. (B) shows the sequence of the pelB signal peptide (in orange), Vpu (in green) and histidine tag (in blue). Chymotrypsin cleavage sites are denoted by (⬇) for strong catalytic sites and by (*) for secondary catalytic sites.

Bacterial cells harboring pTM875 were grown to mid-logarithmic phase when 0.1 mM IPTG was added to the culture medium to induce expression of the recombinant Vpu. At 6 h post induction, cells were harvested and lyzed by a microfluidizer. Following cell lysis, cellular components were fractionated into aqueous and non-aqueous fractions and their proteins resolved by SDS-PAGE. Immunoblot analysis revealed the almost-exclusive presence of Vpu in the water-insoluble fraction. However, Vpu could be extracted from the water-insoluble fraction with detergents. Particularly effective in extraction of Vpu were the maltoside detergents βDM and βDDM and the zwitterionic detergent, DPC (Figure III-2). These three detergents have relatively long and flexible hydrophobic chains, which may

be necessary for the ability of these detergents to effectively extract the highly hydrophobic Vpu protein. Accordingly, the shorter-chained OG and CHAPS, whose hydrophobic tail consists of a rigid steroidal ring system, have relatively ineffective extraction power. Long flexible hydrophobic tails may be necessary for successful extraction of Vpu, but apparently are not sufficient as LDAO performed poorly: its solubilization power may be hampered by a very small hydrophilic head (18 .2 as compared

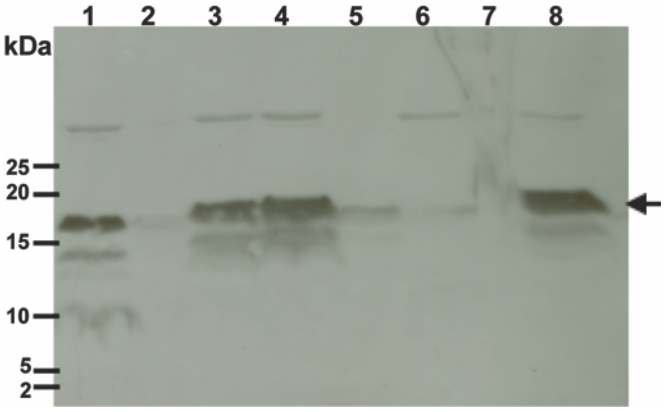

Figure III-2: Vpu fractionates with the water insoluble fraction and can be subsequently solubilized by detergents.
Whole cell lysates of BL21 strains of *E. coli* were fractionated into non- aqueous (lane 1) and aqueous (lane 2) fractions by centrifugation. The non-aqueous fraction (pellets) were resuspended in extraction buffer containing various detergents (1% final concentration): βDM (lane 3), βDDM (lane 4), CHAPS (lane 5), OG (lane 6), LDAO (lane 7) and DPC (lane 8). Following overnight incubation at 4 ºC, Detergent-soluble proteins were separated from detergent-insoluble proteins by centrifugation and fractionated by SDS-PAGE followed by immunoblot analysis. Vpu is indicated by a black arrow.

to 59 .2 and 179 .2 of DPC and the two maltoside detergents, respectively) (National Center for Biotechnology Information, 2016a, b, c) and a high octanol/water partition coefficient (logP > 5.3) (National Center for Biotechnology Information, 2016a). Based on its performance and its suitability for downstream applications, I elected to use βDDM in all subsequent experiments.

Vpu is targeted to the membranes and inserted as a type I membrane protein.

In mammalian cells, the Vpu transmembrane domain serves as a signal-anchor to target the protein for insertion into the membrane, but when expressed in bacteria, the domain cannot support this targeting function, resulting in the accumulation and aggregation of the protein in inclusion bodies (Ma et al. , 2002). The PelB leader sequence

targets its cargo protein pectate lyase B of *Erwinia carotovora* into the periplasm via the Sec-dependent pathway (Berks et al. , 2000, Steiner et al. , 2006, Thie et al. , 2008), which is also used for targeting integralmembrane proteins to the inner membrane (Hartl et al. , 1990). While PelB is commonly used to direct recombinant proteins to the periplasm of Gram-negative bacteria, there are not many examples of its application in targeting membrane proteins to the bacterial inner membrane as was intended here. Because the non-aqueous fraction obtained after cell lysis contain both membranes with their respective membrane proteins and aggregated proteins in the form of inclusion bodies, the question arose as to the partition of the recombinant Vpu between these two compartments.

To answer this question, I used differential extraction of Vpu from samples of water-insoluble protein fractions obtained at various times after the beginning of recombinant protein induction. To this end, I used the mild detergent of choice, βDDM, to extract membrane proteins and subjected the residual detergent-insoluble proteins to extraction with 8 M Urea, a chaotropic agent that can solubilize protein inclusion bodies (Alexander et al. , 1992, Kuhelj et al. , 1995, Patra et al. , 2000). Extractions were carried out at the specified time points following the induction with IPTG. The amount of Vpu extractable with βDDM increased with time during the first 6 hr post-induction (Figure III-3A). However, there was only a slight increase of the Vpu amount that could be extracted from homogenization pellets of cells harvested after overnight growth in the presence of IPTG as compared to 6 hr. In striking contrast, the overnight sample had a significant increase in amount of urea-extractable Vpu between the same time points. This could be explained by saturation of the bacterial inner membrane by 6 hr post induction and subsequent accumulation of the over-expressed protein in intracellular inclusion bodies. Urea cannot extract integral membrane proteins embedded in membranes, but

such proteins can be extracted by detergents. Conversely, detergent-extractable proteins may be present in inclusion bodies, but such proteins should also be solubilized by urea. To rule out this second possibility, and to further demonstrate that βDDM predominantly extracts Vpu from the cell membranes rather than from inclusion bodies, I reversed the order of extraction such that the non-aqueous fraction was first subjected to urea extraction followed by βDDM extraction. Most of the protein from cells harvested 2 h and 4 h after induction was in the βDDM extractable fraction (Figure III-3B). This indicates that most of the protein localizes in the membrane fraction until around 6 h after induction with IPTG, after which the membranes may saturate and the subsequently produced recombinant protein forms aggregates that can be solubilized by urea. Based on this finding, the cells were harvested after 6 hr of IPTG induction for all subsequent experiments.

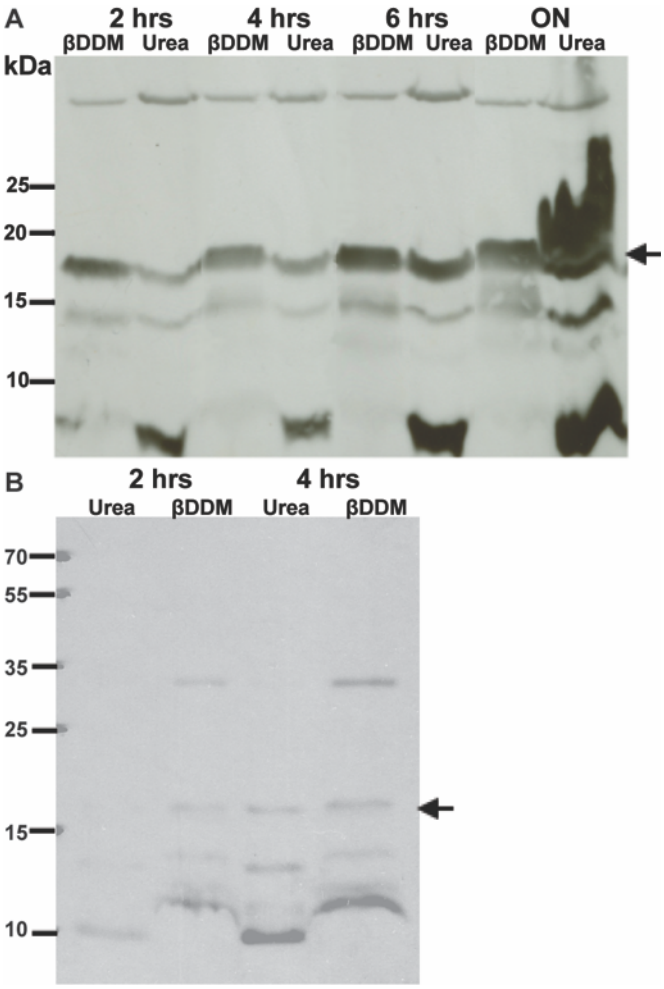

Figure III-3: Fractionation of Vpu between membranes and inclusion bodies.
Vpu fractionates between membrane fraction and inclusion bodies depending on time post- induction with IPTG. The βDDM extractable fraction increases with time until it reaches saturation around 6 hr (A). When the non–aqueous fraction is first treated with urea and then βDDM (B), the protein first fractionates in the detergent fraction, implying that protein does integrate in the membranes that is extractable by βDDM. Vpu is indicated by a black arrow.

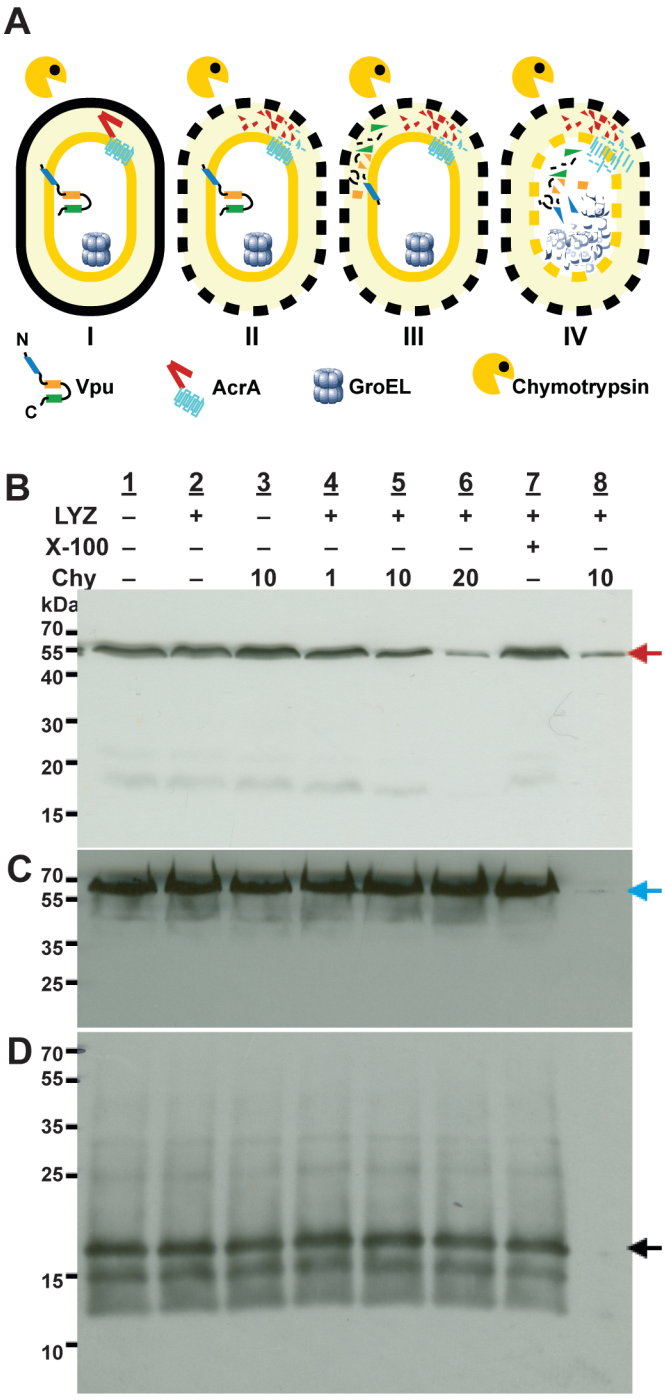

Figure III-4: Vpu is inserted into the bacterial inner membrane with its C-terminal domain within the cytoplasm. Panel A depicts the possible outcomes when *E. coli* cells (I) and protoplasts (II III and IV) that express Vpu are challenged with chymotrypsin (I-IV) and Triton X-100 (IV). If the C-terminal domain of Vpu is protected by the inner membrane (I and II), it is expected to be resistant to chymotrypsin digestion, similar to the case of the cytoplasmic resident protein GroEL. If the C-terminal domain of Vpu is exposed at the periplasmic space of the cells (III), it is expected to be digested in the same way as AcrA. All three proteins should undergo chymotrypsin cleavage when the inner membranes are compromised by the addition of Triton X-100 (IV). *E. coli* cells (lanes 1 and 3) and protoplasts (lanes 2 and 4-8) were incubated without chymotrypsin (lanes 1, 2, and 7) or with the indicated concentrations of chymotrypsin (µg/mL); in the presence of 1% Triton X-100 (lanes 7 and 8) or its absence (lanes 1-6). Following treatments, cells were lysed in the presence of SDS sample buffer and protein samples were resolved by SDS-PAGE followed by immunoblotting. Detecting Abs were against the periplasmic domain of the inner-membrane protein AcrA (Panel B, indicated by a red arrow), against the cytoplasmic protein GroEL (panel C, indicated by a blue arrow) and against the C-terminal domain of Vpu (Panel D, indicated by a black arrow).

The PelB sequence allows the insertion of recombinant Vpu into the membrane, however the presence of two in tandem hydrophobic domains may complicates the membrane topology of the protein. To settle this question, I next sought to determine *in*

vivo whether the protein is oriented with its N-terminus outside of the cell (in the periplasm, functionally equivalent to the ER lumen in human cells) and its C-terminus inside the cell (in the cytoplasm). To this end I converted *E. coli* cells expressing PelB-Vpu into protoplasts by lysozyme treatment. The protoplasts were subjected to mild chymotrypsin proteolysis. The C-terminal domain of Vpu contains several chymotrypsin proteolytic sites, which should be protected from the protease if the protein is inserted with its C-terminus in the cytoplasm. However, if the orientation of the protein is such that the C-terminus is externally-exposed, it will be cleaved and should not react with the polyclonal antibodies against Vpu.

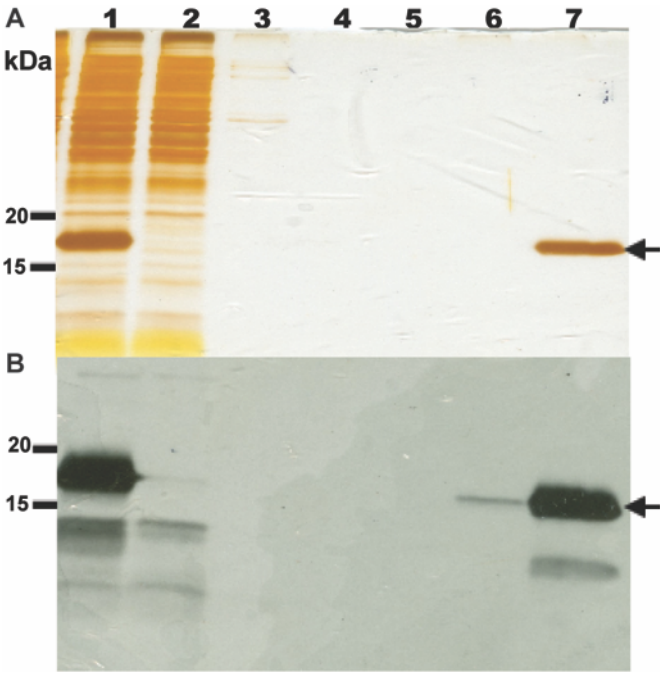

Figure III-5: Talon metal affinity chromatography purification of Vpu.
Protein fractions were subjected to SDS-PAGE followed by silver staining (A) and immublot analysis. (B). Detergent (βDDM)-soluble fraction containing Vpu (Lane 1) was loaded onto a column containing Talon resin that was pre-equilibrated with 20 mM HEPES, pH 7.5, supplemented with 500 mM NaCl, 5 mM imidazole, and 0.02% βDDM. Unbound proteins in the flow through were collected (Lane 2) and the column was washed consecutively with four different buffer solutions (20 mM HEPES, pH 7.5): W1 (Lane 3, buffer plus 500 mM NaCl), W2 (Lane 4, buffer plus 500 mM NaCl and 0.02% βDDM), W3 (Lane 5, buffer plus 250 mM NaCl and 0.02% βDDM), and W4 (Lane 6, buffer plus 250 mM NaCl, 0.02% βDDM and 10 mM imidazole). Pure Vpu (Lane 7) was eluted with W4 buffer supplemented with 300 mM imidazole, indicated by a black arrow on (A) and (B).

Indeed, the chymotrypsin digestion assay revealed that the C-terminal domain of Vpu is shielded from proteolytic digestion by the *E. coli* inner membrane (Figure III-4). In contrast, the periplasmic domain of AcrA, a native *E. coli* inner-membrane efflux pump, was vulnerable to proteolytic cleavage. (Figure III-4A). The cytoplasmic chaperone GroEL, like

the cytoplasmic domain of Vpu, was immune to the effects of chymotrypsin (Figure III-4B and 4C respectively). Vpu and GroEL could be digested by chymotrypsin only when the integrity of the *E. coli* inner membranes was compromised by treatment with the detergent triton X-100. The results of this experiment support the hypothesis that PelB-Vpu is inserted into the membrane with its C-terminal domain located in the cytoplasm and its N-terminus projecting into the periplasm.

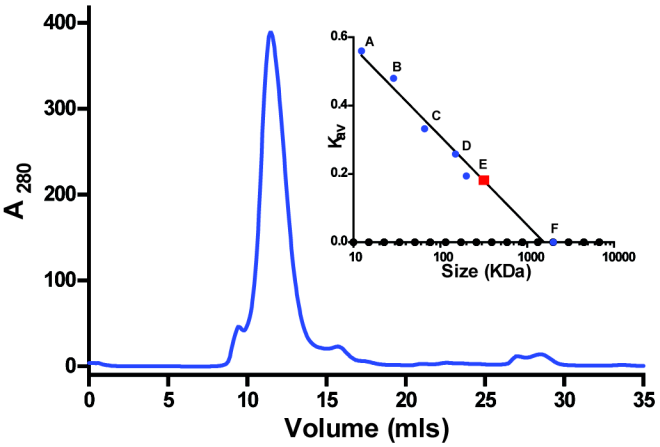

Figure III-6: Size-exclusion chromatography of concentrated metal-affinity chromatography-purified Vpu.
Eluate from Figure III-5 was subjected to SEC-FPLC. Sec resin: Superdex 200 10/300 GL; Flow-rate: 0.5 mL/min, Running buffer: 20 mM HEPES, pH 7.5, 250 mM NaCl, 5% glycerol and 0.02% βDDM. The minor peak at 8 mL corresponded to void volume, and the major peak at 11.48 mL contained Vpu. The column was calibrated with cytochrome c (A), carbonic anhydrase (B), albumin (C), alcohol dehydrogenase (D), β-amylase (E) and blue dextran (F) and a standard curve was obtained as shown in the inset. The size of the Vpu- βDDM complex was estimated to be 315 kDa.

Purification of Vpu

Immobilized metal affinity purification of membrane protein- detergent complexes can be challenging in terms of amount and purity of the enriched protein. The choice of detergent and buffers can have some effect on the efficiency of the purification procedure (Loo and Clarke, 1995, Peters et al. , 1995). The conformation of the protein could also play a vital role towards the retention of the protein in the affinity resin (Janssen et al. , 1995, Lindner et al. , 1992). The folding state can also dictate the placement of the affinity tag in the protein and its accessibility to the metal resin (Waeber et al. , 1993). Towards my effort to isolate His-tagged Vpu from the rest of the cellular biomolecules, the βDDM solubilized fraction was subjected to TALON metal affinity. I observe that the protein in the elution fraction was

obtained in a highly pure form (Figure III-5A). I was also able to obtain our target protein with minimal loss during the purification procedure in the flow-through and wash steps (Figure III-5B). Although the quality of the eluate was demonstrated by denaturing gels, it is also important to analyze the sample for high molecular weight aggregates, which may be undetectable due to the denaturing and reducing nature of SDS-PAGE. With this objective, concentrated IMAC purified protein was analyzed by size exclusion chromatography. I observe that the protein eluted as mostly a solitary peak. Void volume aggregates eluted as a distinctly small distinct peak before the major peak, which was easily separated and discarded before proceeding onto further characterization procedures (Figure III-6).

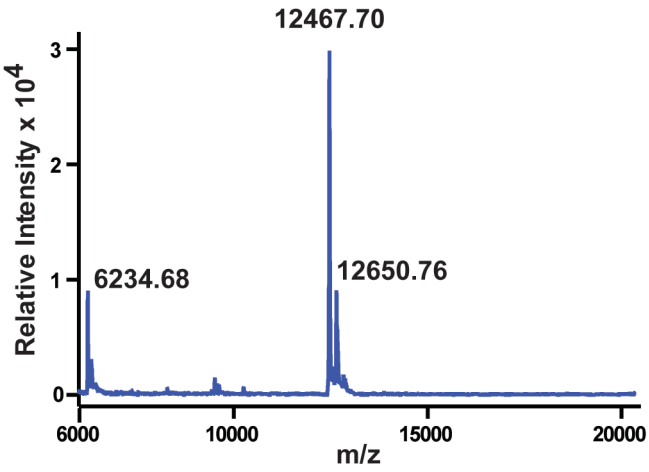

Figure III-7: Mass spectrometry analysis of PelB-Vpu.
MALDI-TOF spectrum of Vpu reveals that the purified protein retains the PelB peptide. The major peak corresponding to the MH^+ form of the protein was noticed at 12467.7 Da

Size of Vpu

My results so far suggest that the fusion of the PelB signal sequence converted *de facto* Vpu, a Type III membrane protein, into a protein more akin to a Type I membrane protein. However, unlike most Type I proteins, from which the signal peptide is typically cleaved concomitantly to their insertion into the membrane, the apparent molecular mass of the recombinant protein of approximately 17.5 kDa, as estimated from denaturing gels, suggests that the PelB sequence is not cleaved off Vpu. Vpu is known to align with a size of 16 kDa when analyzed with SDS-PAGE (Strebel, Klimkait, 1988a). The predicted

molecular mass of Vpu based on its primary structure including the engineered poly-histidine tag and PelB is 12463.7 Da. If the signal peptide would be cleaved the predicted molecular mass would be 10,064.7 Da. To precisely determine the size of the bacterially-produced human protein, I subjected the protein mass spectrometry (MALDI-TOF, Figure III-7). The peak representing the MH^+ form of the protein at 12467.7 Da, corresponds well to the scenario in which the PelB signal peptide remains uncleaved. Inefficient cleavage by periplasmic peptidases could be a result of steric hindrance due to the proximity of the cleavage site and the five residue-long N-terminal ectodomain to the hydrophilic heads of phospholipids in the outer leaflet the plasma membranes of *E. coli*. The size of the non-denatured Vpu within the context of its associated βDDM micelle is shown by size exclusion

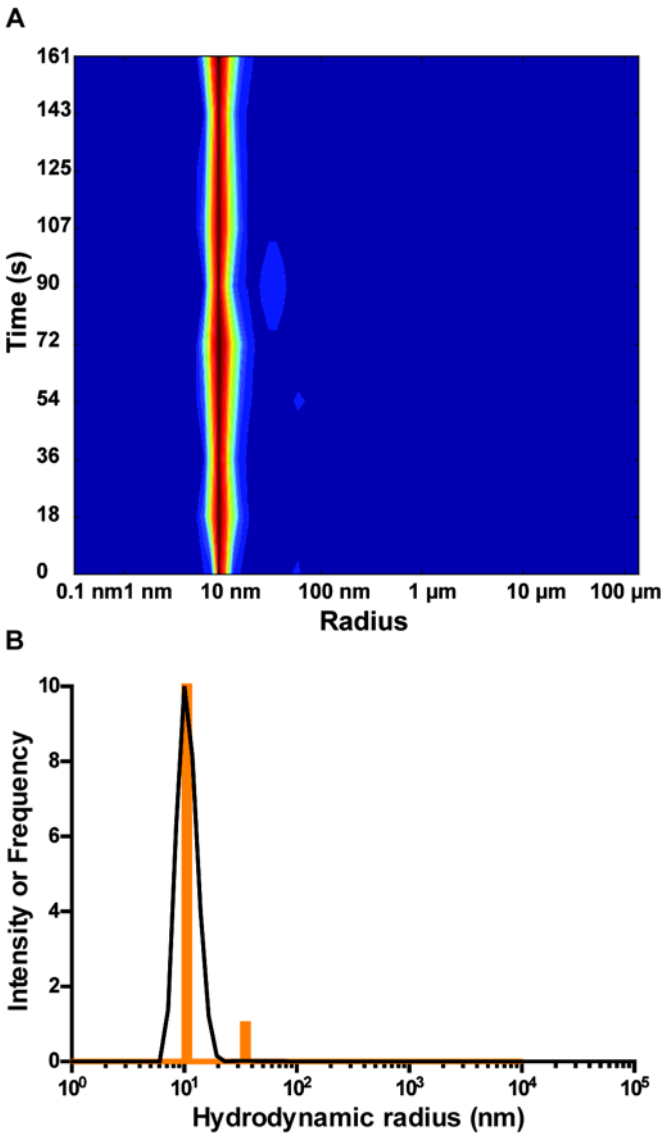

Figure III-8: Dynamic light scattering measurement of PelB-Vpu.

DLS measurement proves that PelB-Vpu is monodisperse. I could detect by DLS the complex of detergent and PelB-Vpu as a narrow peak at 10 nm. A molecular weight of 448.6 KDa was predicted for the protein-detergent complex using this technique. Monodispersity of Vpu at a concentration of 10 mg/mL is shown by the heat map diagram (A) and a plot of frequency of each particle size estimated by multiple runs of the experiment (B).

chromatography to be around 315 kDa (Figure III-6). This indicates that Vpu exists as an oligomer in complex with the βDDM micelles. The size of empty βDDM micelles size of has been estimated to be 60-70 kDa (Jumpertz et al. , 2011, Prive, 2007, Strop and Brunger, 2005, VanAken et al. , 1986), however, it is difficult to predict the size of the βDDM-protein micelles. Consequently, the accurate determination of the oligomeric state of the protein is very challenging in a protein-detergent micelle complex.

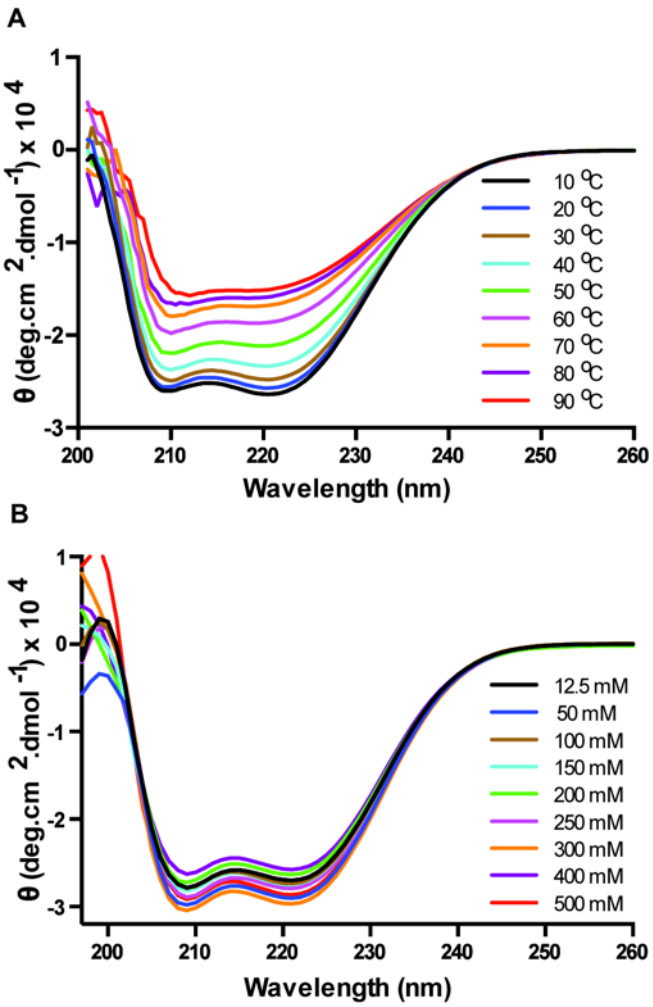

Figure III-9: Circular dichroism analysis of PelB-Vpu.
CD spectrometry analysis at various temperatures (A) reveals that PelB-Vpu is stable upto 40 °C. CD spectrometry of the protein at various salt concentrations (B) reveals that Pel-Vpu is stable across a wide spectrum of salt concentrations.

Preparations of purified Vpu are uniform and the protein is folded and stable.

Dynamic light scattering of purified Vpu preparations reveals very low dispersity at a concentration of 5 mg/mL and 10 mg/mL with a 10.44 ± 0.1 nm hydrodynamic radius (data not shown and Figure III-8). This estimation was fairly consistent upon re-runs of the experiment as is evident by the histogram depicting the frequency of each size estimation over 10 runs (Figure III-8B). The hydrodynamic radius

corresponds to a protein-detergent complex of about 332.2 kDa, corresponding well to the molecular mass estimates reported above for size-exclusion chromatography.

Circular dichroism was used to estimate the secondary structure content of Vpu. The CD spectrum of Vpu displayed two negative peaks at 208 and 222 nm, characteristic of a α-helical protein. Spectra for wavelengths below 200 nm could not be obtained because of interference from the chloride ions in the buffer. Analysis of the CD data (in 20 mM HEPES pH 7.5, 250 mM NaCl, 0.02% βDDM, and 5% glycerol) by CONTINLL in the CDPro software package revealed 55.6% right handed helix, 23% left handed helix, 3.3% sheets, 2% turns and 16% random elements, corresponding well to in silico analysis by the secondary structure prediction tool, GOR 54, which estimated 65.2% helices in the sequence.

Purified PelB-Vpu was observed to be stable up to around 40 ºC after which a temperature dependent disintegration of the α-helical secondary structure was observed (Figure III-9A). It was also observed that the protein was stable across a wide range of salt concentrations (Figure III-9B).

Purified Vpu can selectively associates with CD4

The interaction with CD4 and its subsequent degradation is one of the well-characterized functions of Vpu. This interaction has been shown to be dependent on an intriguing combination of specific amino acids and structural features in the transmembrane and cytoplasmic domain of both proteins. Scrambling the amino acids of the transmembrane domain of Vpu, while preserving its hydrophobicity, decreased its capability to down-regulate surface expression of CD4 in HeLa CD4+ cells (Hout et al. , 2005). This indicates a potential of loss of usual interaction between the two proteins. It has also been shown that specific amino acids are required in the cytoplasmic domain of CD4 (Lenburg and Landau, 1993) and Vpu for their interaction (Margottin et al. , 1996).

Furthermore, it was also demonstrated that the formation of α-helical structures in the cytoplasmic domains of both Vpu and CD4 was critical for CD4-Vpu interactions (Tiganos et al. , 1997). The transmembrane and cytoplasmic domains of CD4 were expressed with an N-terminal fusion with maltose binding protein (MBP) in BL21(DE3) *E. coli* cells. The fusion protein embedded in βDDM micelles was purified by using metal affinity chromatography and size exclusion chromatography purifications in βDDM micelles (data not shown). I was able to demonstrate that PelB-Vpu in βDDM micelles precipitated with MBP-CD4 (Figure III-10). The exclusivity of the binding was illustrated by the fact that PelB-Vpu did not precipitate with MBP nor does it cross react with anti- MBP antibody or the agarose beads. It does appear that the affinity of interactions between the two proteins is substantial enough to overcome the challenges imposed by the fact that both proteins are surrounded by bulky detergent micelles.

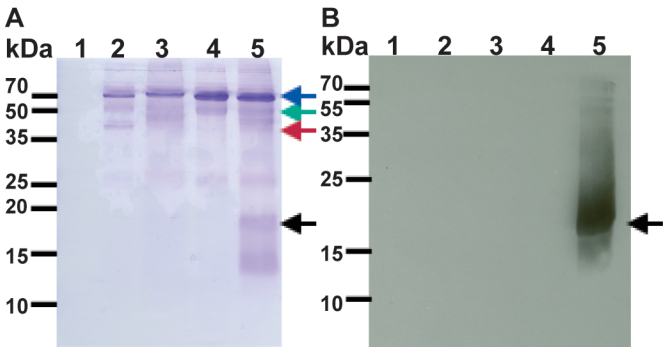

Figure III-10: Co-immunoprecipitation of Vpu with CD4.
A fusion of maltose binding protein (MBP) and the trans-membrane and cytoplasmic domains of CD4 was incubated with Vpu. The complex was captured by anti- MBP antibodies conjugated with beads and pelleted by centrifugation. Vpu was pelleted with MBP-CD4 and the samples were analyzed by SDS-PAGE followed by coomassie staining (A) and immunoblot analysis with antibodies raised against Vpu (B). Panel A depicts the all the proteins pulled down by the agarose beads (Lane 1) and agarose beads conjugated with Anti-MBP (Lanes 2-5). Anti-MBP, MBP-CD4, MBP and Vpu are denoted by blue, green, red and black arrows respectively. In the immunoblot analysis (B), Vpu was not detected in Lane 1 (beads with MBP-CD4), Lane 2 (beads conjugated with anti- MPB with MBP and Vpu), Lane 3 (beads conjugated with anti- MPB with MBP-CD4), Lane 4 (beads conjugated with anti- MPB with Vpu) but, was detected in Lane 5 (beads conjugated with anti-MPB with MBP-CD4 and Vpu).

Conclusions

The requirement of obtaining substantial quantities of pure, folded, functional and monodisperse protein samples has been a major factor that hampers the elucidation of structural models of membrane proteins. Here I demonstrate that I was able to express good quantities of HIV-1 Vpu. The protein was folded, mono disperse and functional. This is in spite of the fact that the signal peptide seems to be uncleaved from the protein. I hypothesize that efficient cleavage of the signal peptide was inhibited by the inability of the periplasmic peptidases to access the cleavage site. Nevertheless, this expression strategy could provide an excellent template towards producing high quality membrane proteins towards structural studies.

IV. Crystallization of Vpu.

Abstract

Viral protein U (Vpu) is an important accessory protein of the Human Immuno-deficiency Virus (HIV) -1 which is primarily involved in viral release from the host cells and viral propagation, using a multi-pronged approach. This protein has some interesting structural attributes that are yet to be elucidated on which, there are strong indications, that the functions of the proteins could be dependent on. Thus, it is an attractive target to structurally characterize using crystallization followed by X-ray diffraction. I had earlier reported the successful expression, purification followed by functional and biophysical characterization of bacterially produced Vpu with the PelB signal peptide. I was able to obtain pure, functional, monodisperse samples of the protein which are excellent precursor conditions to satisfy before setting up crystallization trials. In this chapter, I detail our efforts to crystallize the protein in detergent micelles. I also employ the relatively new, promising technique of crystallizing membrane proteins in a more native environment by integrating them in lipid cubic phases.

Introduction

Integral membrane proteins, for example, channels, transporters, receptors, are critical components of many essential biological processes and make up about 20- 35% of the proteins encoded by an organism's genome. Overexpression of membrane proteins for structural studies is a major challenge. During the synthesis of a membrane protein, the secretory machinery of the cell is engaged, and that protein must be targeted to and inserted into the membrane (de Gier and Luirink, 2001, Johnson and van Waes, 1999, Muller et al. , 2001). High-level expression of a membrane protein often saturates the secretory pathway, leading either to the buildup of toxic intermediates or to inclusion body formation.

Having achieved satisfactory levels of expression, the recombinant membrane protein must be purified, using standard biochemical techniques. This typically requires using detergents to solubilize the membrane protein. The choice of detergent is a critical issue to consider while extracting proteins from the membranes and maintain them in solution thereafter. Ideally, a detergent (or detergent mixture) should solubilize the target protein in an unaggregated state. It is important to assess the effects of detergent on protein stability (Engel et al. , 2002); an appropriate detergent will selectively stabilize the native structure of the protein (Rosenbusch, 2001) and also maintain it in its functional conformation.

It is also important that the structural integrity of the protein be maintained and that nonspecific aggregates be avoided. Dynamic light scattering could be used to test a protein sample for monodispersity to streamline crystallization trials and eliminate less favorable samples (Ferre-D'Amare and Burley, 1994). Dynamic light scattering is frequently used to evaluate the monodispersity of protein samples prior to crystallization trials (Ferré-D'Amaré and Burley, 1997). However, solutions of integral membrane proteins could appear polydisperse by dynamic light scattering, owing to the presence of detergent micelles which could mimic the size of the protein–detergent complex or form heterogeneous protein-detergent complexes. (Hitscherich et al. , 2001).

Finally, the growth of well-ordered 3D crystals, which is a prerequisite for X-ray crystallography, has often been a major challenge, in which case, the presence of detergent complicates matters. Crystallization is driven by the increase of precipitant concentration in a drop of protein solution by vapor diffusion. Although protein–protein interactions are the most important interactions for obtaining a high-quality of crystal, the detergent molecules present in the protein-detergent complex must also be adapted in size. Therefore, searching for crystallization conditions for protein–detergent complexes

is of paramount importance towards exploring a complicated phase diagram upon which protein phase transitions and detergent phase transitions are superimposed and in which each component affects the behavior of the other (Garavito and Ferguson-Miller, 2001).

Crystallizing membrane proteins within a more native lipid bilayer environment was achieved when well-diffracting crystals of bacteriorhodopsin were obtained in the presence of a lipidic cubic phase (Landau and Rosenbusch, 1996). The lipidic cubic mesophases form gel-like materials containing continuous bilayer structures, arranged so as to form topologically distinct lipid and aqueous regions (Larsson, 2000, Rummel et al. , 1998) which, is a membrane mimetic environment that could be suitable for the stabilization and crystallization of membrane proteins. Proteins are first added to preformed lipidic cubic phases, upon which they partition into the bilayer. This is followed by the addition of precipitating agents to induce crystallization (Figure IV-1) (Caffrey, 2000, Nollert et al. , 2002).

Lipid cubic phase crystallization has been remarkably successful for complex transmembrane proteins such as archaeal seven-transmembrane helix proteins, leading

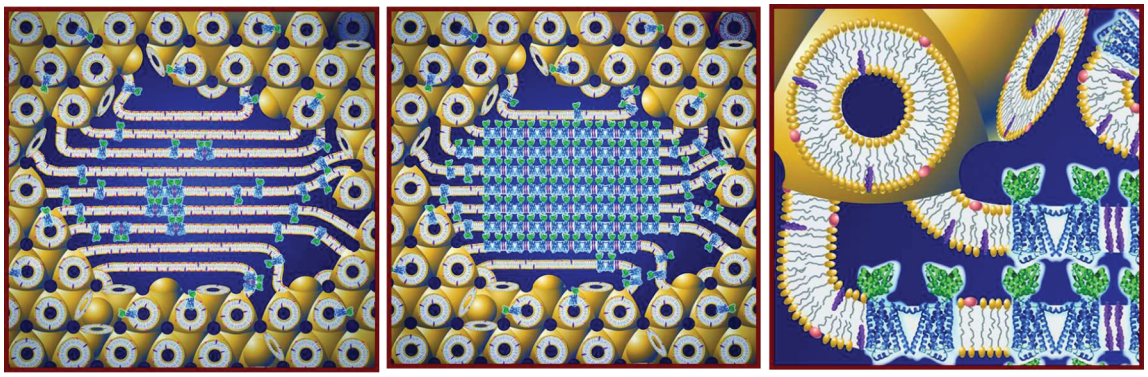

Figure IV-1: Crystallization of IMPs in LCP.
Upon the addition of precipitants to proteins reconstituted in LCP, phase separation occurs and the protein molecules diffuse from the bilayer environment into a sheet like lamellar phase (A). The proteins start concentrating in the lamellar phase and begin to nucleate, leading to crystal growth (B). An expanded view of the bilayer (C) depict the protein in blue and green, and the lipids in yellow with tail. The blue color represents the aqueous channels. Adapted from Caffrey (2015).

to structures for sensory rhodopsin II from *Natronobacterium pharaonis* (Gordeliy et al. , 2002, Luecke et al. , 2001, Royant et al. , 2001) and halorhodopsin and bacteriorhodopsin from *H. salinarum* (Kolbe et al. , 2000, Luecke et al. , 1998, Pebay-Peyroula et al. , 1997). This technique has been highly successful in crystallization and structure determination of human G protein-coupled receptors (GPCRs) (Cherezov et al. , 2007, Chien et al. , 2010, Jaakola et al. , 2008, Shimamura et al. , 2011, Wu et al. , 2010). Most of the lipidic cubic phase crystals have been grown in hydrated monoolein. However, a variety of other lipid species can also be incorporated without causing the disruption of the cubic phase but, on the contrary, leading to an expansion in the range of proteins that can be accommodated with this technique (Cherezov et al. , 2002). Although data are now becoming available detailing which detergents and precipitating agents are compatible with the lipid matrix (Ai and Caffrey, 2000, Cherezov et al. , 2001), the method is under active development.

Translational diffusion of membrane proteins embedded in LCP matrix is essential for crystal nucleation and growth. The structural features of LCP, however, can restrict motions of large proteins or oligomeric protein aggregates, thus preventing their crystallization. Fluorescence recovery after photo-bleaching (FRAP) was used to study the diffusion of integral membrane proteins in LCP (Cherezov et al. , 2008). It was found that the diffusion properties within LCP matrix strongly depend on protein stability and screening conditions. Common precipitants often induce fast non-specific aggregation of membrane proteins, limiting their mobility within LCP, and thereby impeding their chances for crystallization. A good correlation between a high protein mobile fraction and successful crystallization conditions has been observed. Based on these studies, a high throughput pre-screening assay (HT LCP-FRAP) was developed. This assay can be used to select the most promising protein construct, ligand and LCP host lipid, and rule out

conditions that are not conducive to diffusion from subsequent crystallization trials (Xu et al. , 2011). HT LCP-FRAP was instrumental in obtaining initial crystallization conditions for the CXCR4 chemokine and dopamine D3 GPCRs (Chien, Liu, 2010, Wu, Chien, 2010).

As discussed in Chapter III, I was able to obtain sufficient amounts of extremely pure, functional, monodisperse samples of PelB-Vpu in βDDM micelles. The protein detergent complex was stable across various salt concentrations and up to approximately 40 ºC. These presented me with very favorable parameters to set up wide range of experiments towards my efforts to crystallize PelB-Vpu.

Materials and Methods

Setting up sitting- drop crystallization trials.

Expression, purification and characterization of PelB-Vpu was described in Chapter III. A Rigaku CrystalMation high-throughput machine, was used to disperse 0.1 µL and 0.2 µL of PelB-Vpu from a stock of 10 mg/mL of protein into each of the mini-wells of a 2 drop 96 well crystallization plate (Molecular Dimensions, cat# MD11-00U-100). Similarly, 0.1 µL of each of the 96 crystallization conditions were dispersed into the mini-wells such that one of the mini-well had a protein to precipitant ratio of 1:1 (v/v) and the other had a ratio of 2:1 (v/v). 50 µL of the corresponding crystallization conditions were dispersed in the reservoir for each of the 2 drops with the same condition. The plates were sealed tightly and incubated at 20 ºC. The wells were monitored by visualizing them under UV and polarized light microscopes. A variety of commercial crystallization screens were used, such as, Crystal screen HT (Hampton Research, cat# HR2-130), Natrix HT (Hampton Research, cat# HR2-131), Index HT (Hampton Research, cat# HR2-134), MembFac HT (Hampton Research, cat# HR2-137), PEG/Ion HT (Hampton Research, cat# HR2-139), GridScreen Salt HT (Hampton Research, cat# HR2-248), MemGold (Molecular

Dimensions, cat# MD1-39), MemGold2 (Molecular Dimensions, cat# MD1-63), The PEGs (Qiagen, cat# 130704), The Classics (Qiagen, cat# 130701), The MbClass (Qiagen, cat# 130711), The MbClass II (Qiagen, cat# 130712), and MPD (Qiagen, cat# 130706).

Labeling PelB-Vpu for LCP-FRAP.

Cy3-mono NHSester dye (GE Healthcare Life Sciences, cat# PA13101) was prepared as a 5 mg/mL stock in dimethylformamide (DMF, Sigma, cat# D-4254). 10 mg of PelB-Vpu in βDDM micelles, purified by size exclusion chromatography as described in Chapter III, was incubated with 10 μg of Cy3-mono NHSester dye. The labelling reaction was incubated for 3 hr in the dark at 4 ºC and was loaded onto a 1.5 mL bed volume Talon metal affinity resin, which was prequilibrated with a buffer consisting of 20 mM HEPES pH 7.5, 250 mM NaCl, 0.02% βDDM. The column was washed with 20 column volumes of the same buffer to remove unbound and weakly bound dyes and the labelled protein was eluted with buffer supplemented with 300 mM imidazole. The labelled protein was concentrated to 10 mg/mL before setting up LCP-FRAP experiments. The metal affinity purification and concentration of the labelled samples were performed at 4 ºC in dark to preserve the functional integrity of the dye.

Setting up LCP crystallization and LCP FRAP plates.

PelB-Vpu complexed with βDDM micelles and 1-Oleoyl-rac-glycerol (Monoolein) (Sigma, Cat# M7765) were mixed using two Hamilton micro-syringes connected by a coupler. The protein-detergent complex was placed in one syringe and monoolein was placed in the other such that the next mixture contained 60% monoolein and 40% protein by weight. Mixing was achieved by repeatedly moving the contents of the two syringes back and forth through the coupler. For dispensing the homogeneous mesophase onto glass sandwich crystallization plates, the coupler was replaced by a needle and 0.1 μL

was dispensed onto each well by a Gryphon high-throughput LCP screen set up machine by Art Robbins Instrument. Precipitant solutions (1 µL) of various compositions were placed over the mesophase and the wells were finally sealed with a cover glass. The screens were incubated at 20 ºC for one week before monitoring for crystal growth. Commercial screens used for this process include Crystal screen HT (Hampton Research, cat# HR2-130), MembFac HT (Hampton Research, cat# HR2-137), PEG/Ion HT (Hampton Research, cat# HR2-139), MemGold (Molecular Dimensions, cat# MD1-39), MemGold2 (Molecular Dimensions, cat# MD1-63), The PEGs (Qiagen, cat# 130704), The MbClass II (Qiagen, cat# 130712), and MPD (Qiagen, cat# 130706).

Setting up LCP-FRAP Experiment

In order to set up LCP FRAP plates, the labelled protein sample was used at a concentration of 10 mg/mL. The protein was incorporated into LCP and 96 well screening tray was set up with different precipitants as mentioned above. The 96 different conditions were based of StockOptions Salt screen (Hampton Research, cat# HR2-245). The 48 different salts were used at 100 mM and 400 mM concentrations, and combined with a buffer (100 mM TRIS, pH 7), and a precipitant such as polyethylene glycol 400 (30% v/v). The screens were incubated at 20 ºC for 1 day.

LCP-FRAP data collection

LCP-FRAP data acquisition and image analysis were fully automated using the Formulatrix benchtop FRAP machine. Each well was sequentially bleached at an automatically chosen location in the drop by firing laser pulses at a 25 Hz pulse rate. Fluorescence images before and immediately after bleaching were recorded and saved for further analysis. After bleaching all the 96 wells (approximately 30 min incubation time for each well), the plate was scanned to record the end-state fluorescence recovery

images for each sample. Recorded images were processed automatically to locate the bleached spot and to calculate the intensity of the recovered fluorescence. Conditions above 30% recovery were chosen and the pattern of recovery was analyzed individually over 1000 sec.

Dynamic light scattering

Dynamic light-scattering (DLS) measurements were performed using a NaBiTec GmbH setup comprising a SpectroSize 302 (Molecular Dimensions) in combination with an S6D microscope (Leica). PelB-Vpu was purified by size exclusion chromatography and concentrated to 10 mg/mL as described in Chapter II and then was illuminated in a 2 µL hanging drop using a 24-well crystallization plate (VDX Greased Plate, Hampton Research) covered with siliconized-glass circular cover slides (22 mm; Hampton Research). The well itself was filled with 400 µL SEC running buffer. Prior to the measurement, the protein solution was centrifuged at 18000 ×*g*, 30 min, 4 ºC to remove possible dust and other suspended particles. All measurements were done at 20 ºC. Ten consecutive measurements, each with an integration time of 20 s, were averaged. Hydrodynamic size of the particles was estimated with the instrument software using the following parameters: refractive index 1.33, viscosity 1.006, shape factor 1.0 and hydrated shell 0.2 nm.

Results and Discussion

Conventional crystallization trials resulted in amorphous precipitates.

PelB-Vpu in complex with βDDM micelles was previously shown to be pure, mono-disperse and in a functionally active conformation. These are very promising conditions to go into experiments screening for conditions for crystallization of the protein detergent complex. I observed that, in the majority of the wells, the protein immediately precipitated

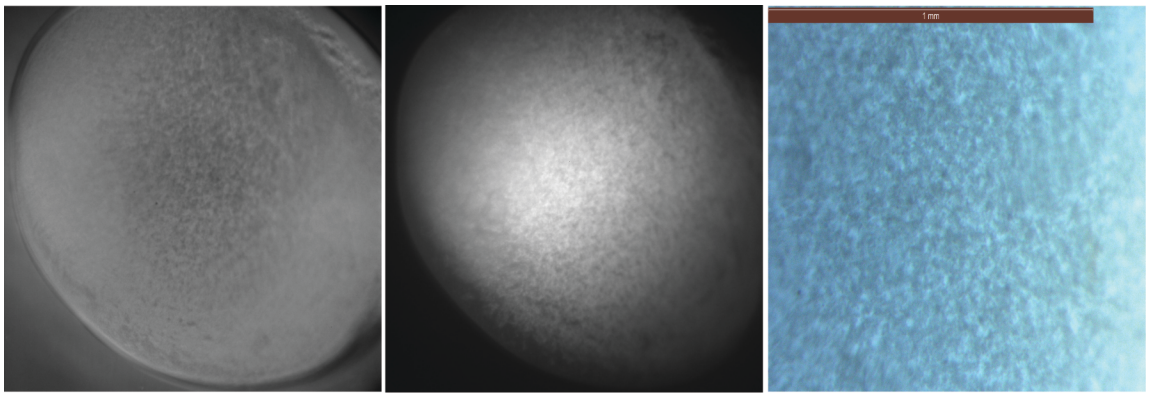

Figure IV-2: Potential nano-crystals in precipitate obtained by sitting drop vapor diffusion crystallization trials.
Purified, mono - dispersed sample of PelB-Vpu, expressed from BL21- pTM875, at a concentration 10 mg/mL and was used in a 2:1 (v/v) ratio with 0.8M ammonium sulfate, 0.1M citric acid at pH 5. The well was imaged by bright field microscope (A), UV microscope (B) and a polarized light microscope (C).

upon the addition of the precipitating conditions. Upon visualization on subsequent days, I could not isolate any promising conditions to fine tune our crystallization attempts and mostly yielded amorphous precipitates. Precipitates usually consists of denatured proteins. But, they could also contain precipitates of nanocrystals (<1 μm) which can be too small to be detected by optical microscopes. Second order nonlinear imaging of chiral crystals (SONICC), a method based on the principle of second harmonic generation, has been used for the efficient detection of protein nanocrystals (Haupert and Simpson, 2011, Wampler et al. , 2008). Recent advancement in detection of protein nanocrystals demonstrates that protein nanocrystals, which are first visualized by SONICC, retain the ability to dissolve after dilution of the reservoir solution while a denatured precipitate does not (Dörner et al. , 2016). But, since SONICC is most efficiently applied to proteins containing chromophoric cofactors, Vpu was invisible to any SONICC signals. Hence I was unable to characterize wells, such as in Figure IV-2, for the presence of protein nanocrystals.

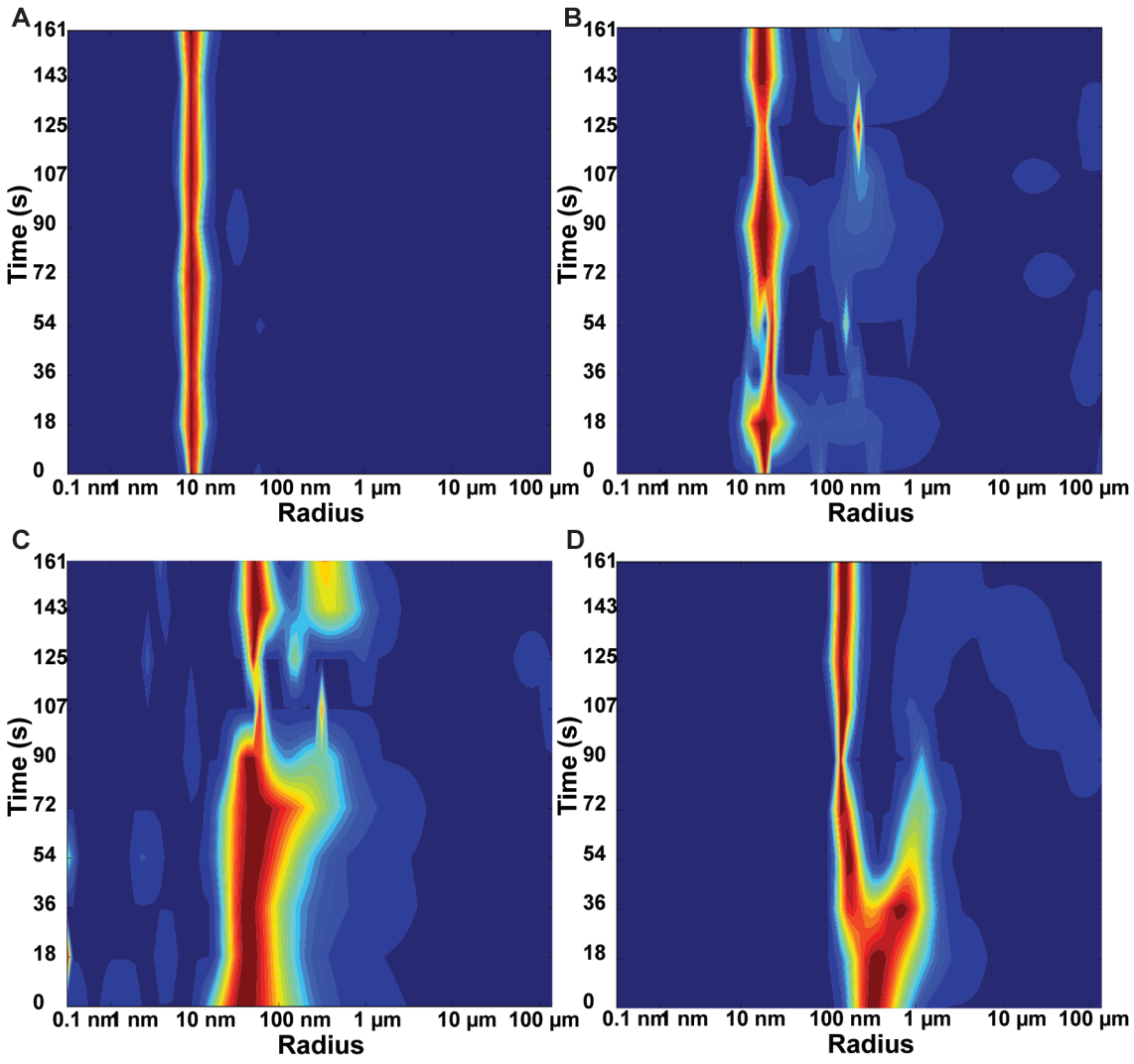

Figure IV-3: Heat map diagram representing DLS of 10 mg/mL PelB-Vpu over time at 20 ºC.
The sample showed as a narrow peak after freshly concentrating the protein, indicating a mono-disperse protein population, day 0 (A). I observe a broadening of the peak around day 2 (B) and then gradual appearance of high molecular weight aggregates around day 4 (C) and day 6 (D).

The precipitants that were used to induce crystallization could have profound effects on detergent phase behavior which could lead to inducing or changing the position of phase separations (Garavito et al. , 1996, Rosenow et al. , 2001). One such consequence of detrimental phase behaviors could be a scenario where the solution separates into detergent rich and detergent poor states at the cloud point boundary.

Integral membrane proteins like Vpu will partition into the detergent-rich phase(Ward et al. , 1987), where a substantial increase in detergent concentration can lead to denaturation of the protein and be deleterious to crystal growth.

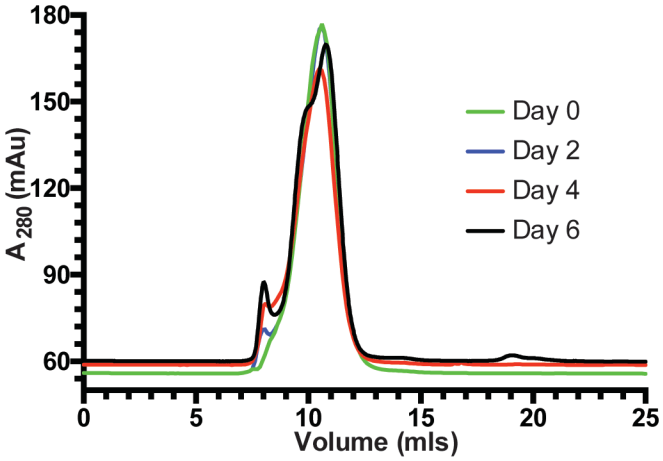

Figure IV-4: FPLC-SEC of concentrated PelB-Vpu over time.
50 µL of a sample of 10 mg/mL PelB-Vpu in βDDM micelles was injected in to a Superdex 200 10/300 GL column after 2, 4 and 6 days of setting up a crystallization trial with freshly purified and concentrated protein. The mobile fraction constists of 20 mM HEPES pH 7.0, 250 mM NaCl, 0.02% βDDM and 5% glycerol. Void volume aggregates are found at 8 mL which is observed to increase in amount over time.

Another factor that could play a big role in the eventual crystallization of the protein is the stability of the protein in the detergent micelles at high concentrations over time. Dynamic light scattering characterization of PelB-Vpu at 10 mg/mL concentration reveals that the protein is relatively unstable over time (Figure IV-3). I observe from the heat-map diagram that the sharp band at 10 nm , indicating a monodisperse PelB-Vpu-βDDM complex when the crystallization trials were set up, progressively disintegrates and there is a shift towards a 100 nm particle over time. Analysis of a sample by size exclusion chromatography also reveals similar trends (Figure IV-4). With increasing time, in units of days, I observe higher amounts of aggregates which elute at the void volume of the column (8 mL). Furthermore, I also observe splitting of the otherwise single peak in case of the 6th day sample. These indicate towards an unstable protein-detergent complex at higher concentrations, and this tendency to aggregate could make the prospect of the protein-detergent complex forming crystals, quite challenging. The DLS and SEC results of each time point, when compared to each other, also reveals

a concentration dependent dynamic shift in the oligomerization status of the protein. The DLS result shows a strong shift towards a 100 nm radius particle over time from a 10 nm radius particle size on day 0. This could indicate that at a constant high concentration, there is a strong tendency towards protein aggregation, forming high molecular weight species over time. But, when the samples are diluted as a result of the mobile phase of SEC, even if I do observe a greater proportion of void volume aggregates over time, most of the protein till day 4 elutes as a single major peak, same as the fresh sample. From these results, I could hypothesize that most of the aggregation of the protein at high concentrations is reversible upon dilution. Probability of crystallization could thus be increased by finding conditions which increase the stability of PelB-Vpu at high concentrations.

Diffusion in LCP

With indications that PelB-Vpu may be unstable at higher concentrations in βDDM micelles, I decided to explore the possibility of crystallizing the protein in a more native environment. Lipid cubic phase (LCP) is a membrane-mimetic matrix which stabilizes integral membrane protein and has proved to be a robust approach for crystallizing membrane proteins for structure determination. But, for crystal nucleation and growth in the LCP matrix, the membrane proteins are required to translationally diffuse within the matrix. Thus, large proteins or multi-order oligomeric proteins, with their restrictive rates of diffusion would find it very difficult to crystallize. Indeed, there exists correlation between the degree of mobility of protein in the LCP and success of crystal formation for a given condition. Thus, I used fluorescence recovery after photo-bleaching (FRAP) to investigate the manner of diffusion of PelB-Vpu in the LCP under the effects of various crystallization conditions. The results obtained depicts that only two conditions (G2 and H4) showed moderate levels of diffusion (Figure IV-5). Highly mobile proteins have a value close to 1.

There were three other conditions which facilitated lower rates of diffusion (F3, G6 and H1). A curve depicting the fraction of fluorescence recovered over time is an excellent way of avoiding false positives (Figure IV-6). An exponential curve is indicative of protein diffusion in the LCP. Hence I was optimistic about the prospects of a few conditions, which showed decent levels of protein mobility in the LCP, as determined by LCP-FRAP, towards being amiable to crystallization.

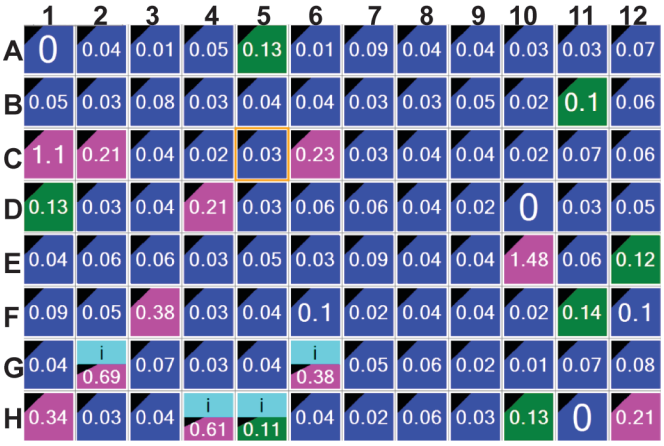

Figure IV-5: Fraction of fluorescence recovered after photo-bleaching for the 96 conditions.
Highly mobile species would have a value close to 1. The conditions marked “i" were further probed for the nature of fluorescence recovery over time to eliminate false positives.

LCP crystallization screen yielded no promising conditions.

Crystallization of proteins by the lipid cubic phase technique has resulted in structural models of a wide variety of proteins such as microbial rhodopsins, GPCRs, photosynthetic proteins, small peptides, heme-copper oxidases and bacterial outer membrane proteins (Cherezov, 2011). In spite of extensive screening, I was unable to identify any condition that showed any degree of promise towards obtaining well-diffracting crystals. Unlike the more traditional methods of crystallization of proteins, where membrane proteins typically nucleate by virtue of their soluble domains (type II crystal packing), lipid cubic phase crystallization facilitates the interaction of both the soluble and the hydrophobic transmembrane domains of a membrane protein (type I crystal packing) (Caffrey, 2000, Caffrey, 2009, Cherezov, Rosenbaum, 2007, Tiefenbrunn et al. , 2011). Hence, the fact that Vpu lacks a prominent soluble N-terminal domain was seen as a less

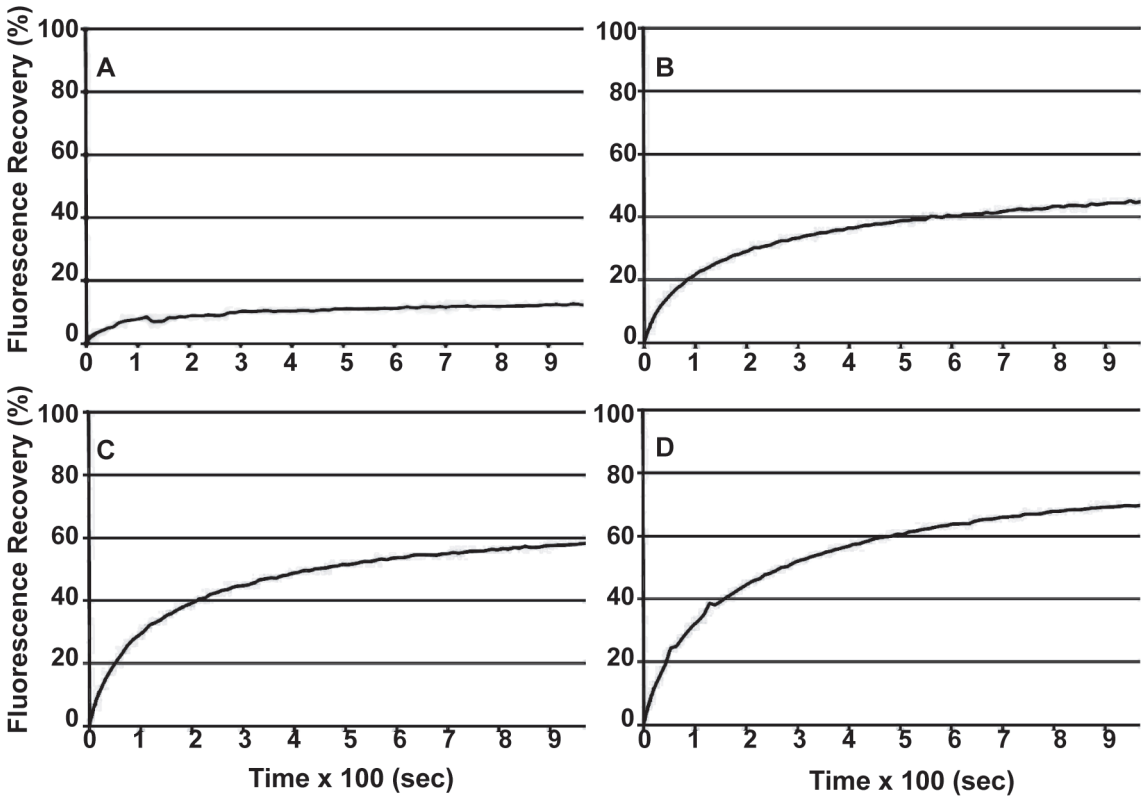

Figure IV-6: Fluorecense recovery data for PelB-Vpu in LCP under different conditions. Condition H5 was used as a negative control (A). In condition G6 (100 mM TRIS, pH 7.0; 400 mM potassium phosphate dibasic, 30% PEG400 (v/v)) PelB-Vpu in LCP demonstrates moderate levels of diffusion (B). Conditions H4 (100 mM TRIS, pH 7.0; 400 mM sodium phosphate dibasic, 30% PEG400 (v/v)) and G2 (100 mM TRIS, pH 7.0; 400 mM potassium citrate tribasic, 30% PEG400 (v/v)) show higher levels of diffusion of PelB-Vpu in LCP, (C) and (D) respectively.

of a hindrance when crystallizing the proteins in LCP. But, I speculate that the presence of the hydrophobic PelB signal peptide with Vpu could play a role in non- homogeneous insertion of PelB-Vpu in lipid bilayers. This not only could have resulted in lower percentage of conditions being successful with LCP FRAP, but also could be a very detrimental factor towards nucleation and crystal growth of the conditions that showed appreciable amounts of mobility. A known disadvantage of LCP matrices is the curved nature of the lipid membranes. The resulting microstructures could limit the ability of larger membrane proteins to diffuse freely and thus hamper the chances of crystallization (Cherezov et al. , 2006). Although this problem has been circumvented by the addition of

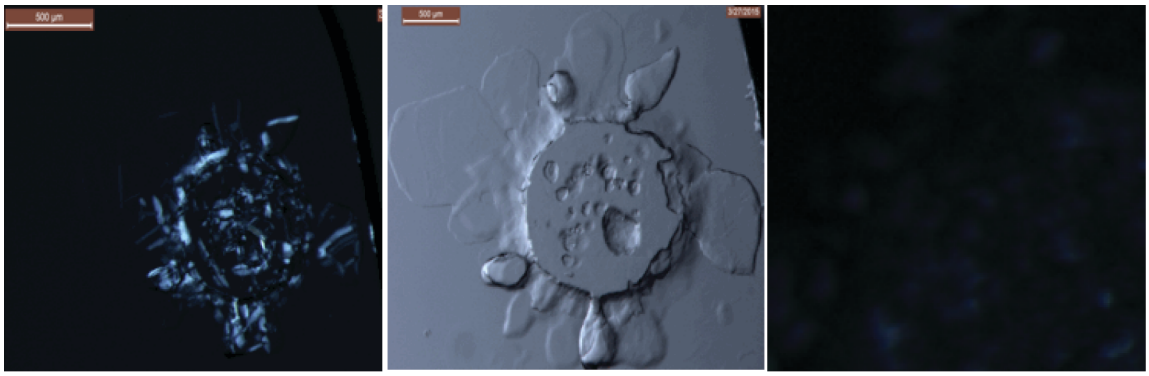

Figure IV-7: Image of a well from the LCP crystallization trials.
Purified, mono - dispersed sample of Vpu at a concentration of 10 mg/mL and was mixed in a ratio of 2:3 with 1 – Oleoyl – rac – glycerol to integrate PelB-Vpu into lipid cubic phases. Then, crystallization trials were set up with various crystallization conditions. The well shown used 0.1M bicine, pH 8.9, 31% w/v PEG 2000 and imaged by a polarized light microscope (A), bright field microscope (B) and UV microscope (C). Although the polarized light image showed some potential of crystal formation, the contents of the well were UV invisible.

non-volatile alcohols, low molecular weight PEGs and polymers that lead to the swelling of the LCP (Cherezov, Clogston, 2006, Wadsten et al. , 2006), the uncertainty that shrouds the manner of interaction between PelB-Vpu and the lipid complicates the scenario.

Conclusions

Although there have been significant advances in membrane protein crystallization, the crystallization of PelB-Vpu has proven to be incredibly challenging. The lack of any promising conditions that could lead to formation of crystals, in spite of extensive screening, prompts us to revisit our strategy of protein expression, especially the presence of the hydrophobic PelB signal peptide. It would be interesting to structurally characterize PelB-Vpu in solution using techniques such as nuclear magnetic resonance (NMR) spectroscopy that could elucidate key details on the effect that the hydrophobic signal peptide could have on the protein in general. This would also guide us onto learning about the prospects of this expression strategy and/or help us design effective strategies for crystallization of Vpu.

V. Characterization of Vpu using Nuclear Magnetic Resonance (NMR) Spectroscopy

Abstract

Vpu is an HIV-1 protein that is essential for virus propagation *in vivo* where it performs important functions that promote virion assembly and egress. It belongs to the viroporin protein family encompassing small homo-oligomeric ion channel proteins with members in many of the most successful human viruses (influenza, coronaviruses). In addition to its ion-transport function, Vpu exhibits affinity to various cellular proteins, including HIV-1's receptor (CD4) and a major host restriction factor (tetherin). With its multiplicity of functions, Vpu represents a promising, underexplored target for drug development. Nuclear magnetic resonance (NMR) spectroscopy is a perfect technology to study Vpu's structure and function. Our extensive crystallization experiments of protein-detergent micelles of PelB-Vpu have not been successful, whereas, NMR studies by other groups have revealed a great deal of structural information. Moreover, most of the ascribed functions of Vpu involve protein-protein interactions – either with itself in forming oligomers, or with the cellular targets mentioned above. These interactions involve both the transmembrane and cytoplasmic tail domains of the proteins that are suspected to exhibit conformational flexibility. In this study, I present the results of an evaluation of the conformational integrity of PelB-Vpu in different membrane mimetic environments.

Introduction

HIV-1 and its closest simian relative SIV_{cpz} express a small hydrophobic protein called viral protein U (Vpu) (Cohen et al. , 1988, Strebel et al. , 1988), which is not found in most of the other known primate lentiviruses (e.g. HIV-2 and most SIVs) (Strebel, 2014, Yang et al. , 2010). Vpu is vital for efficient virus propagation *in vivo* and is considered a major factor in the rapid evolution of HIV-1 from a relatively ineffective zoonotic pathogen

to the successful pandemic-causing agent that we know today (Andrew and Strebel, 2010, McCarthy and Johnson, 2014, Sauter et al. , 2009, Yang, Lopez, 2010). It is a 16-kDa type III trans-membrane protein of 77-86 amino acids in length depending on the HIV-1 subtype. Vpu has a very short N-terminal extracellular domain; a trans-membrane domain (TMD) and a longer cytoplasmic domain (CTD) which has two predicted α-helical regions separated by a hinge. The hinge region contains two phosphorylation sites (Schubert et al. , 1992) and is partially responsible for the flexibility of the CTD (Wittlich et al. , 2009).

Vpu plays a number of roles in promoting virion assembly and release (Dube et al. , 2010, Roy et al. , 2014, Strebel, 2014). Vpu functions through protein-protein interactions to down-regulate key host-cell proteins (Andrew and Strebel, 2010). More specifically, Vpu interacts with the CD4 surface receptor through their respective TMDs, causing the retention of the receptor in the ER (Magadan and Bonifacino, 2012, Magadan et al. , 2010). Subsequently, the CTD recruits ubiquitination factors that mark CD4 for proteosomal degradation(Magadan and Bonifacino, 2012, Magadan, Perez-Victoria, 2010). Similar mechanisms were invoked for the roles that the Vpu TMD and CTD play in the downregulation of tetherin, an integral membrane protein that functions to limit the escape of newly formed virions from cells infected by HIV-1 and other enveloped viruses (e.g. Ebola) (Douglas et al. , 2010, Evans et al. , 2010, Kluge et al. , 2013, Kueck and Neil, 2012). In addition, the CTD of Vpu directly functions to displace tetherin away from the sites of viral assembly in the host cell membrane (McNatt et al. , 2013).

The importance of Vpu for efficient assembly and egress of HIV-1 (Giese and Marsh, 2014, Jafari et al. , 2014, Pickering et al. , 2014) makes it a promising, but so far underexplored, therapeutic target. Developing its therapeutic utility requires establishing reliable structural information. The Vpu CTD and TMD have been studied by solution and solid state nuclear magnetic resonance spectroscopy (NMR) resulting in independent

structures of the CTD or TMD (Sharpe et al. , 2006, Wittlich, Koenig, 2009) which have been combined in a molecular model (Lemaitre et al. , 2006). A full-length NMR structure of the protein was recently elucidated (Zhang et al. , 2015). Interestingly, the relative mobility of the cytoplasmic helices was dependent on the membrane mimetic environments used. In 1,2-dimyristoyl-*sn*-glycero-3-phosphocholine (DMPC) proteoliposomes, the helices were flexible and could be either arranged in a linear or in a U -shaped orientation as against in 1,2-Dihexanoyl-sn-Glycero-3-Phosphocholine (DHPC) micelles, where the backbone dynamics were more restricted and the cytoplasmic helices adopted well-defined U-shaped loop region between them.

It was also notable in the full-length structure that the transmembrane domain influences the conformation, structure and dynamics of the C-terminal domain and *vice versa*. Hence our goal was to characterize the PelB-Vpu protein, described in Chapter III, by NMR spectroscopy for its structural attributes. Additionally, while the individual domains and the full length Vpu were studied in form of monomers, I have strong evidence that the full length Vpu forms oligomers. Vpu belongs to a diverse group of small transmembrane viral proteins called viroporins that form homo-oligomeric ion channels. While Vpu's channel activity has been well demonstrated (Ewart et al. , 1996, Herrero et al. , 2013), its physiological role is less clear (Strebel, 2014). NMR experiments could also explain why conventional crystallization attempts have failed so far in case of PelB-Vpu and indicate towards more promising crystallization strategies.

Materials and Methods

Expression of PelB-Vpu and MBP-Vpu in M9 minimal media.

An *E. coli* vector (pTM875) directing the expression of PelB-Vpu was described in Chapter III. 1 mL of LB media supplemented with 1 µg/mL kanamycin (Phytotechnology lab; cat# K378) was inoculated with a colony of BL21- pTM875 or BL21- pTM975

(described in Chapter II) and was grown for about 8 hr at 37 ºC at 170 rpm agitation. M9 minimal media was prepared with 45 mM Na_2HPO_4, 22 mM KH_2PO_4, 8.5 mM NaCl and 20 mM NH_4Cl (Sambrook and Russell, 2001). The media was autoclaved and supplemented with 1x MEM vitamin mix (Sigma; cat# M6895), 2 mM $MgCl_2$, 0.1 mM $CaCl_2$ and 0.4% glucose. Supplements were sterilized using a 0.45 µm filter. M9 minimal media (100 mL) was inoculated with the LB-kanamycin- overnight-grown culture (5 µL or a ratio of 1:20,000) and was incubated overnight at 37 ºC at 170 rpm. This overnight culture was used to inoculate a 1 L culture, which constituted of 20 mM $^{15}NH_4Cl$ (Cambridge Isotope Laboratories, Inc; cat# NLM-467) instead of NH_4Cl, at a ratio of 1:100 that was grown at 37 ºC at 170 rpm until culture density reaches $OD_{600} \approx 0.4$. The culture was then moved to 15 ºC and bacteria were allowed to grow until density reached $OD_{600} \approx 0.5$. At this point, recombinant Vpu expression was induced by addition of IPTG (Roche; cat# 11411446001) to a final concentration of 0.2 mM. in case of BL21- pTM875 and 0.4 mM IPTG in case of BL21 cells harboring pTM975, an *E. coli* expression vector directing the expression of $MBP_{\text{-PPCS-}}$Vpu as described in Chapter III, and incubated at 15 ºC for 14 hr with 170 rpm agitation. The cells were harvested by centrifugation at 7000 *xg* at 4 ºC for 20 min and stored at -20 ºC until further use.

Membrane isolation

Bacterial cells were harvested by centrifugation cultures (4 L of culture yielded approximately 12 g of pelleted cells) and then re-suspended in 100 mL of ice-cold phosphate buffer saline (PBS; 137 mM NaCl, 2.7 mM KCl, 10 mM Na_2HPO_4, 1.8 mM KH_2PO_4, pH 7.4) supplemented with EDTA-Free SIGMA*FAST*™ Protease Inhibitor Cocktail tablets (Sigma; cat# S8830), to prevent protein degradation. The cells were lysed by double passage through a microfluidizer (Microfluidics Microfluidizer). The lysate was collected and centrifuged at 36,000 ×*g* for 30 min at 4 ºC. The insoluble fraction was

washed once by repeated re-suspension (50 mL of ice-cold PBS with protease inhibitor cocktail) and centrifugation. The pellet was frozen at -80 ºC until further use.

Detergent extraction

For large-scale extractions from 4L cultures, the pellet, containing the membrane fraction, was fully re-suspended in 100 mL PBS supplemented with EDTA-Free SIGMA*FAST*™ Protease Inhibitor Cocktail tablets. N-Dodecyl-N,N- dimethylglycine (Empigen BB, Sigma; cat# 30326) was used for solubilization at a final concentration of 3% (w/v). The protein was extracted and at 4℃ overnight with agitation at 200 rpm. The detergent soluble fraction was obtained by collecting the supernatant after centrifugation at 36,000 ×*g* for 30 min at 4 ºC.

Purification

A gravity driven column (Biorad Econo-column) containing TALON® Superflow metal affinity resin (15 mL bed volume, Clontech Laboratories Ltd; Cat# 635507) was equilibrated with binding buffer (20 mM HEPES pH 7.5, 500 mM NaCl, 1.5% Empigen, 5 mM imidazole). The sample was then loaded onto the column, flow-through was collected and reloaded onto the same column to collect the final flow-through. The column was sequentially washed with ten bed volumes each of wash buffers containing various combinations of salt and imidazole, for example, for expression from pTM875, 20 mM HEPES pH 7.5 with 500 mM NaCl (Wash I), 500 mM NaCl, 1.5% Empigen (Wash II), 250 mM NaCl, 1.5% Empigen (Wash III), 250 mM NaCl, 1.5% Empigen, 5 mM imidazole (Wash IV) and 250 mM NaCl, 1.5% Empigen, 5% glycerol, 10 mM imidazole (Wash V) to remove weakly bound proteins. Tightly bound proteins were eluted by application of 3 bed volumes of elution buffer (20mM HEPES pH 7.5, 250 mM NaCl, 1.5% Empigen, 5% glycerol, 300 mM imidazole). When purifying the protein produced using pTM975, wash buffers IV and V were replaced with wash buffers VI and VII, respectively. They contained

20 mM HEPES pH 7.5, 250 mM NaCl, 1.5% Empigen supplemented with 10 mM imidazole (Wash VI) and with 15 mM imidazole and 5% glycerol (Wash VII).

The eluted sample was concentrated by 30 kDa molecular weight cutoff (MWCO) concentrators (Millipore; cat# UFC903024) to approximately 10 times its original volume. Concentrated samples were further purified by size exclusion chromatography (GE Life sciences, Superdex 200 10/300 GL; column volume: 24 mL; fluid phase: 8 mL) using a fast pressure liquid chromatography instrument (FPLC, Pharmacia, Äkta Explorer). The running buffer contained 20 mM HEPES pH 7.5, 250 mM NaCl, 1.5% Empigen, and 5% glycerol. For preparatory separations, a 1 mL sample of concentrated Vpu was loaded onto the SEC column and chromatography was performed at a flow rate of 0.5 mL/min. The protein elution was detected by absorption at 280 nm. The concentration of protein in the desired peak was determined spectrophotometrically (A_{280}) based on the primary sequence of Vpu; Σ_{280} was calculated with ProtParam web application (http://web.expasy.org/protparam/).

Detergent exchange

A gravity driven column (Biorad Econo-column) containing 1 mL bed volume of TALON® Superflow metal affinity resin (Clontech laboratories Ltd; Cat# 635507) was equilibrated with binding buffer (20 mM HEPES pH 7.5, 250 mM NaCl, 1.5% Empigen). Purified PelB-Vpu- Empigen complex was then loaded onto the column, flow-through was collected and reloaded onto the same column to collect the final flow-through. The column was washed with twenty bed volumes of a wash buffer containing 20 mM HEPES, pH 7.5, 250 mM NaCl, 5% glycerol and the detergent of choice for NMR spectroscopy, for example, LysoFosCholine 16 or 1-Palmitoyl-2-Hydroxy-sn-Glycero-3-Phosphocholine (LPPC) (Anatrace, cat# L216), LysoFos Glycerol 16 or 1-Palmitol-2-Hydroxy-sn-Glycero-3-Phospho-(1'-rac-Glycerol)-Sodium Salt (LPPG) (Anatrace, cat# L316), 1,2-Dihexanoyl-

sn-Glycero-3-Phosphocholine (DHPC) (Anatrace, cat# D606) and LysoFos Glycerol 14 or 1-Myristoyl-2-Hydroxy-sn-Glycero-3-Phospho-(1'-rac-Glycerol) -Sodium Salt) (LMPG) (Anatrace, cat# L314). The critical micelle concentration (CMC) of each of the detergents and the concentrations used to solubilize Vpu are shown in Table V-1. The wash buffer was applied one bed volume at a time to obtain most effective detergent exchange without consuming excess detergents. Protein was eluted with 2 bed volumes of the same wash buffer, supplemented with 300 mM imidazole.

Table V-1: Ionic properties and CMCs of detergents used in the study.

Detergents	Charge	CMC (mM)	Concentration Used (mM)	References
Empigen BB	Zwitterionic	1.8	5	(Beckett and Woodward, 1963)
LysoFosCholine 16 (LPPC)	Zwitterionic	0.004 - 0.008	0.03	(Kumar and Baumann, 1991, le Maire et al. , 2000, Stafford et al. , 1989)
LysoFos Glycerol 16 (LPPG)	Anionic	0.02-0.6	1.2	(Chou et al. , 2004, Stafford, Fanni, 1989)
1,2-Dihexanoyl-sn-Glycero-3-Phosphocholine (DHPC)	Zwitterionic	15	30	(Chou, Baber, 2004, Lin et al. , 1986)
LysoFos Glycerol 14 (LMPG)	Anionic	0.2-3	5	(Stafford, Fanni, 1989)
n-Dodecylphosphocholine (DPC)	Zwitterionic	1.5	3	(Lauterwein et al. , 1979, le Maire, Champeil, 2000)

To purify and exchange PelB-Vpu into n-Dodecylphosphocholine (DPC, Anatrace, cat# F308S) micelles, a gravity driven column containing 15 mL bed volume of TALON® Superflow metal affinity resin was equilibrated with binding buffer (20 mM HEPES pH 7.5, 500 mM NaCl, 1.5% Empigen, 5 mM imidazole). The Empigen-extracted protein sample from the non-aqueous fraction of BL21-pTM875 was then loaded onto the column, flow-through was collected and reloaded onto the same column to collect the final flow-through. The column was sequentially washed with ten bed volumes each of wash buffers containing various combinations of salt, DPC and imidazole concentrations, for example, 20 mM HEPES, pH 7.5 with 500 mM NaCl (Wash I), 500 mM NaCl, 0.2% DPC (Wash II), 250 mM NaCl, 0.1% DPC (Wash III), and 250 mM NaCl, 0.1% DPC, 10 mM imidazole (Wash IV) to remove weakly bound proteins. Tightly bound proteins were eluted by application of 3 bed volumes of elution buffer (20mM HEPES pH 7.5, 250 mM NaCl, 0.1% DPC, 5% glycerol, 300 mM imidazole).

Solution NMR experiments.

Solution NMR experiments were performed on a Bruker Avance III HD 850 MHz spectrometer, equipped with 5 mm TCI cryoprobes. Transverse relaxation optimized spectroscopy – heteronuclear single quantum coherence (^{15}N-TROSY-HSQC) experiments were performed at 40 ºC except for PelB-Vpu in LPPG micelles which were performed at 45 ºC. I used 416 transients to obtain a desired signal to noise ratio for ^{15}N-TROSY-HSQC experiments for PelB-Vpu in DHPC, LPPG and DPC micelles and 160 transients for similar experiments on PelB-Vpu in LMPG micelles. All protein – detergent complexes were held in a solution of 20 mM sodium phosphate, pH 6.5 with 0.5 mM EDTA. The data acquisition size (TD) used for all the experiments was 128 and 2048 along the ^{15}N and ^{1}H dimensions respectively. The raw NMR data was processed using NMRPipe

(Delaglio et al. , 1995) and analyzed using the CcpNmr software suite (Vranken et al. , 2005).

Cyanogen bromide digestion of PelB-Vpu.

To digest PelB-Vpu with cyanogen bromide (Gross and Witkop, 1961) a protocol was adopted which was amenable to digestion in buffer containing 20 mM HEPES pH 7.5, 250 mM NaCl, 1.5% Empigen, and 5% glycerol (Andreev et al. , 2010). Briefly, the buffer containing the purified protein was acidified by adding HCl up to a final concentration of 0.5 M. 1 mM PelB-Vpu was digested with 100 mM cyanogen bromide for 16 hr at room temperature, in dark. Cyanogen bromide was removed post-reaction by washing with fresh buffer over a 3 kDa molecular weight cutoff (MWCO) concentrators (Millipore; cat# UFC900324).

SDS-PAGE gel electrophoresis, staining and immunoblot analysis were done as described in Chapters II and III.

Results and Discussion

Expression of Vpu in bacteria grown on minimal medium

Biomolecular NMR studies require the use of isotopically labeled samples obtained from cells grown in minimal (M9) medium to ensure isotopical uniformity. I initially substituted LB medium with unlabeled M9 medium using our optimized culture protocols to reduce costs. The switch resulted in longer generation times of the bacteria. Since glucose was used as the only source of carbon in the media, I anticipated a repressive effect on the lac operon system on our expression vectors. To counter this, I used IPTG at higher concentrations than what I previously used to express the protein from the same expression vector in rich media. Hence 0.2 mM IPTG was used to induce expression of recombinant PelB-Vpu in bacterial cells, which were grown to mid- logarithmic phase. I used the same line of thought to induce bacterial cells harboring pTM975 with 0.4 mM

IPTG. Due to the metabolic challenges presented to the bacterial cells by growing them in minimal medium, I also anticipated a reduced rate and yield of recombinant protein synthesis. This led us to prolonging the time of incubation post- induction with IPTG for both the bacterial cultures. Following lysis of the cells by a microfluidizer, cellular components were fractionated into aqueous and non-aqueous fractions and the proteins were resolved by SDS-PAGE. Immunoblot analysis of such fractions of BL21- pTM975 revealed that most of desired protein separated in the non-aqueous fraction, which was extractable by detergents (Figure V-1).

Detergent extraction of Vpu

As described in Chapter III, I have identified βDDM as a suitable membrane mimic for PelB-Vpu. However, βDDM forms large micelles (Jumpertz et al. , 2011, Prive, 2007, Strop and Brunger, 2005, VanAken et al. , 1986), decreasing experimental resolution and sensitivity and is therefore not compatible with NMR studies (Columbus et al. , 2009). For the purposes of protein extraction from bacterial non-aqueous fraction, I made use of a relatively cost-effective, zwitterionic detergent called Empigen BB. It is a useful detergent that has been previously used in the solubilization of membrane proteins and biochemical analysis of keratins (Lowthert et al. , 1995). It has been shown to be very effective in membrane protein extraction, solubilizing larger amounts of proteins (Lowthert, Ku, 1995, Lukacova et al. , 1994, Vancraenenbroeck et al. , 2012). Even though it is a relatively harsher detergent than non-ionic detergents like βDDM, it has been shown to maintain proteins in their native conformations, as confirmed by antibody reactivity and other protein binding assays. (Guo et al. , 2013, Wahl, 2002). Interestingly, viral antigens prepared with Empigen have been shown to illicit a greater antibody response than non-ionic detergents (Jennings and Erturk, 1990). The remarkable effectiveness of Empigen in the extraction of membrane proteins, even at concentrations twice its critical micelle concentration

(CMC) of 1.8 mM (Beckett and Woodward, 1963), could be because of the pattern of charge distribution in the zwitterionic molecule which, resembles membrane phospholipids such as phosphatidylcholine and thereby functions as an effective membrane mimic (Allen and Humphries, 1975). The membrane penetrative ability of Empigen could also be attributed to its small molecular size. Furthermore, given its relatively higher CMC, I would also expect to face minimal challenges in exchanging Empigen for other less harsh and/or compatible detergents for down-stream applications. Thus, based on its known performance and suitability, Empigen was the detergent of choice for extracting bacterial membrane proteins for our purposes.

Purification of MBP$_{-PPCS-}$Vpu

The combination of a poly-histidine tag and Maltose binding protein (MBP) presents us with a great deal of flexibility and options regarding purification strategies of recombinant proteins (Nallamsetty and Waugh, 2007, Pryor and Leiting, 1997, Waugh, 2005). As a first step towards the removal of cellular proteins and enrichment in the amount of MBP-Vpu, Empigen extracted non-aqueous fraction of BL21 cells harboring pTM975 was subjected to metal affinity purification (Figure V-1). The purification resulted in minimal loss of the MBP$_{-PPCS-}$Vpu fusion in the flow-through and the wash steps. This could be due to the enhanced affinity of the N-terminal histidine tag on the MBP$_{-PPCS-}$Vpu fusion with the cobalt ions due to a longer chain (10) of histidine residues. The challenging aspect of the recombinant protein expression through this strategy was that the yield of protein was significantly less than the yield from BL21- pTM875. I could speculate that the reason behind this could be the higher metabolic load imposed on the bacterial cells towards over-expressing a bulky fusion tag, especially in minimal media. Furthermore, the fusion was unstable upon storage at a range of cold temperatures and resulted in an array of degradation products. Since resolving such bands seemed challenging over a size

exclusion column, I proceed to perform a second round of purification exploiting the ability of Maltose binding protein to bind with amylose (di Guana et al. , 1988, Maina et al. , 1988, Riggs, 2001). I observed that there was no significant affinity between the MBP part of the fusion and amylose (Figure V-2) and most of the proteins were found in the flow-through. Although this purification strategy has been relatively successful, there have been previous instances on the challenges encountered in this process by the lack of substantial binding between MBP and amylose (Lo-Man et al. , 1993, Rhyum et al. , 1994). The binding of the MBP to amylose is strictly dependent on the correct biological activity and thus, proper folding of the MBP. Structural disturbances of the fusion partner, Vpu, in the present case, can also compromise the biologically active

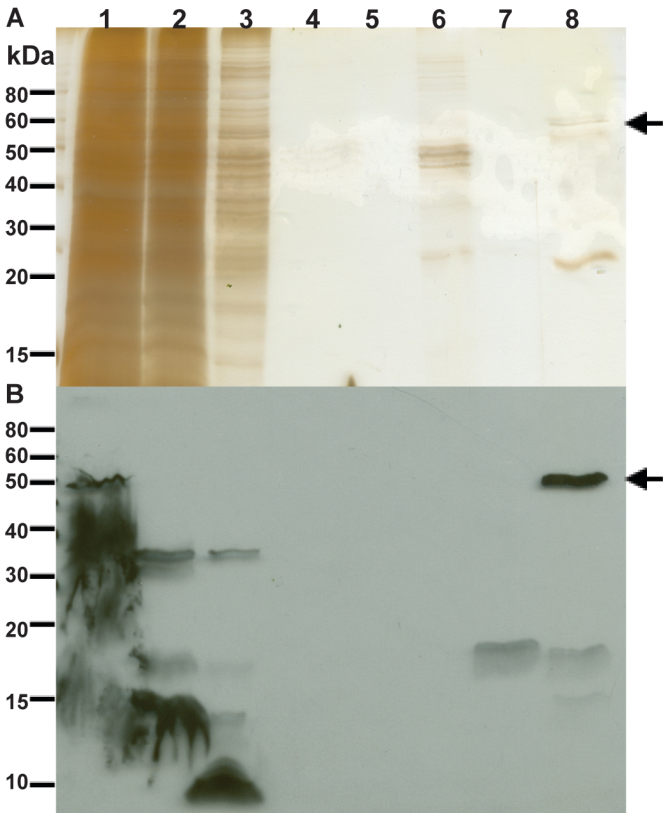

Figure V-1: Talon metal affinity chromatography purification of $MBP_{-PPCS-}Vpu$.
BL21 cells harboring pTM 975 were lysed after overnight expression and separated into aqueous and non-aqueous fractions, which, was treated with Empigen. Protein fractions were subjected to SDS-PAGE followed by silver staining (A) and immuno-blot analysis. (B). Detergent (Empigen)-soluble fraction containing $MBP_{-PPCS-}Vpu$ (Lane 1) was loaded onto a column containing Talon resin that was pre-equilibrated with 20 mM HEPES, pH 7.5, supplemented with 500 mM NaCl, 5 mM imidazole, and 1.5%% Empigen. Unbound proteins in the flow through were collected (Lane 2) and the column was washed consecutively with five different buffer solutions (20 mM HEPES, pH 7.5): W1 (Lane 3, buffer plus 500 mM NaCl), W2 (Lane 4, buffer plus 500 mM NaCl and 1.5% Empigen), W3 (Lane 5, buffer plus 250 mM NaCl and 1.5% Empigen), W4 (Lane 6, buffer plus 250 mM NaCl, 1.5% Empigen and 10 mM imidazole) and W5 (Lane 7, buffer plus 250 mM NaCl, 1.5% Empigen and 15 mM imidazole). Most of the protein $MBP_{-PPCS-}Vpu$ (Lane 8, indicated by arrows) was eluted with W5 buffer supplemented with 300 mM imidazole.

folding of MBP with respect to its amylose binding affinity (Park et al. , 1998). Comparing the amylose purification of MBP$_{-PPCS-}$Vpu complex in βDDM micelles (Figure II-17 in which, I did observe a small fraction of the fusion eluting by the addition of 10 mM maltose, I can also envision the effects of detergents in this process. MBP$_{-PPCS-}$Vpu in complex with a zwitterionic detergent, Empigen, appears to be in a biologically inactive form than some of the same protein in complex with a relatively mild, non-ionic detergent, βDDM. Since the binding affinities between MBP and amylose isn't significantly affected by ionic strength of the buffer, the inability of MBP$_{-PPCS-}$Vpu in Empigen micelles to bind to amylose can be attributed to the effect of the detergent on the structure/function relationship of the fusion protein rather than the possible unfavorable ionic interaction dynamics between amylose and the zwitterionic detergent. Owing to these challenges in purification and stability, I did not further pursue this strategy of obtaining Vpu for NMR characterization.

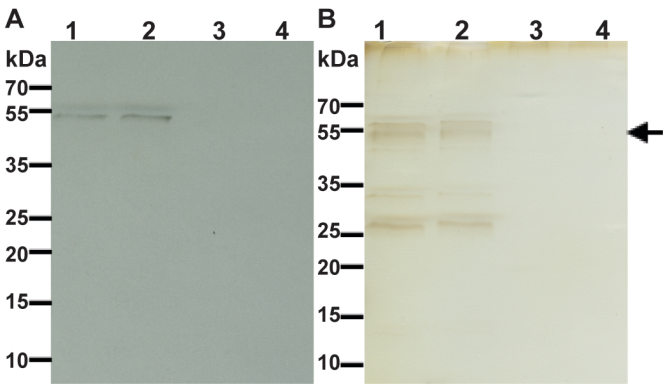

Figure V-2: Amylose resin purification of the MBP$_{-PPCS-}$Vpu complex.
Protein fractions were subjected to SDS-PAGE followed by immuno-blot analysis, probed with anti-Vpu (**A**) and silver staining (**B**). Eluate from Figure V-1 was loaded onto an amylose resin pre-equilibrated with 20 mM HEPES, pH 7.5, supplemented with 250 mM NaCl, 1.5% Empigen and 1 mM EDTA. Most of the protein remained unbound to the column, and was collected as flow-through (Lane 2). There was no visible trace of the protein when the column was washed with 10 CV of the equilibration buffer (Lane 3) and when the column was subjected to 3 CV of the equilibration buffer supplemented with 10 mM maltose (Lane 4).

Purification of PelB- Vpu

Towards our effort to isolate His-tagged Vpu, expressed with the PelB leader sequence, the Empigen-solubilized fraction was subjected to metal affinity purification. In accordance with previous literature that was discussed above, I observed a net increase

in the amount of total protein extracted from the non-aqueous fraction of the bacterial cells. This led us to incorporate stringent washes with imidazole for both the proteins, compared to the protocols that involved extraction with a less harsh, non-ionic detergent like βDDM. I observed that some higher molecular weight proteins co-purified with PelB-Vpu. Contaminants around 25 kDa and higher were found to be in greater proportions than shown in (Figure V-3) in the absence of $FeCl_3$, $ZnSO_4$, $CuSO_4$ and $MnCl_2$. Cobalt and Nickel affinity purification are often contaminated with endogenous *E. coli* metal binding proteins like GlmS, SlyD, ArnA and Can (Andersen et al. , 2013, Robichon et al. , 2011). The majority of these contaminants are stress-responsive proteins that are expressed in conditions such as heat shock,

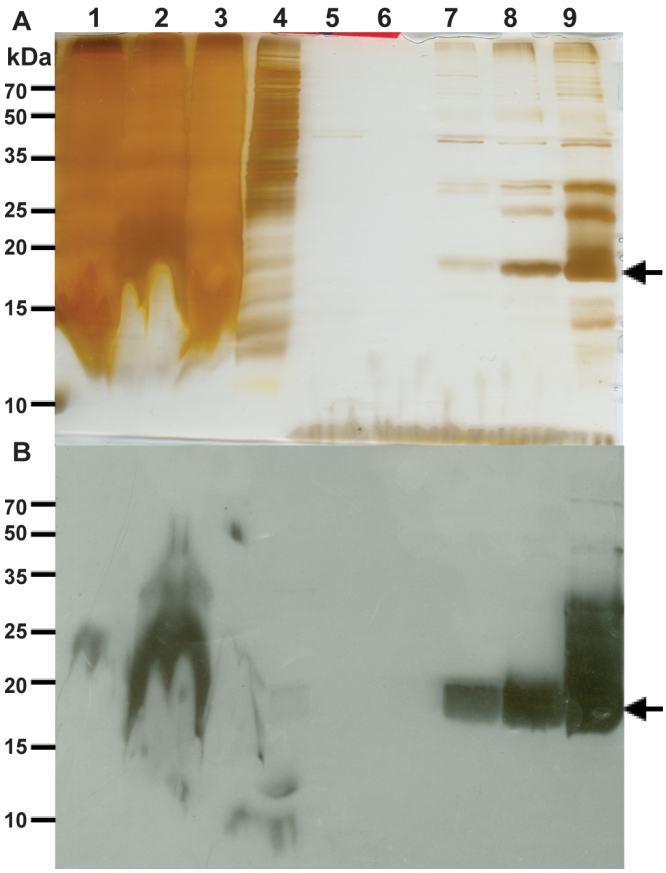

Figure V-3: Talon metal affinity chromatography of PelB-Vpu.
BL21-pTM875 cells were lysed after overnight expression and separated into aqueous (Lane 1) and non-aqueous fractions, which, was treated with Empigen. Protein fractions were subjected to SDS-PAGE followed by silver staining (A) and immuno-blot analysis. (B). Detergent soluble fraction containing Vpu (Lane 2) was loaded onto a Talon column that was pre-equilibrated with 20 mM HEPES pH 7.5, 500 mM NaCl, 5 mM imidazole, and 1.5% Empigen. Unbound proteins in the flow through were collected (Lane 3) and the column was washed consecutively with five different buffer solutions (20 mM HEPES, pH 7.5): W1 (Lane 4, buffer plus 500 mM NaCl), W2 (Lane 5, buffer plus 500 mM NaCl and 1.5% Empigen), W3 (Lane 6, buffer plus 250 mM NaCl and 1.5% Empigen), W4 (Lane 7, buffer plus 250 mM NaCl, 1.5% Empigen and 5 mM imidazole) and W5 (Lane 8, buffer plus 250 mM NaCl, 1.5% Empigen and 10 mM imidazole). Most of the protein Vpu (Lane 9) was eluted with W5 buffer supplemented with 300 mM imidazole.

nutrient starvation and oxidative damage (Bolanos-Garcia and Davies, 2006). Supplementing the minimal media with various trace metals indeed helped decrease the expression levels of these contaminants to enrich our protein of interest. I did observe some fraction of PelB-Vpu eluting in the lower imidazole washes. This could be because of changed interaction dynamics between cobalt ions and the protein surrounded by zwitterionic detergent micelles. To remove the co-purified contaminants, the eluate was concentrated and the proteins were resolved by size exclusion chromatography. PelB-Vpu eluted as a single major peak, which was easily fractionated (Figure V-4). The size of the protein detergent complex in this case, approximately 60 kDa, roughly indicates a possibility of a dimeric oligomerization arrangement of PelB-Vpu in Empigen micelles.

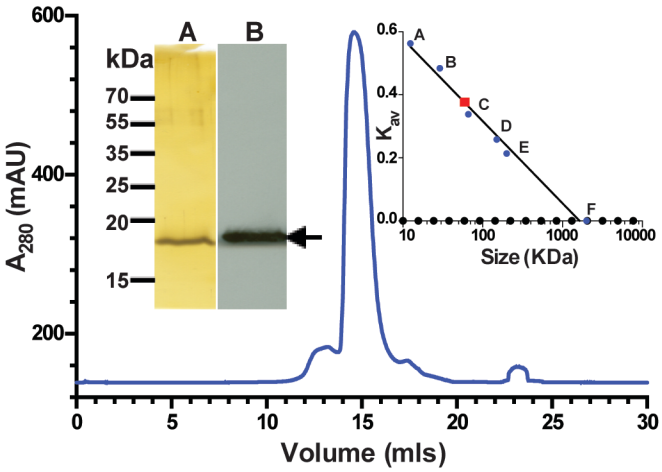

Figure V-4: Size-exclusion chromatography of concentrated metal-affinity purified PelB-Vpu. Eluate from Figure V-3 was subjected to SEC-FPLC. Sec resin: Superdex 200 10/300 GL; Flow-rate: 0.5 mL/min, Running buffer: 20 mM HEPES, pH 7.5, 250 mM NaCl, 5% glycerol and 1.5% Empigen. The major peak at 14.58 mL contained Vpu. The column was calibrated with cytochrome c (A), carbonic anhydrase (B), albumin (C), alcohol dehydrogenase (D), β-amylase (E) and blue dextran (F) and a standard curve was obtained as shown in the inset. The size of the Vpu- Empigen complex was estimated to be 60 kDa.

Detergent exchange

After I purified PelB-Vpu in complex with Empigen to substantial levels of purity by using metal affinity purification and size exclusion chromatography, I proceeded towards replacing Empigen for more NMR compatible detergents. A major obstacle to membrane protein structure determination is the selection of a detergent micelle that mimics the native lipid bilayer. Since the effects of protein-detergent interactions on the structure of

membrane proteins are hard to predict, detergents are selected by exhaustive screening. NMR structures of a large number of single- helix membrane protein have been solved in DPC micelles (Damberg et al. , 2001). Lysolipids, which are derivatives of *E. coli* lipids dipalmitoyl glyceorolphosphoglycerol and dipalmitoyl glycerolphosphocholine, like 1-Palmitol-2-Hydroxy-sn-Glycero-3-Phospho-(1'-rac-Glycerol) -Sodium Salt (LPPG)and 1-Palmitoyl-2-Hydroxy-sn-Glycero-3-Phosphocholine (LPPC) respectively, have also been shown to be very favorable towards elucidating membrane protein structures (Krueger-Koplin et al. , 2004). The short chain lipid, 1,2-Dihexanoyl-sn-Glycero-3-Phosphocholine (DHPC), was used to solve the structure of the M2 proton channel of the influenza A virus (Schnell and Chou, 2008) and most importantly, the full length structure of Vpu (Zhang, Lin, 2015) while LysoFos Glycerol 14 or 1-Myristoyl-2-Hydroxy-sn-Glycero-3-Phospho-(1'-rac-Glycerol) -Sodium Salt) (LMPG) was instrumental in characterizing the solution structure of influenza B virus proton channel (Wang et al. , 2009). I exchanged Empigen with the above mentioned detergents by first, binding the Empigen solubilized PelB-Vpu first to a metal affinity resin and then gradually replace Empigen with the new detergent by applying wash and elution buffers in multiple batches. The elutions, when analyzed with SDS-PAGE followed by silver staining and immunoblot analysis, reveal that depending on the initial detergent before the addition of the SDS

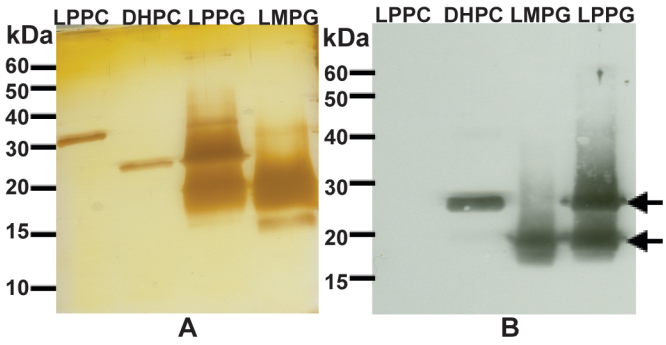

Figure V-5: Talon metal affinity chromatography purification and detergent exchange.
The major peak from Figure V-4 containing purified Vpu- Empigen complex was subjected to another round of talon purification to exchange Empigen to LPPC, DHPC, LPPG and LMPG detergents. The elutions of each of the purification were analyzed by SDS PAGE followed by silver staining (A) and immuno-blotting (B). Arrows indicate the different oligomeric states of PelB-Vpu.

loading buffer, the protein migrated as a monomer and/or an oligomer (Figure V-5). I was unable to elute any detectable amounts of PelB-Vpu with LPPC. In case of DHPC, the protein that was illuminated by immunoblot analysis with antibodies against Vpu was roughly around 25 kDa. I hypothesize that the larger size could be due to the protein migrating in an oligomeric state. The same band is also visualized with LPPG, along with another protein band at approximately 17 kDa, the usual size marker PelB-Vpu aligns with. Higher molecular weight bands were not observed in LMPG samples and the protein aligned with the usual size of PelB-Vpu. Proteins migrating in their oligomeric states in a denaturing gel, in spite of the lack of *in vitro* crosslinking, especially in case of DHPC, has also been observed in case of *Thermotoga*

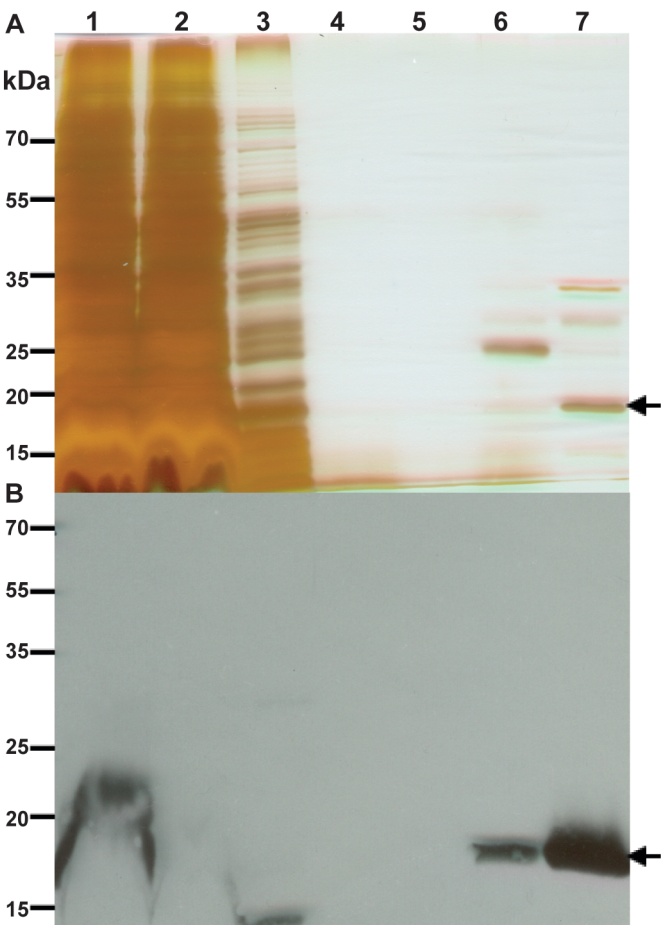

Figure V-6: Extraction of Vpu with Empigen and metal affinity purification and detergent exchange into DPC micelles.
Non- aqueous fraction of BL21-pTM 875 cells was harvested after overnight protein expression and was treated with Empigen. Protein fractions were subjected to SDS-PAGE followed by silver staining (**A**) and immuno-blot analysis. (**B**). Empigen soluble fraction containing Vpu (Lane 1) was loaded onto a Talon column that was pre-equilibrated with 20 mM HEPES pH 7.5, 500 mM NaCl, 5 mM imidazole, and 1.5% Empigen. Unbound proteins in the flow through were collected (Lane 2) and the column was washed consecutively with four different buffer solutions (20 mM HEPES, pH 7.5): W1 (Lane 3, buffer plus 500 mM NaCl), W2 (Lane 4, buffer plus 500 mM NaCl and 0.2% DPC), W3 (Lane 5, buffer plus 250 mM NaCl and 0.1% DPC), and W4 (Lane 6, buffer plus 250 mM NaCl, 0.1% DPC and 10 mM imidazole). Most of the protein Vpu (Lane 7) was eluted with W4 buffer supplemented with 300 mM imidazole.

maritima membrane protein TM1514 (Columbus et al. , 2006).

To obtain PelB-Vpu in DPC micelles, protein extracted from the non-aqueous fraction of BL21- pTM 875 by Empigen was purified and underwent detergent exchange in a single metal affinity purification step (Figure V-6). The protein was relatively pure than the first round of metal affinity purification when the protein was eluted complexed with Empigen micelles (Figure V-3). I proceeded to concentrate the fraction eluted with high imidazole and further purify PelB-Vpu in DPC micelles from unwanted contaminants by size exclusion chromatography (Figure V-7). The major peak, which contained PelB-Vpu, was fractionated stringently so as to totally eliminate the possibility of contamination with proteins eluting later and closely following the major peak.

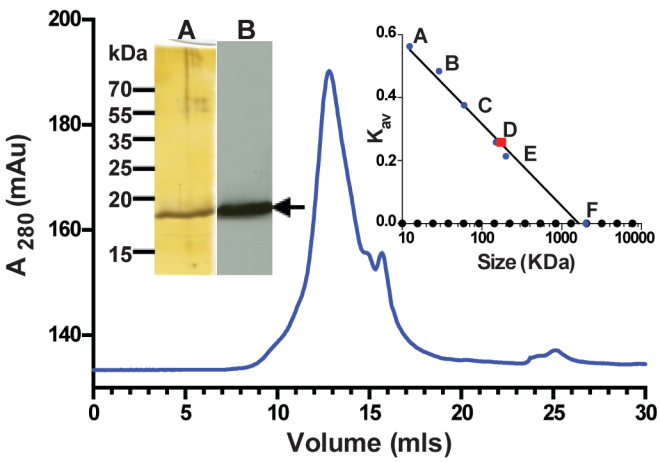

Figure V-7: Size-exclusion chromatography of concentrated metal-affinity chromatography - purified Vpu.
Eluate from Figure V-6 was subjected to SEC-FPLC. Sec resin: Superdex 200 10/300 GL; Flow-rate: 0.5 mL/min, Running buffer: 20 mM HEPES, pH 7.5, 250 mM NaCl, 5% glycerol and 0.1% Fos-choline-12. The major peak at 12.8 mL contained Vpu.

Solution NMR of PelB-Vpu in different detergents

Having obtained Pel-Vpu in complex with different detergent micelles, I proceeded towards characterizing the protein- detergent complexes by biomolecular solution NMR spectroscopy. Suitability for structural studies can be judged by spectral quality. I employed Transverse relaxation optimized spectroscopy – heteronuclear single quantum coherence (^{15}N-TROSY-HSQC) experiments towards this purpose. This technique is a common measure of protein folding and monitoring backbone glycine (Gly) amide and tryptophan (Trp) side-chain resonances, with their characteristic chemical shifts allowing

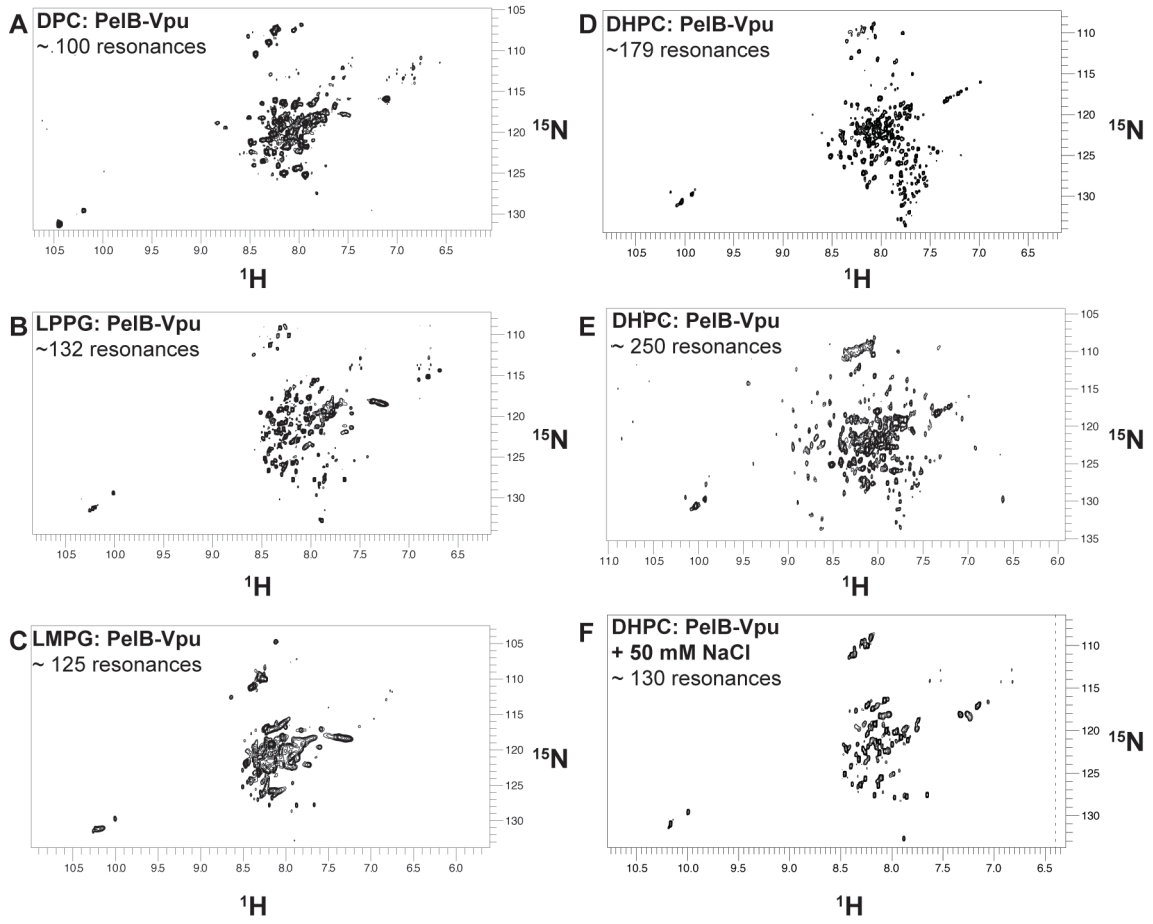

Figure V-8: ^{15}N-^{1}H HSQC spectra of Vpu in complex with various detergents.

me to accurately judge the conformational stability of the protein. I observe that the spectra of PelB-Vpu in most detergent micelles, except in DPC, over-estimates the total number of resonances that are to be expected (112). Specifically, I observe more than the expected two Trp resonances for the PelB-Vpu in complex with LPPG and DHPC micelles. Interestingly, in case of PelB-Vpu in DHPC micelles, I observe nearly two fold of expectant resonances. Furthermore, these resonances tend to decrease in number with increase in data acquisition time. The addition of 50 mM NaCl to the NMR sample did not significantly improve the spectra. I suspect that this heterogeneity of the spectra could be a result of protein aggregates or the presence of different oligomers at the sample conditions the spectra was obtained at. The presence of such oligomers was described in the previous

section (Figure V-5) for DHPC and LPPG. Another cause of this heterogeneity of spectra could be that fact that some micelles may have only one protein molecule per micelle while other micelles may have a different number of a protein to micelle ratio. In a study by McDonnell and Opella (1993), problem of similar kind was solved under conditions where the micelle concentration was much higher than the apparent protein concentration. But, in our case, increasing the concentration of DHPC above 50 mM resulted in most of the protein coming out of the solution as a precipitate. The number of Trp resonances obtained in case of PelB-Vpu in complex with LMPG and DPC micelles is in accordance to our expectations. Comparison of the shape of the two spectra in each detergent implies that each Trp could be in a different physiological environment. Indeed, in case of PelB-Vpu, one of the Trp is localized in the transmembrane domain and the other in the soluble cytoplasmic domain. But, in case of both these detergent –protein complexes, the overall spectral quality was poor and would be extremely challenging to resolve. In case of PelB-Vpu in DPC micelles, the under-estimation of detectable resonances could be because of slow tumbling rates of the protein-detergent complex. The size of the PelB-Vpu – DPC complex can be estimated to be approximately 150 kDa from the major peak of the size exclusion chromatogram (Figure V-7). Such a size could result in lower dynamics resulting in a few undetectable resonances.

Role of the PelB signal peptide.

Despite the seemingly uniform preparation (as judged by DLS and SEC-HPLC), the NMR results clearly point to conformational heterogeneity that reveals itself at the molecular level. I hypothesized that one of the factors that was responsible for the heterogeneity of the NMR spectra discussed above was the possible co-existence of multifarious conformations of the protein-detergent complexes. Specifically, I suspected that this conformational complexity may be ascribed to the hydrophobic PelB signal

peptide that was left uncleaved. The presence of two hydrophobic helical domains in tandem could complicate the manner in which detergent micelles interact with the protein. So, I proceeded to undertake efforts to remove PelB signal peptide from Vpu *in vitro* by digesting the protein with cyanogen bromide. Cyanogen bromide cleaves a peptide at methionine residues (Gross, 1967, Gross and Witkop, 1961, Villa et al. , 1989). A complete digestion of the PelB-Vpu protein would generate a largest fragment consisting of the N-terminal domain, transmembrane domain and the first C-terminal helical domain of Vpu. I observe that the reaction did not achieve completion even after prolonged incubation and our efforts to separate each fragment by metal affinity purification resulted into multiple fragments in each fraction

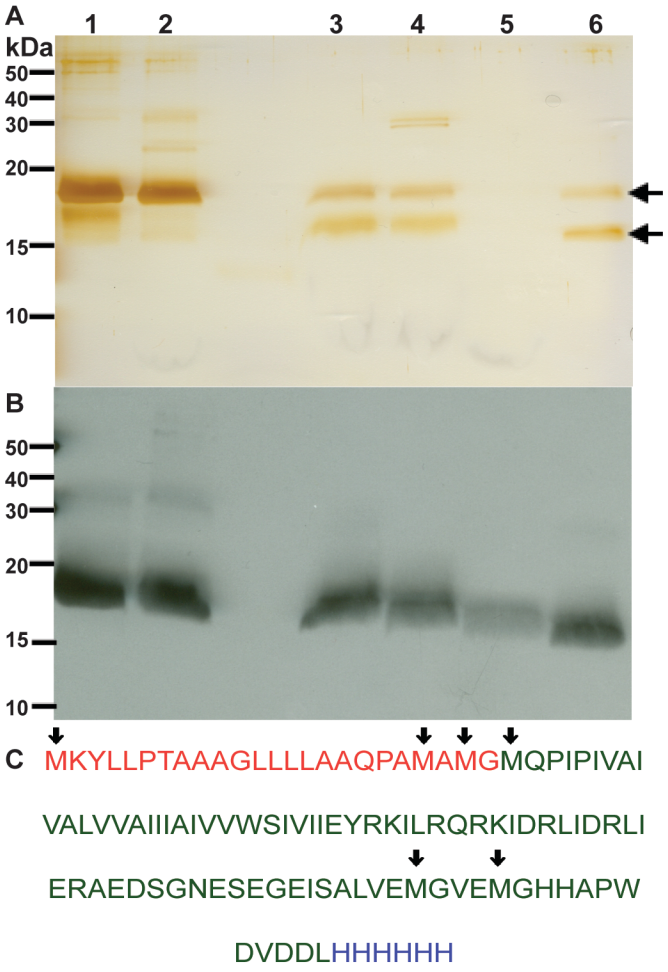

Figure V-9: Cyanogen bromide digestion of PelB-Vpu.
Purified Vpu from Figure V-4 (lane 2) was subjected to cyanogen bromide cleavage. After incubation, the reaction (lane 3) was loaded onto a Talon resin that was pre-equilibrated with 20 mM HEPES, pH 7.5, supplemented with 250 mM NaCl and 1.5% empigen. Unbound proteins in the flow through were collected (lane 4). The column was washed with 5 CV of the equilibration buffer (lane 5) and bound proteins were eluted with the same buffer supplemented with 300 mM imidazole (lane 6). The protein fractions were subjected to SDS-PAGE followed by silver staining (**A**) and immuno-blot analysis, probed with anti-Vpu. (**B**). Black arrows depict the potential cleavage sites on the PelB-Vpu sequence (**C**).

(Figure V-9). The challenging aspect of separating these fragments was further illustrated

by performing a size exclusion chromatography where I observe that most of the peaks within the first column volume of the SEC column (24 mL), within which Vpu is expected to elute, were poorly resolved (Figure V-10). The challenges with this procedure were further compounded by the fact that the harsh nature of the reaction conditions led to the precipitation of the protein, which seriously hampers the possibility of obtaining sufficient amount of protein for structural studies.

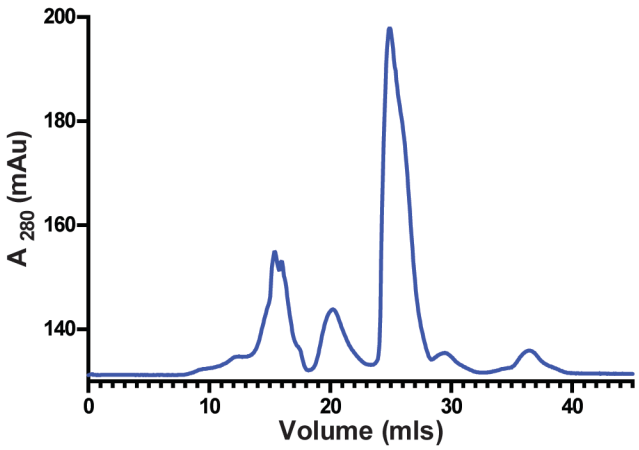

Figure V-10: Size-exclusion chromatography of cyanogen bromide digested products.
The sample from Figure V-9, Lane 3 was subjected to SEC-FPLC. Sec resin: Superdex 200 10/300 GL; Flow-rate: 0.5 mL/min, Running buffer: 20 mM HEPES, pH 7.5, 250 mM NaCl and 1.5% Empigen.

Conclusions

I conclude that it is necessary to revisit our strategies of obtaining recombinant Vpu. It is demonstrated from the NMR spectroscopy studies that the presence of additional hydrophobic tags, such as an uncleaved signal peptide, greatly impairs the possibility of obtaining well-resolved signals. This could be due to sample heterogeneity. The presence of an additional hydrophobic segment closely preceding the hydrophobic transmembrane domain of Vpu could potentially complicate the manner of interactions of PelB-Vpu with the various membrane-mimetic environments used, compared to a situation where the PelB signal peptide was cleaved *in vivo* in the bacterial cells and the protein was obtained in a relatively native state. It could also be possible that the PelB segment and the transmembrane domain of Vpu could interact with each other, potentially masking surfaces on the transmembrane domain which otherwise interact with the lipid. Since the

dynamics of the soluble C-terminal domain of Vpu have been found to be dependent on the transmembrane domain (Zhang et al. , 2015), it can be clearly envisioned that that the unwanted hydrophobic interactions mentioned above can have far reaching consequences on the whole protein. When there is an existence of such dynamic, interconverting conformations, each conformation results in spin states with different intrinsic resonance frequency. Depending on the comparative rate of exchange between these different states and the difference in resonance frequencies, peaks corresponding to each conformation could be observed, thereby over-estimating the number of theoretical expected peaks (Sanders et al. 2006).

Key questions about attributes of Vpu such as, its oligomeric state, combined with the fact that Vpu interacts with a range of host factors that are critical towards understanding the structure-function relationship in this protein remain unanswered.

VI. Summary and outlook

HIV-1 Viral protein U (Vpu) is a type III membrane protein which is expressed in infected host cells. It is involved in efficient viral release and propagation from the host cells. The protein achieves it by binding to host cell viral restriction factors like CD4 and BST-2 and in most cases, tagging them for lysosomal and/or proteasomal degradation. As detailed in Chapter I, binding is achieved by the involvement of both the trans-membrane and the cytoplasmic domain and key structural components in these domains are implicated to be critical for these functions. Unravelling this structural-function relationship of Vpu was the primary motivation behind this study to elucidate a structural model of the protein by X-ray crystallography.

During the course of this research, there were significant challenges towards my goal. Obtaining protein samples which are amenable for setting up crystallization trials proved challenging, especially when Vpu was expressed in fusion with a soluble bacterial protein like Mistic and the maltose binding protein (MBP). Although there are fewer cases of successful vs unsuccessful heterologous expression and enriched isolation of eukaryotic membrane proteins in bacteria for structural studies, the choice of the bacterial expression system, in case of Vpu, was dictated by the fact that the protein lacked typical eukaryotic post translational modifications, such as glycosylation. In the natural host, targeting and retention of this protein to the membranes is driven by amino acid motifs in the trans-membrane and cytoplasmic domain itself (Pacyniak et al. , 2005, Ruiz et al. , 2008, Vigan and Neil, 2011). Since such an arrangement was shown to be non-adaptive in a vastly different prokaryotic expression system, I relied on known bacterial targeting elements to target and integrate Vpu in the bacterial inner membranes.

Expression of Vpu with Mistic did result in fair amounts of recombinant proteins. Mistic is an unusual membrane associating protein that has been shown to tightly

associate with membranes *in vivo* and membrane-mimetic environments *in vitro*, even if it lacks characteristic membrane interaction segments. The post-translational self-association of Mistic in biological membranes and its interactions *in vitro* with ionic and zwitterionic detergents is brought about by polar rather than hydrophobic interactions (Broecker et al. , 2014). Subsequently it was used to express functional versions of typically difficult to express proteins like the G protein coupled receptors (GPCRs) in *E. coli* (Chowdhury et al. , 2012, Petrovskaya et al. , 2010). Contrary to expectations, the Mistic-Vpu fusion protein was very unstable and prone to degradation and aggregation over time. Furthermore, the fusion was cleavable only under extreme conditions which not only resulted in an unfavorable environment for the stability of the proteins but also yielded very less quantities of cleaved Vpu.

Even more than Mistic, the *E. coli* maltose binding protein (MBP) has been extensively used in facilitating the production of recombinant proteins in bacterial systems as detailed in Chapter III. I experimented with different construct designs with regards to linkers and site-specific proteases. MBP-Vpu fusion containing a Tobacco etch Virus (TEV) protease site ($MBP_{\text{-TEV-}}Vpu$) was found to fractionate equally between the water soluble and insoluble fractions of the bacterial cell. Although this protein was very conducive to extraction from the membranes by a wide range of detergents, metal affinity purified $MBP_{\text{-TEV-}}Vpu$ was completely resistant to cleavage with TEV protease. Due to the use of Gateway recombination sequences for the creation of the expression vector, the linker between MBP and Vpu translated to a long stretch of amino acids which were predicted to render the whole fusion too flexible to crystallize. Hence, I resorted to the usage of a shorter linker which also served as a site for cleavage with PreScission protease ($MBP_{\text{-PPCS-}}Vpu$). This fusion was seen to be efficiently targeted to the membranes with the help of the PelB leader peptide. But, the fusion remained resistant to cleavage by

PreScission protease when attempted under preparative conditions. Progress towards the further use of the uncleaved fusion was hampered by the fact that MBP_{-PPCS-}Vpu co-eluted with a similar-sized impurity by metal affinity chromatography. Moreover, Vpu and the contaminant could not be efficiently resolved by size exclusion chromatography. Next, I attempted a different strategy based on affinity chromatography using immobilized-amylose resin relying on the ability of MBP to bind to short alpha-glucose polymers. This also proved to yield unsatisfactory results. In addition, the amylose affinity chromatography also indicated the fact that MBP_{-PPCS-}Vpu was present in solution as a mixture of well-folded and mal-folded forms judging by its affinity to amylose. This in turn could point towards the protein being present in different conformations in solution which would be a major hindrance towards crystallization.

My efforts to express Vpu as a type I membrane protein in *E. coli* with the help of the PelB signal peptide proved successful. Extensive characterization revealed that the protein was efficiently targeted to the inner membranes of the bacteria. In addition, towards the membrane topology of this protein, I showed that the C-terminal domain of Vpu was protected by the bacterial inner membranes. I was able to extract the protein using mild detergents such as βDDM and isolate the protein from other cellular impurities in an extremely pure form using metal affinity chromatography and size exclusion chromatography. Although mass spectrometry revealed the failure of periplasmic peptidases to remove PelB from Vpu, the protein was tested to be in a functional conformation when it bound selectively to the transmembrane and cytoplasmic domain of heterologously expressed human CD4. The presence of expected secondary structure elements was shown alternatively using circular dichroism, which also revealed the stability of the protein in conditions of varying ionic strengths and up to a temperature of approximately 40 ºC. Lastly, its excellent theoretical suitability for crystallization was also

demonstrated by the presence of a mono-disperse PelB-Vpu-βDDM complex at concentrations of 10 mg/mL.

Despite the promising biochemical and biophysical characteristics of the purified Vpu preparations, crystallization of the PelB-Vpu-βDDM complex was largely unsuccessful so far. When subjected to extensive screening with various salts, buffers, precipitants, ionic strength among others, immediate precipitation was observed for most of the conditions. In order to crystallize PelB-Vpu in an environment more native to protein, I employed the technique of Lipid cubic phase (LCP) crystallization. Some conditions showed promise towards this technique when I was able to detect appreciable rates of labeled PelB-Vpu diffusion in the LCP using fluorescence detection after photo-bleaching (FRAP). But, in spite of this, I hitherto could not identify any conditions that supported the crystallization of the protein and would lead to further optimization of conditions.

In parallel to our thus-far unsuccessful crystallization efforts, I turned to another method for structure determination, namely NMR spectroscopy. Bacterial cells harboring plasmids for the expression of PelB-Vpu were successfully adapted to protein expression in M9 minimal medium. Upon successful purification, the protein was obtained in complex with various detergents and lipid. Solution NMR spectroscopy experiments like ^{15}N- ^{1}H HSQC revealed heterogeneous spectra of PelB-Vpu in complex with various membrane-mimetic environments. Non-reproducibility of well-defined, expectant number of resonances when compared to a recently published full length solution NMR structure of Vpu in DHPC micelles (Zhang et al. , 2015) strongly indicated the possible role of the hydrophobic PelB sequence towards the discrepancies observed in the NMR spectra. Specifically, the presence of a second hydrophobic segment with the hydrophobic transmembrane domain of Vpu could result in heterogeneous interaction of PelB-Vpu with membrane mimetic environments.

The Vpu cytoplasmic domain and the transmembrane domain have been previously studied by solution and solid state nuclear magnetic resonance spectroscopy (NMR) resulting in independent structures of the either domain (Sharpe et al. , 2006, Wittlich et al. , 2009). A full-length NMR structure of the protein was recently published (Zhang, Lin, 2015). From these studies, it was observed that the relative mobility of the cytoplasmic helices was dependent on the membrane mimetic environments used. In 1,2-dimyristoyl-*sn*-glycero-3-phosphocholine (DMPC) proteoliposomes, the helices were flexible and could be either arranged in a linear or in a U -shaped orientation as against in 1,2-Dihexanoyl-sn-Glycero-3-Phosphocholine (DHPC) micelles, where the backbone dynamics were more restricted and the cytoplasmic helices adopted well-defined U-shaped loop region between them. It was also shown in the full-length structure that the transmembrane domain influences the conformation, structure and dynamics of the C-terminal domain and *vice versa*.

Judging by the above mentioned dependence of the protein on the membrane-mimetic environment, I predict that the way forward in future structural studies in Vpu is to over-express the protein in a more native environment, such as mammalian cells. Insect cell expression systems can also be considered (Sarramegna et al. , 2003). Cell free systems, especially the eukaryotic wheat germ extracts (Anderson et al. , 1983, Madin et al. , 2000, Sawasaki and Endo, 2004), could also be used for protein synthesis. Addition of suitable lipids in solution can create a favorable environment for the membrane protein to be synthesized directly into a defined membrane-mimetic environment of choice that would allow solubility and functional folding of the proteins (Elbaz et al. , 2004, Ishihara et al. , 2005, Klammt et al. , 2004, Klammt et al. , 2005). *Xenopus laevis* oocytes can also be used for expression (Buckingham et al. , 2006). This system has been used widely for

the expression of receptors and ion-channels, including Vpu, to demonstrate its ion channel activity (Coady et al. , 1998)

A major challenge towards structural studies of hydrophobic membrane proteins using X-ray crystallography is the growth of well-ordered 3D crystals of membrane proteins. Especially, proteins with small extra-membrane domains, such are Vpu could be difficult to crystallize because they have reduced surface area for type II crystal contacts and the presence of detergent micelles could have a restrictive effect as well. One of the ways to facilitate the process could be to generate monoclonal antibodies against Vpu and co-crystallize the protein with these structural monoclonal antibody fragments (Hunte and Michel, 2002).

For the purposes of crystallization, lipid cubic phase could play an important role because of its flexibility to allow the incorporation of various kinds of lipids thus providing a stabilizing environment in which the protein is initially embedded and then crystallization is driven by lateral diffusion of the protein in LCP upon the addition of precipitants (Nollert et al. , 2002). Due to the relatively slow diffusion rates of membrane proteins in LCP, crystals obtained by this method are usually found to be smaller than the ones obtained from *in surfo* methods (Liu et al. , 2014b). Small crystals could be challenging to detect and harvest and are more susceptible to X-ray radiation damage, thereby hampering the collection of high-resolution diffraction data from these crystals. The technique of Serial femtosecond crystallography was developed to obtain time-resolved diffraction patterns from small crystals with minimal radiation damage (Chapman et al. , 2011, Kupitz et al. , 2014). This technique has been adapted to use with LCP crystallization (Liu et al. , 2014a, Liu et al. , 2013, Liu, Wacker, 2014b, Weierstall et al. , 2014) thereby greatly benefitting the prospects of this technique.

The HIV-1 Vpu has been an active subject of research in the scientific community. The various important roles played by the protein towards efficient viral release from infected host cells makes it an attractive anti-viral drug target. The above mentioned options will be explored in the future in the hope of elucidating a reliable structural model of not only Vpu, but also its manner of interactions with its binding partners. This could help in the formulation of a successful strategy to halt the spread of the devastating epidemic caused by HIV-1.

REFERENCES

Ai X, Caffrey M. Membrane protein crystallization in lipidic mesophases: detergent effects. Biophys J. 2000;79:394-405.

Alexander DM, Hesson T, Mannarino A, Cable M, Dalie BL. Isolation and purification of a biologically active human platelet-derived growth factor BB expressed in *Escherichia coli*. Protein Expr Purif. 1992;3:204-11.

Allen JC, Humphries C. The use of zwitterionic surfactants in the agarose chromatography of biological membranes. FEBS Lett. 1975;57:158-62.

Andersen KR, Leksa NC, Schwartz TU. Optimized *E. coli* expression strain LOBSTR eliminates common contaminants from His-tag purification. Proteins. 2013;81:1857-61.

Anderson CW, Straus JW, Dudock BS. Preparation of a cell-free protein-synthesizing system from wheat germ. Methods Enzymol. 1983;101:635-44.

Andreev YA, Kozlov SA, Vassilevski AA, Grishin EV. Cyanogen bromide cleavage of proteins in salt and buffer solutions. Anal Biochem. 2010;407:144-6.

Andrew A, Strebel K. HIV-1 Vpu targets cell surface markers CD4 and BST-2 through distinct mechanisms. Mol Aspects Med. 2010;31:407-17.

Arvola M, Keinänen K. Characterization of the ligand-binding domains of Glutamate Receptor (GluR)-B and GluR-D subunits expressed in *Escherichia coli* as periplasmic proteins. Journal of Biological Chemistry. 1996;271:15527-32.

Basmaciogullari S, Pizzato M. The activity of Nef on HIV-1 infectivity. Frontiers in Microbiology. 2014;5:232.

Bassford PJ, Jr. Export of the periplasmic maltose-binding protein of *Escherichia coli*. J Bioenerg Biomembr. 1990;22:401-39.

Beckett A, Woodward R. Surface-active betaines: n-alkyl-nn-dimethylglycines and their critical micelle concentrations. Journal of Pharmacy and Pharmacology. 1963;15:422-31.

Bedouelle H, Bassford PJ, Jr., Fowler AV, Zabin I, Beckwith J, Hofnung M. Mutations which alter the function of the signal sequence of the maltose binding protein of *Escherichia coli*. Nature. 1980;285:78-81.

Berks BC, Sargent F, Palmer T. The Tat protein export pathway. Mol Microbiol. 2000;35:260-74.

Bolanos-Garcia VM, Davies OR. Structural analysis and classification of native proteins from *E. coli* commonly co-purified by immobilised metal affinity chromatography. Biochem Biophys Acta. 2006;1760:1304-13.

Bolduan S, Hubel P, Reif T, Lodermeyer V, Hohne K, Fritz JV, et al. HIV-1 Vpu affects the anterograde transport and the glycosylation pattern of NTB-A. Virology. 2013a;440:190-203.

Bottino C, Falco M, Parolini S, Marcenaro E, Augugliaro R, Sivori S, et al. Gntb-A, a novel Sh2d1a-associated surface molecule contributing to the inability of Natural Killer Cells to kill Epstein-Barr Virus–infected B Cells in X-linked lymphoproliferative disease. The Journal of Experimental Medicine. 2001;194:235-46.

Bour S, Boulerice F, Wainberg MA. Inhibition of gp160 and CD4 maturation in U937 cells after both defective and productive infections by human immunodeficiency virus type 1. Journal of Virology. 1991;65:6387-96.

Bowie JU. Solving the membrane protein folding problem. Nature. 2005;438:581-9.

Broecker J, Fiedler S, Gimpl K, Keller S. Polar interactions trump hydrophobicity in stabilizing the self-inserting membrane protein Mistic. J Am Chem Soc. 2014;136:13761-8.

Buckingham SD, Pym L, Sattelle DB. Oocytes as an expression system for studying receptor/channel targets of drugs and pesticides. In: Liu XJ, editor. Xenopus Protocols: Cell Biology and Signal Transduction. Totowa, NJ: Humana Press; 2006. p. 331-45.

Caffrey M. A lipid's eye view of membrane protein crystallization in mesophases. Current Opinion in Structural Biology. 2000;10:486-97.

Caffrey M. Crystallizing membrane proteins for structure determination: use of lipidic mesophases. Annu Rev Biophys. 2009;38:29-51.

Caffrey M. A comprehensive review of the lipid cubic phase or in meso method for crystallizing membrane and soluble proteins and complexes. Structural Biology and Crystallization Communications. 2015;71:3–18.

Carrington JC, Dougherty WG. A viral cleavage site cassette: identification of amino acid sequences required for tobacco etch virus polyprotein processing. Proc Natl Acad Sci U S A. 1988;85:3391-5.

Chapman HN, Fromme P, Barty A, White TA, Kirian RA, Aquila A, et al. Femtosecond X-ray protein nanocrystallography. Nature. 2011;470:73-77 © 2011 Nature Publishing Group, a division of Macmillan Publishers Limited. All Rights Reserved..

Cherezov V. Lipidic cubic phase technologies for membrane protein structural studies. Current opinion in structural biology. 2011;21:559–66.

Cherezov V, Clogston J, Misquitta Y, Abdel-Gawad W, Caffrey M. Membrane protein crystallization in meso: lipid type-tailoring of the cubic phase. Biophys J. 2002;83:3393-407.

Cherezov V, Clogston J, Papiz MZ, Caffrey M. Room to move: crystallizing membrane proteins in swollen lipidic mesophases. J Mol Biol. 2006;357:1605-18.

Cherezov V, Fersi H, Caffrey M. Crystallization screens: compatibility with the lipidic cubic phase for in meso crystallization of membrane proteins. Biophysical journal. 2001;81:225–42.

Cherezov V, Liu J, Griffith M, Hanson MA, Stevens RC. LCP-FRAP Assay for Pre-Screening Membrane Proteins for in Meso Crystallization. Cryst Growth Des. 2008;8:4307-15.

Cherezov V, Rosenbaum DM, Hanson MA, Rasmussen SG, Thian FS, Kobilka TS, et al. High-resolution crystal structure of an engineered human beta2-adrenergic G protein-coupled receptor. Science. 2007;318:1258-65.

Chien EY, Liu W, Zhao Q, Katritch V, Han GW, Hanson MA, et al. Structure of the human dopamine D3 receptor in complex with a D2/D3 selective antagonist. Science. 2010;330:1091-5.

Chou JJ, Baber JL, Bax A. Characterization of phospholipid mixed micelles by translational diffusion. J Biomol NMR. 2004;29:299-308.

Chowdhury A, Feng R, Tong Q, Zhang Y, Xie XQ. Mistic and TarCF as fusion protein partners for functional expression of the cannabinoid receptor 2 in *Escherichia coli*. Protein Expr Purif. 2012;83:128-34.

Coady MJ, Daniel NG, Tiganos E, Allain B, Friborg J, Lapointe JY, et al. Effects of Vpu expression on Xenopus oocyte membrane conductance. Virology. 1998;244:39-49.

Cohen EA, Terwilliger EF, Sodroski JG, Haseltine WA. Identification of a protein encoded by the vpu gene of HIV-1. Nature. 1988a;334:532-34 © 1988 Nature Publishing Group.

Columbus L, Lipfert J, Jambunathan K, Fox DA, Sim AY, Doniach S, et al. Mixing and matching detergents for membrane protein NMR structure determination. J Am Chem Soc. 2009;131:7320-6.

Columbus L, Lipfert J, Klock H, Millett I, Doniach S, Lesley SA. Expression, purification, and characterization of *Thermotoga maritima* membrane proteins for structure determination. Protein Sci. 2006;15:961-75.

Crise B, Buonocore L, Rose JK. CD4 is retained in the endoplasmic reticulum by the human immunodeficiency virus type 1 glycoprotein precursor. Journal of Virology. 1990;64:5585-93.

Damberg P, Jarvet J, Graslund A. Micellar systems as solvents in peptide and protein structure determination. Methods Enzymol. 2001;339:271-85.

de Gier JW, Luirink J. Biogenesis of inner membrane proteins in *Escherichia coli*. Mol Microbiol. 2001;40:314-22.

Delaglio F, Grzesiek S, Vuister GW, Zhu G, Pfeifer J, Bax A. NMRPipe: a multidimensional spectral processing system based on UNIX pipes. J Biomol NMR. 1995;6:277-93.

di Guana C, Lib P, Riggsa PD, Inouyeb H. Vectors that facilitate the expression and purification of foreign peptides in *Escherichia coli* by fusion to maltose-binding protein. Gene. 1988;67:21-30.

Dörner K, Martin-Garcia JM, Kupitz C, Gong Z, Mallet TC, Chen L, et al. Characterization of protein nanocrystals based on the reversibility of crystallization. Crystal Growth & Design. 2016.

Dougherty WG, Carrington JC, Cary SM, Parks TD. Biochemical and mutational analysis of a plant virus polyprotein cleavage site. EMBO J. 1988;7:1281-7.

Dougherty WG, Parks TD, Cary SM, Bazan JF, Fletterick RJ. Characterization of the catalytic residues of the tobacco etch virus 49-kDa proteinase. Virology. 1989;172:302-10.

Douglas JL, Gustin JK, Viswanathan K, Mansouri M, Moses AV, Fruh K. The great escape: viral strategies to counter BST-2/tetherin. PLoS Pathog. 2010a;6:e1000913.

Douglas JL, Viswanathan K, McCarroll MN, Gustin JK, Fruh K, Moses AV. Vpu directs the degradation of the human immunodeficiency virus restriction factor BST-2/Tetherin via a βTrCP-dependent mechanism. J Virol. 2009;83:7931-47.

Dube M, Bego M, Paquay C, Cohen E. Modulation of HIV-1-host interaction: role of the Vpu accessory protein. Retrovirology. 2010a;7:114.

Duplay P, Hofnung M. Two regions of mature periplasmic maltose-binding protein of Escherichia coli involved in secretion. J Bacteriol. 1988;170:4445-50.

Dvir H, Choe S. Bacterial expression of a eukaryotic membrane protein in fusion to various Mistic orthologs. Protein Expression and Purification. 2009;68:28-33.

Dvir H, Lundberg ME, Maji SK, Riek R, Choe S. Mistic: Cellular localization, solution behavior, polymerization, and fibril formation. Protein Science. 2009;18:1564–70 Copyright © 2009 The Protein Society.

Elbaz Y, Steiner-Mordoch S, Danieli T, Schuldiner S. In vitro synthesis of fully functional EmrE, a multidrug transporter, and study of its oligomeric state. Proc Natl Acad Sci U S A. 2004;101:1519-24.

Engel CK, Chen L, Prive GG. Stability of the lactose permease in detergent solutions. Biochim Biophys Acta. 2002;1564:47-56.

Engelman A, Cherepanov P. The structural biology of HIV-1: mechanistic and therapeutic insights. Nature Reviews Microbiology. 2012;10:279-90 © 2012 Nature Publishing Group.

Evans DT, Serra-Moreno R, Singh RK, Guatelli JC. BST-2/tetherin: a new component of the innate immune response to enveloped viruses. Trends in Microbiology. 2010a;18:388-96.

Ewart GD, Mills K, Cox GB, Gage PW. Amiloride derivatives block ion channel activity and enhancement of virus-like particle budding caused by HIV-1 protein Vpu. European Biophysics Journal. 2002;31:26-35.

Ewart GD, Sutherland T, Gage PW, Cox GB. The Vpu protein of human immunodeficiency virus type 1 forms cation-selective ion channels. Journal of Virology. 1996a;70:7108-15.

Fecker LF, Kaufmann A, Commandeur U, Commandeur J, Koenig R, Burgermeister W. Expression of single-chain antibody fragments (scFv) specific for beet necrotic yellow vein virus coat protein or 25 kDa protein in *Escherichia coli* and *Nicotiana benthamiana*. Plant Molecular Biology. 1996;32:979-86.

Ferre-D'Amare AR, Burley SK. Use of dynamic light scattering to assess crystallizability of macromolecules and macromolecular assemblies. Structure. 1994;2:357-9.

Ferré-D'Amaré AR, Burley SK. Dynamic light scattering in evaluating crystallizability of macromolecules. Methods in Enzymology: Academic Press; 1997. p. 157-66.

Flaig RM, Stark S, Watzl C. Cutting Edge: NTB-A activates NK cells via homophilic interaction. The Journal of Immunology. 2004;172:6524-27.

Gao F, Bailes E, Robertson DL, Chen Y, Rodenburg CM, Michael SF, et al. Origin of HIV-1 in the chimpanzee Pan troglodytes troglodytes. Nature. 1999;397:436-41 © 1999 Nature Publishing Group.

Garavito RM, Ferguson-Miller S. Detergents as tools in membrane biochemistry. Journal of Biological Chemistry. 2001;276:32403 -06 0267.

Garavito RM, Picot D, Loll PJ. Strategies for crystallizing membrane proteins. J Bioenerg Biomembr. 1996;28:13-27.

Garcia JV, Miller AD. Serine phosphorylation-independent downregulation of cell-surface CD4 by Nef. Nature. 1991;350:508-11 © 1991 Nature Publishing Group.

Geyer BC, Kannan L, Garnaud PE, Broomfield CA, Cadieux CL, Cherni I, et al. Plant-derived human butyrylcholinesterase, but not an organophosphorous-compound hydrolyzing variant thereof, protects rodents against nerve agents. Proc Natl Acad Sci U S A. 2010;107:20251-6.

Giese S, Marsh M. Tetherin can restrict cell-free and cell-cell transmission of HIV from primary macrophages to T cells. PLoS Pathog. 2014;10:e1004189.

Goder V, Junne T, Spiess M. Sec61p contributes to signal sequence orientation according to the positive-inside rule. Mol Biol Cell. 2004;15:1470-8.

Goffinet C, Allespach I, Homann S, Tervo H-M, Habermann A, Rupp D, et al. HIV-1 antagonism of CD317 is species specific and involves Vpu-mediated proteasomal degradation of the restriction factor. Cell Host & Microbe. 2009;5:285-97.

Gonzalez ME, Carrasco L. Viroporins. FEBS Letters. 2003;552:28-34.

Gordeliy VI, Labahn J, Moukhametzianov R, Efremov R, Granzin J, Schlesinger R, et al. Molecular basis of transmembrane signalling by sensory rhodopsin II-transducer complex. Nature. 2002;419:484-87.

Greenfield NJ. Using circular dichroism spectra to estimate protein secondary structure. Nature protocols. 2006;1:2876-90.

Gross E. The cyanogen bromide reaction. Methods in Enzymology: Academic Press; 1967. p. 238-55.

Gross E, Witkop B. Selective cleavage of the methionyl peptide bonds in ribonuclease with cyanogen bromide. Journal of the American Chemical Society. 1961;83:1510-11.

Guenzel CA, Hérate C, Benichou S. HIV-1 Vpr-a still "enigmatic multitasker". Frontiers in Microbiology. 2014;5:127.

Guo W, Cleveland B, Davenport TM, Lee KK, Hu SL. Purification of recombinant vaccinia virus-expressed monomeric HIV-1 gp120 to apparent homogeneity. Protein Expr Purif. 2013;90:34-9.

Hartl FU, Lecker S, Schiebel E, Hendrick JP, Wickner W. The binding cascade of SecB to SecA to SecY/E mediates preprotein targeting to the *E. coli* plasma membrane. Cell. 1990;63:269-79.

Haupert LM, Simpson GJ. Screening of protein crystallization trials by second order nonlinear optical imaging of chiral crystals (SONICC). Methods. 2011;55:379-86.

Helenius A, Aebi M. Roles of N-linked glycans in the endoplasmic reticulum. Annu Rev Biochem. 2004;73:1019-49.

Herrero L, Monroy N, Gonzalez ME. HIV-1 Vpu protein mediates the transport of potassium in *Saccharomyces cerevisiae*. Biochemistry. 2013a;52:171-77.

Hilf RJC, Dutzler R. X-ray structure of a prokaryotic pentameric ligand-gated ion channel. Nature. 2008;452:375-79 © 2008 Nature Publishing Group.

Hitscherich C, Jr., Aseyev V, Wiencek J, Loll PJ. Effects of PEG on detergent micelles: implications for the crystallization of integral membrane proteins. Acta Crystallogr D Biol Crystallogr. 2001;57:1020-9.

Hout DR, Gomez ML, Pacyniak E, Gomez LM, Inbody SH, Mulcahy ER, et al. Scrambling of the amino acids within the transmembrane domain of Vpu results in a simian-human immunodeficiency virus (SHIVTM) that is less pathogenic for pig-tailed macaques. Virology. 2005;339:56-69.

Hunte C, Michel H. Crystallisation of membrane proteins mediated by antibody fragments. Curr Opin Struct Biol. 2002;12:503-8.

Hussain A, Das SR, Tanwar C, Jameel S. Oligomerization of the human immunodeficiency virus type 1 (HIV-1) Vpu protein – a genetic, biochemical and biophysical analysis. Virology Journal. 2007;4:1-11.

Ikemura T. Correlation between the abundance of *Escherichia coli* transfer RNAs and the occurrence of the respective codons in its protein genes. J Mol Biol. 1981;146:1-21.

Ikemura T. Correlation between the abundance of yeast transfer RNAs and the occurrence of the respective codons in protein genes. Differences in synonymous codon choice patterns of yeast and *Escherichia coli* with reference to the abundance of isoaccepting transfer RNAs. J Mol Biol. 1982;158:573-97.

Ishihara G, Goto M, Saeki M, Ito K, Hori T, Kigawa T, et al. Expression of G protein coupled receptors in a cell-free translational system using detergents and thioredoxin-fusion vectors. Protein Expr Purif. 2005;41:27-37.

Iwabu Y, Fujita H, Kinomoto M, Kaneko K, Ishizaka Y, Tanaka Y, et al. HIV-1 accessory protein Vpu internalizes cell-surface BST-2/tetherin through transmembrane interactions leading to lysosomes. J Biol Chem. 2009;284:35060-72.

Iwasaki Y, Mishima N, Mizumoto K, Nakano H, Yamane T. Extracellular production of phospholipase D of *Streptomyces* antibioticus using recombinant *Escherichia coli*. Journal of Fermentation and Bioengineering. 1995;79:417-21.

Jaakola VP, Griffith MT, Hanson MA, Cherezov V, Chien EY, Lane JR, et al. The 2.6 angstrom crystal structure of a human A2A adenosine receptor bound to an antagonist. Science. 2008;322:1211-7.

Jabbar MA, Nayak DP. Intracellular interaction of human immunodeficiency virus type 1 (ARV-2) envelope glycoprotein gp160 with CD4 blocks the movement and maturation of CD4 to the plasma membrane. Journal of Virology. 1990;64:6297-304.

Jafari M, Guatelli J, Lewinski MK. Activities of transmitted/founder and chronic clade B HIV-1 Vpu and a C-terminal polymorphism specifically affecting virion release. J Virol. 2014;88:5062-78.

Janssen JJ, Bovee-Geurts PH, Merkx M, DeGrip WJ. Histidine tagging both allows convenient single-step purification of bovine rhodopsin and exerts ionic strength-dependent effects on its photochemistry. J Biol Chem. 1995;270:11222-9.

Jennings R, Erturk M. Comparative studies of HSV-1 antigens solubilised from infected cells by using non-ionic or zwitterionic detergents. J Med Virol. 1990;31:98-108.

Johnson AE, van Waes MA. The translocon: a dynamic gateway at the ER membrane. Annu Rev Cell Dev Biol. 1999;15:799-842.

Jumpertz T, Tschapek B, Infed N, Smits SH, Ernst R, Schmitt L. High-throughput evaluation of the critical micelle concentration of detergents. Anal Biochem. 2011;408:64-70.

Kanaya S, Yamada Y, Kinouchi M, Kudo Y, Ikemura T. Codon usage and tRNA genes in eukaryotes: correlation of codon usage diversity with translation efficiency and with CG-dinucleotide usage as assessed by multivariate analysis. J Mol Evol. 2001;53:290-8.

Kapust RB, Routzahn KM, Waugh DS. Processive degradation of nascent polypeptides, triggered by tandem AGA codons, limits the accumulation of recombinant tobacco etch virus protease in *Escherichia coli* BL21(DE3). Protein Expr Purif. 2002;24:61-70.

Kapust RB, Tozser J, Fox JD, Anderson DE, Cherry S, Copeland TD, et al. Tobacco etch virus protease: mechanism of autolysis and rational design of stable mutants with wild-type catalytic proficiency. Protein Eng. 2001;14:993-1000.

Kapust RB, Waugh DS. *Escherichia coli* maltose-binding protein is uncommonly effective at promoting the solubility of polypeptides to which it is fused. PRS. 1999;8:1668–74.

Kefala G, Kwiatkowski W, Esquivies L, Maslennikov I, Choe S. Application of Mistic to improving the expression and membrane integration of histidine kinase receptors from *Escherichia coli*. Journal of Structural and Functional Genomics. 2007;8:167-72.

Kellermann OK, Ferenci T. Maltose-binding protein from *Escherichia coli*. Methods Enzymol. 1982;90 Pt E:459-63.

Kessans SA, Linhart MD, Matoba N, Mor T. Biological and biochemical characterization of HIV-1 Gag/dgp41 virus-like particles expressed in *Nicotiana benthamiana*. Plant Biotechnol J. 2013;11:681-90.

Kimura T, Nishikawa M, Ohyama A. Intracellular Membrane Traffic of Human Immunodeficiency Virus Type 1 Envelope Glycoproteins: Vpu Liberates Golgi-Targeted gp160 from CD4-Dependent Retention in the Endoplasmic Reticulum. Journal of Biochemistry. 1994;115:1010-20.

Klammt C, Lohr F, Schafer B, Haase W, Dotsch V, Ruterjans H, et al. High level cell-free expression and specific labeling of integral membrane proteins. Eur J Biochem. 2004;271:568-80.

Klammt C, Schwarz D, Fendler K, Haase W, Dotsch V, Bernhard F. Evaluation of detergents for the soluble expression of alpha-helical and beta-barrel-type integral membrane proteins by a preparative scale individual cell-free expression system. FEBS J. 2005;272:6024-38.

Kluge SF, Sauter D, Vogl M, Peeters M, Li Y, Bibollet-Ruche F, et al. The transmembrane domain of HIV-1 Vpu is sufficient to confer anti-tetherin activity to SIV_{cpz} and SIV_{gor} Vpu proteins: cytoplasmic determinants of Vpu function. Retrovirology. 2013;10:32.

Kolbe M, Besir H, Essen LO, Oesterhelt D. Structure of the light-driven chloride pump halorhodopsin at 1.8 A resolution. Science. 2000;288:1390-6.

Korepanova A, Moore JD, Nguyen HB, Hua Y, Cross TA, Gao F. Expression of membrane proteins from *Mycobacterium tuberculosis* in *Escherichia coli* as fusions with maltose binding protein. Protein Expression and Purification. 2007;53:24-30.

Kota J, Ljungdahl PO. Specialized membrane-localized chaperones prevent aggregation of polytopic proteins in the ER. J Cell Biol. 2005;168:79-88.

Krueger-Koplin RD, Sorgen PL, Krueger-Koplin ST, Rivera-Torres IO, Cahill SM, Hicks DB, et al. An evaluation of detergents for NMR structural studies of membrane proteins. J Biomol NMR. 2004;28:43-57.

Kueck T, Neil SJ. A cytoplasmic tail determinant in HIV-1 Vpu mediates targeting of tetherin for endosomal degradation and counteracts interferon-induced restriction. PLoS Pathog. 2012a;8:e1002609.

Kuhelj R, Dolinar M, Pungercar J, Turk V. The preparation of catalytically active human cathepsin B from its precursor expressed in *Escherichia coli* in the form of inclusion bodies. Eur J Biochem. 1995;229:533-9.

Kumar VV, Baumann WJ. Lanthanide-induced phosphorus-31 NMR downfield chemical shifts of lysophosphatidylcholines are sensitive to lysophospholipid critical micelle concentration. Biophys J. 1991;59:103-7.

Kupitz C, Basu S, Grotjohann I, Fromme R, Zatsepin NA, Rendek KN, et al. Serial time-resolved crystallography of photosystem II using a femtosecond X-ray laser. Nature. 2014;513:261-5.

Kupzig S, Korolchuk V, Rollason R, Sugden A, Wilde A, Banting G. Bst-2/HM1.24 is a raft-associated apical membrane protein with an unusual topology. Traffic (Copenhagen, Denmark). 2003;4:694-709.

Landau EM, Rosenbusch JP. Lipidic cubic phases: a novel concept for the crystallization of membrane proteins. Proceedings of the National Academy of Sciences. 1996;93:14532–35.

Larsson K. Aqueous dispersions of cubic lipid–water phases. Current Opinion in Colloid & Interface Science. 2000;5:64-69.

Lauterwein J, Bosch C, Brown LR, Wuthrich K. Physicochemical studies of the protein-lipid interactions in melittin-containing micelles. Biochim Biophys Acta. 1979;556:244-64.

Lavner Y, Kotlar D. Codon bias as a factor in regulating expression via translation rate in the human genome. Gene. 2005;345:127-38.

le Maire M, Champeil P, Moller JV. Interaction of membrane proteins and lipids with solubilizing detergents. Biochim Biophys Acta. 2000;1508:86-111.

Lee HH, Cherni I, Yu H, Fromme R, Doran JD, Grotjohann I, et al. Expression, purification and crystallization of CTB-MPR, a candidate mucosal vaccine component against HIV-1. IUCrJ. 2014;1:305-17.

Lee KE, Kim HM, Lee JO, Jeon H, Han SS. Regulation of CD40 reconstitution into a liposome using different ratios of solubilized LDAO to lipids. Colloids Surf B Biointerfaces. 2008;62:51-7.

Lei SP, Lin HC, Wang SS, Callaway J, Wilcox G. Characterization of the *Erwinia carotovora* pelB gene and its product pectate lyase. Journal of Bacteriology. 1987;169:4379-83.

Lemaitre V, Willbold D, Watts A, Fischer WB. Full length Vpu from HIV-1: combining molecular dynamics simulations with NMR spectroscopy. J Biomol Struct Dyn. 2006;23:485-96.

Lenburg ME, Landau NR. Vpu-induced degradation of CD4: requirement for specific amino acid residues in the cytoplasmic domain of CD4. J Virol. 1993;67:7238-45.

Lewinski MK, Jafari M, Zhang H, Opella SJ, Guatelli J. Membrane Anchoring by a C-terminal tryptophan enables HIV-1 Vpu to displace BST2 from sites of viral assembly. Journal of Biological Chemistry. 2015:jbc–M114.

Lin TL, Chen SH, Gabriel NE, Roberts MF. The use of small-angle neutron scattering to determine the structure and interaction of dihexanoylphosphatidylcholine micelles. Journal of the American Chemical Society. 1986;108:3499-507.

Lindner P, Guth B, Wülfing C, Krebber C, Steipe B, Müller F, et al. Metal affinity protein separations: Purification of native proteins from the cytoplasm and periplasm of *Escherichia coli* using IMAC and histidine tails: A comparison of proteins and protocols. Methods. 1992;4:41-56.

Liu W, Ishchenko A, Cherezov V. Preparation of microcrystals in lipidic cubic phase for serial femtosecond crystallography. Nature protocols. 2014a;9:2123–34.

Liu W, Wacker D, Gati C, Han GW, James D, Wang D, et al. Serial Femtosecond Crystallography of G Protein–Coupled Receptors. Science. 2013;342:1521-24.

Liu W, Wacker D, Wang C, Abola E, Cherezov V. Femtosecond crystallography of membrane proteins in the lipidic cubic phase. Philosophical Transactions of the Royal Society B: Biological Sciences. 2014b;369:20130314.

Liu X, Wu L, Deng G, Li N, Chu X, Guo F, et al. Characterization of mitochondrial trifunctional protein and its inactivation study for medicine development. Biochim Biophys Acta. 2008;1784:1742-9.

Lo-Man R, Martineau P, Hofnung M, Leclerc C. Induction of T cell responses by chimeric bacterial proteins expressing several copies of a viral T cell epitope. Eur J Immunol. 1993;23:2998-3002.

Loo TW, Clarke DM. Rapid purification of human P-glycoprotein mutants expressed transiently in HEK 293 cells by nickel-chelate chromatography and characterization of their drug-stimulated ATPase activities. J Biol Chem. 1995;270:21449-52.

Lowthert LA, Ku NO, Liao J, Coulombe PA, Omary MB. Empigen BB: a useful detergent for solubilization and biochemical analysis of keratins. Biochem Biophys Res Commun. 1995;206:370-9.

Lu J-X, Sharpe S, Ghirlando R, Yau W-M, Tycko R. Oligomerization state and supramolecular structure of the HIV-1 Vpu protein transmembrane segment in phospholipid bilayers. Protein Science. 2010;19:1877-96 Copyright © 2010 The Protein Society.

Luecke H, Richter HT, Lanyi JK. Proton transfer pathways in bacteriorhodopsin at 2.3 angstrom resolution. Science. 1998;280:1934-7.

Luecke H, Schobert B, Lanyi JK, Spudich EN, Spudich JL. Crystal structure of sensory Rhodopsin II at 2.4 angstroms: Insights into color tuning and transducer interaction. Science. 2001;293:1499-503.

Lukacova M, Gajdosova E, Skultety L, Kovacova E, Kazar J. Characterization and protective effect of a 29 kDa protein isolated from *Coxiella burnetii* by detergent Empigen BB. Eur J Epidemiol. 1994;10:227-30.

Luo J, Choulet J, Samuelson JC. Rational design of a fusion partner for membrane protein expression in *E. coli*. 2009;18:1735-44.

Ma C, Marassi FM, Jones DH, Straus SK, Bour S, Strebel K, et al. Expression, purification, and activities of full-length and truncated versions of the integral membrane protein Vpu from HIV-1. Protein Sci. 2002;11:546-57.

Madin K, Sawasaki T, Ogasawara T, Endo Y. A highly efficient and robust cell-free protein synthesis system prepared from wheat embryos: plants apparently contain a suicide system directed at ribosomes. Proc Natl Acad Sci U S A. 2000;97:559-64.

Magadán JG, Bonifacino JS. Transmembrane Domain Determinants of CD4 Downregulation by HIV-1 Vpu. Journal of Virology. 2012;86:757-72.

Magadan JG, Perez-Victoria FJ, Sougrat R, Ye Y, Strebel K, Bonifacino JS. Multilayered mechanism of CD4 downregulation by HIV-1 Vpu involving distinct ER retention and ERAD targeting steps. PLoS Pathog. 2010;6:e1000869.

Maina CV, Riggs PD, Grandea AG, 3rd, Slatko BE, Moran LS, Tagliamonte JA, et al. An *Escherichia coli* vector to express and purify foreign proteins by fusion to and separation from maltose-binding protein. Gene. 1988;74:365-73.

Maldarelli F, Chen MY, Willey RL, Strebel K. Human immunodeficiency virus type 1 Vpu protein is an oligomeric type I integral membrane protein. J Virol. 1993;67:5056-61.

Mangeat B, Gers-Huber G, Lehmann M, Zufferey M, Luban J, Piguet V. HIV-1 Vpu neutralizes the antiviral factor Tetherin/BST-2 by binding it and directing its β-TrCP2-dependent degradation. PLoS pathogens. 2009;5:e1000574.

Margottin F, Benichou S, Durand H, Richard V, Liu LX, Gomas E, et al. Interaction between the cytoplasmic domains of HIV-1 Vpu and CD4: role of Vpu residues involved in CD4 interaction and *in vitro* CD4 degradation. Virology. 1996;223:381-6.

Marin M. Folding at the rhythm of the rare codon beat. Biotechnol J. 2008;3:1047-57.

Masuyama N, Kuronita T, Tanaka R, Muto T, Hirota Y, Takigawa A, et al. HM1.24 is internalized from lipid rafts by clathrin-mediated endocytosis through interaction with alpha-adaptin. The Journal of Biological Chemistry. 2009;284:15927-41.

Matoba N, Griffin TA, Mittman M, Doran JD, Alfsen A, Montefiori DC, et al. Transcytosis-blocking abs elicited by an oligomeric immunogen based on the membrane proximal region of HIV-1 gp41 target non-neutralizing epitopes. Curr HIV Res. 2008;6:218-29.

Matoba N, Magerus A, Geyer BC, Zhang Y, Muralidharan M, Alfsen A, et al. A mucosally targeted subunit vaccine candidate eliciting HIV-1 transcytosis-blocking Abs. Proc Natl Acad Sci U S A. 2004;101:13584-9.

Matsumoto H, Isono K, Pye Q, Pak WL. Gene encoding cytoskeletal proteins in *Drosophila rhabdomeres*. Proc Natl Acad Sci U S A. 1987;84:985-9.

McCarthy KR, Johnson WE. Plastic proteins and monkey blocks: how lentiviruses evolved to replicate in the presence of primate restriction factors. PLoS Pathog. 2014;10:e1004017.

McCormick-Davis C, Dalton SB, Singh DK, Stephens EB. Comparison of Vpu sequences from diverse geographical isolates of HIV type 1 identifies the presence of highly variable domains, additional invariant amino acids, and a signature sequence motif common to subtype C isolates. AIDS Res Hum Retroviruses. 2000;16:1089-95.

McDonnell PA, Opella SJ. Effect of detergent concentration on multidimensional solution NMR spectra of membrane proteins in micelles. Journal of Magnetic Resonance, Series B. 1993;102:120-25.

McNatt MW, Zang T, Bieniasz PD. Vpu binds directly to tetherin and displaces it from nascent virions. PLoS Pathog. 2013a;9:e1003299.

McNatt MW, Zang T, Hatziioannou T, Bartlett M, Fofana IB, Johnson WE, et al. Species-specific activity of HIV-1 Vpu and positive selection of tetherin transmembrane domain variants. PLoS Pathog. 2009;5:e1000300.

Mitchell RS, Katsura C, Skasko MA, Fitzpatrick K, Lau D, Ruiz A, et al. Vpu antagonizes BST-2-mediated restriction of HIV-1 release via β-TrCP and endo-lysosomal trafficking. 2009.

Miyagi E, Andrew AJ, Kao S, Strebel K. Vpu enhances HIV-1 virus release in the absence of Bst-2 cell surface down-modulation and intracellular depletion. Proceedings of the National Academy of Sciences of the United States of America. 2009;106:2868-73.

Muller M, Koch HG, Beck K, Schafer U. Protein traffic in bacteria: Multiple routes from the ribosome to and across the membrane. Prog Nucleic Acid Res Mol Biol. 2001;66:107-57.

Nagamori S, Smirnova IN, Kaback HR. Role of YidC in folding of polytopic membrane proteins. J Cell Biol. 2004;165:53-62.

Nallamsetty S, Austin BP, Penrose KJ, Waugh DS. Gateway vectors for the production of combinatorially-tagged His6-MBP fusion proteins in the cytoplasm and periplasm of *Escherichia coli*. Protein Science. 2005;14:2964–71 Copyright © 005 The Protein Society.

Nallamsetty S, Waugh DS. A generic protocol for the expression and purification of recombinant proteins in *Escherichia coli* using a combinatorial His6-maltose binding protein fusion tag. Nat Protocols. 2007;2:383-91.

National Center for Biotechnology Information. PubChem Compound Database. CID=15433. 2016a.

National Center for Biotechnology Information. PubChem Compound Database. CID=24802064. 2016b.

National Center for Biotechnology Information. PubChem Compound Database. CID=24802120. 2016c.

Neil SJD. The antiviral activities of tetherin. Current Topics in Microbiology and Immunology. 2013;371:67-104.

Nguyen K-L, Llano M, Akari H, Miyagi E, Poeschla EM, Strebel K, et al. Codon optimization of the HIV-1 vpu and vif genes stabilizes their mRNA and allows for highly efficient Rev-independent expression. Virology. 2004;319:163-75.

Nollert P, Navarro J, Landau EM. Crystallization of membrane proteins in Cubo. Methods in Enzymology: Academic Press; 2002. p. 183-99.

Pacyniak E, Gomez ML, Gomez LM, Mulcahy ER, Jackson M, Hout DR, et al. Identification of a region within the cytoplasmic domain of the subtype B Vpu protein of human immunodeficiency virus type 1 (HIV-1) that is responsible for retention in the golgi complex and its absence in the Vpu protein from a subtype C HIV-1. AIDS research and human retroviruses. 2005;21:379-94.

Park JH, Choi EA, Cho EW, Hahm KS, Kim KL. Maltose binding protein (MBP) fusion proteins with low or no affinity to amylose resins can be single-step purified using a novel anti-MBP monoclonal antibody. Mol Cells. 1998;8:709-16.

Parks TD, Leuther KK, Howard ED, Johnston SA, Dougherty WG. Release of proteins and peptides from fusion proteins using a recombinant plant virus proteinase. Anal Biochem. 1994;216:413-7.

Patra AK, Mukhopadhyay R, Mukhija R, Krishnan A, Garg LC, Panda AK. Optimization of inclusion body solubilization and renaturation of recombinant human growth hormone from *Escherichia coli*. Protein Expr Purif. 2000;18:182-92.

Pebay-Peyroula E, Rummel G, Rosenbusch JP, Landau EM. X-ray structure of bacteriorhodopsin at 2.5 angstroms from microcrystals grown in lipidic cubic phases. Science. 1997;277:1676–81.

Peters D, Frank R, Hengstenberg W. Lactose-specific enzyme II of the phosphoenolpyruvate-dependent phosphotransferase system of *Staphylococcus aureus*. Purification of the histidine-tagged transmembrane component IICBLac and its hydrophilic IIB domain by metal-affinity chromatography, and functional characterization. Eur J Biochem. 1995;228:798-804.

Petrovskaya LE, Shulga AA, Bocharova OV, Ermolyuk YS, Kryukova EA, Chupin VV, et al. Expression of G-protein coupled receptors in *Escherichia coli* for structural studies. Biochemistry (Mosc). 2010;75:881-91.

Pickering S, Hue S, Kim EY, Reddy S, Wolinsky SM, Neil SJ. Preservation of tetherin and CD4 counter-activities in circulating Vpu alleles despite extensive sequence variation within HIV-1 infected individuals. PLoS Pathog. 2014;10:e1003895.

Power BE, Ivancic N, Harley VR, Webster RG, Kortt AA, Irving RA, et al. High-level temperature-induced synthesis of an antibody VH-domain in *Escherichia coli* using the PelB secretion signal. Gene. 1992;113:95-99.

Prive GG. Detergents for the stabilization and crystallization of membrane proteins. Methods. 2007;41:388-97.

Pryor KD, Leiting B. High-level expression of soluble protein in *Escherichia coli* using a His6-tag and maltose-binding-protein double-affinity fusion system. Protein Expr Purif. 1997;10:309-19.

Purvis IJ, Bettany AJ, Santiago TC, Coggins JR, Duncan K, Eason R, et al. The efficiency of folding of some proteins is increased by controlled rates of translation *in vivo*. A hypothesis. J Mol Biol. 1987;193:413-7.

Rhyum SB, Jin BR, Park HR, Hong HJ. High level expression of hepatitis B virus preS1 peptide in *Escherichia coli*. J Biotechnol. 1994;36:221-30.

Richard J, Cohen EA. HIV-1 Vpu disarms natural killer cells. Cell Host Microbe. 2010;8:389-91.

Riggs P. Expression and purification of maltose-binding protein fusions. Curr Protoc Mol Biol. 2001;Chapter 16:Unit16 6.

Robichon C, Luo J, Causey TB, Benner JS, Samuelson JC. Engineering *Escherichia coli* BL21(DE3) derivative strains to minimize *E. coli* protein contamination after purification by immobilized metal affinity chromatography. Appl Environ Microbiol. 2011;77:4634-46.

Robinson M, Lilley R, Little S, Emtage JS, Yarranton G, Stephens P, et al. Codon usage can affect efficiency of translation of genes in *Escherichia coli*. Nucleic Acids Res. 1984;12:6663-71.

Rollason R, Korolchuk V, Hamilton C, Schu P, Banting G. Clathrin-mediated endocytosis of a lipid-raft-associated protein is mediated through a dual tyrosine motif. Journal of Cell Science. 2007;120:3850-58.

Rong L, Zhang J, Lu J, Pan Q, Lorgeoux RP, Aloysius C, et al. The transmembrane domain of BST-2 determines its sensitivity to down-modulation by human immunodeficiency virus type 1 Vpu. J Virol. 2009;83:7536-46.

Roosild TP, Greenwald J, Vega M, Castronovo S, Riek R, Choe S. NMR structure of Mistic, a membrane-integrating protein for membrane protein expression. Science. 2005;307:1317-21.

Roosild TP, Vega M, Castronovo S, Choe S. Characterization of the family of Mistic homologues. BMC Struct Biol. 2006;6:10.

Rosenbusch JP. Stability of membrane proteins: relevance for the selection of appropriate methods for high-resolution structure determinations. J Struct Biol. 2001;136:144-57.

Rosenow MA, Williams JC, Allen JP. Amphiphiles modify the properties of detergent solutions used in crystallization of membrane proteins. Acta Crystallogr D Biol Crystallogr. 2001;57:925-7.

Roy N, Pacini G, Berlioz-Torrent C, Janvier K. Mechanisms underlying HIV-1 Vpu-mediated viral egress. Front Microbiol. 2014;5:177.

Royant A, Nollert P, Edman K, Neutze R, Landau EM, Pebay-Peyroula E, et al. X-ray structure of sensory rhodopsin II at 2.1-Å resolution. Proceedings of the National Academy of Sciences. 2001;98:10131-36.

Ruiz A, Hill MS, Schmitt K, Guatelli J, Stephens EB. Requirements of the membrane proximal tyrosine and dileucine-based sorting signals for efficient transport of the subtype C Vpu protein to the plasma membrane and in virus release. Virology. 2008;378:58-68.

Rummel G, Hardmeyer A, Widmer C, Chiu ML, Nollert P, Locher KP, et al. Lipidic cubic phases: new matrices for the three-dimensional crystallization of membrane proteins. Journal of structural biology. 1998;121:82–91.

Sambrook J, Russell DW. Molecular cloning: a laboratory manual 3rd edition. Coldspring-Harbour Laboratory Press, UK. 2001.

Sarramegna V, Talmont F, Demange P, Milon A. Heterologous expression of G-protein-coupled receptors: comparison of expression systems from the standpoint of large-scale production and purification. Cell Mol Life Sci. 2003;60:1529-46.

Sauter D, Schindler M, Specht A, Landford WN, Münch J, Kim K-A, et al. Tetherin-driven adaptation of Vpu and Nef function and the evolution of pandemic and nonpandemic HIV-1 strains. Cell Host & Microbe. 2009a;6:409-21.

Sawasaki T, Endo Y. *In vitro* protein synthesis system: cell-free protein synthesis system prepared from wheat germ. Tanpakushitsu Kakusan Koso. 2004;49:1514-9.

Schnell JR, Chou JJ. Structure and mechanism of the M2 proton channel of Influenza A virus. Nature. 2008;451:591-5.

Schubert U, Ferrer-Montiel AV, Oblatt-Montal M, Henklein P, Strebel K, Montal M. Identification of an ion channel activity of the Vpu transmembrane domain and its involvement in the regulation of virus release from HIV-1-infected cells. FEBS Letters. 1996;398:12-18.

Schubert U, Schneider T, Henklein P, Hoffmann K, Berthold E, Hauser H, et al. Human-immunodeficience-virus-type1-encoded Vpu protein is phosphorylated by casein kinase II. European Journal of Biochemistry. 1992a;204:875-83.

Schwartz S, Felber BK, Fenyö EM, Pavlakis GN. Env and Vpu proteins of human immunodeficiency virus type 1 are produced from multiple bicistronic mRNAs. Journal of Virology. 1990;64:5448-56.

Schwartz S, Felber BK, Pavlakis GN. Mechanism of translation of monocistronic and multicistronic human immunodeficiency virus type 1 mRNAs. Mol Cell Biol. 1992;12:207-19.

Shah AH, Sowrirajan B, Davis ZB, Ward JP, Campbell EM, Planelles V, et al. Degranulation of Natural Killer Cells following interaction with HIV-1-infected cells Is hindered by downmodulation of NTB-A by Vpu. Cell Host & Microbe. 2010;8:397-409.

Sharp PM, Li WH. The codon Adaptation Index--a measure of directional synonymous codon usage bias, and its potential applications. Nucleic Acids Research. 1987;15:1281.

Sharpe S, Yau WM, Tycko R. Structure and dynamics of the HIV-1 Vpu transmembrane domain revealed by solid-state NMR with magic-angle spinning. Biochemistry. 2006;45:918-33.

Shimamura T, Shiroishi M, Weyand S, Tsujimoto H, Winter G, Katritch V, et al. Structure of the human histamine H1 receptor complex with doxepin. Nature. 2011;475:65-70.

Sorensen MA, Kurland CG, Pedersen S. Codon usage determines translation rate in *Escherichia coli*. J Mol Biol. 1989;207:365-77.

Stafford RE, Fanni T, Dennis EA. Interfacial properties and critical micelle concentration of lysophospholipids. Biochemistry. 1989;28:5113-20.

Steiner D, Forrer P, Stumpp MT, Pluckthun A. Signal sequences directing cotranslational translocation expand the range of proteins amenable to phage display. Nat Biotechnol. 2006;24:823-31.

Strebel K. HIV-1 Vpu - an ion channel in search of a job. Biochim Biophys Acta. 2014;1838:1074-81.

Strebel K, Klimkait T, Martin MA. A novel gene of HIV-1, vpu, and its 16-kilodalton product. Science. 1988a;241:1221-23.

Strop P, Brunger AT. Refractive index-based determination of detergent concentration and its application to the study of membrane proteins. Protein Sci. 2005;14:2207-11.

Tate CG. Overexpression of mammalian integral membrane proteins for structural studies. FEBS Letters. 2001;504:94-98.

Taube R, Alhadeff R, Assa D, Krugliak M, Arkin IT. Bacteria-Based Analysis of HIV-1 Vpu Channel Activity. PLoS ONE. 2014;9:e105387.

Tervo H-M, Homann S, Ambiel I, Fritz JV, Fackler OT, Keppler OT. β-TrCP is dispensable for Vpu's ability to overcome the CD317/Tetherin-imposed restriction to HIV-1 release. Retrovirology. 2011;8:9.

Thie H, Schirrmann T, Paschke M, Dubel S, Hust M. SRP and Sec pathway leader peptides for antibody phage display and antibody fragment production in *E. coli*. N Biotechnol. 2008;25:49-54.

Tiefenbrunn T, Liu W, Chen Y, Katritch V, Stout CD, Fee JA, et al. High resolution structure of the ba3 cytochrome c oxidase from *Thermus thermophilus* in a lipidic environment. PLoS One. 2011;6:e22348.

Tiganos E, Friborg J, Allain B, Daniel NG, Yao X-J, Cohen ÉA. Structural and functional analysis of the membrane-spanning domain of the Human immunodeficiency virus type 1 Vpu protein. Virology. 1998;251:96-107.

Tiganos E, Yao XJ, Friborg J, Daniel N, Cohen EA. Putative alpha-helical structures in the human immunodeficiency virus type 1 Vpu protein and CD4 are involved in binding and degradation of the CD4 molecule. J Virol. 1997;71:4452-60.

Tokarev A, Guatelli J. Misdirection of membrane trafficking by HIV-1 Vpu and Nef: Keys to viral virulence and persistence. Cell Logist. 2011;1:90-102.

Urrutia AO, Hurst LD. The signature of selection mediated by expression on human genes. Genome Res. 2003;13:2260-4.

Valent QA, de Gier JW, von Heijne G, Kendall DA, ten Hagen-Jongman CM, Oudega B, et al. Nascent membrane and presecretory proteins synthesized in *Escherichia coli* associate with signal recognition particle and trigger factor. Mol Microbiol. 1997;25:53-64.

VanAken T, Foxall-VanAken S, Castleman S, Ferguson-Miller S. Alkyl glycoside detergents: synthesis and applications to the study of membrane proteins. Methods Enzymol. 1986;125:27-35.

Vancraenenbroeck R, Lobbestael E, Weeks SD, Strelkov SV, Baekelandt V, Taymans JM, et al. Expression, purification and preliminary biochemical and structural characterization of the leucine rich repeat namesake domain of leucine rich repeat kinase 2. Biochim Biophys Acta. 2012;1824:450-60.

Vigan R, Neil SJ. Separable determinants of subcellular localization and interaction account for the inability of group O HIV-1 Vpu to counteract tetherin. J Virol. 2011;85:9737-48.

Villa S, De Fazio G, Canosi U. Cyanogen bromide cleavage at methionine residues of polypeptides containing disulfide bonds. Anal Biochem. 1989;177:161-4.

Vranken WF, Boucher W, Stevens TJ, Fogh RH, Pajon A, Llinas M, et al. The CCPN data model for NMR spectroscopy: development of a software pipeline. Proteins. 2005;59:687-96.

Wadsten P, Wohri AB, Snijder A, Katona G, Gardiner AT, Cogdell RJ, et al. Lipidic sponge phase crystallization of membrane proteins. J Mol Biol. 2006;364:44-53.

Waeber U, Buhr A, Schunk T, Erni B. The glucose transporter of *Escherichia coli*. Purification and characterization by Ni^{2+} chelate affinity chromatography of the IIBCGlc subunit. FEBS Lett. 1993;324:109-12.

Wahl JK, 3rd. Generation of monoclonal antibodies specific for desmoglein family members. Hybrid Hybridomics. 2002;21:37-44.

Wallin E, von Heijne G. Genome-wide analysis of integral membrane proteins from eubacterial, archaean, and eukaryotic organisms. Protein Sci. 1998;7:1029-38.

Walsh NP, Alba BM, Bose B, Gross CA, Sauer RT. OMP peptide signals initiate the envelope-stress response by activating DegS protease via relief of inhibition mediated by its PDZ domain. Cell. 2003;113:61-71.

Wampler RD, Kissick DJ, Dehen CJ, Gualtieri EJ, Grey JL, Wang H-F, et al. Selective detection of protein crystals by Second Harmonic Microscopy. Journal of the American Chemical Society. 2008;130:14076-77.

Wang J, Pielak RM, McClintock MA, Chou JJ. Solution structure and functional analysis of the Influenza B proton channel. Nat Struct Mol Biol. 2009;16:1267-71.

Ward J, Cardoso de Almeida ML, Turner MJ, Etges R, Bordier C. An assay of membrane-bound *Trypanosoma brucei* phospholipase using an integral membrane protein substrate and detergent phase separation. Mol Biochem Parasitol. 1987;23:1-7.

Waugh DS. Making the most of affinity tags. Trends Biotechnol. 2005;23:316-20.

Waugh DS. Crystal structures of MBP fusion proteins. Protein Sci. 2016;25:559-71.

Weierstall U, James D, Wang C, White TA, Wang D, Liu W, et al. Lipidic cubic phase injector facilitates membrane protein serial femtosecond crystallography. Nat Commun. 2014;5:3309.

Willey RL, Maldarelli F, Martin MA, Strebel K. Human immunodeficiency virus type 1 Vpu protein induces rapid degradation of CD4. Journal of Virology. 1992a;66:7193-200.

Willey RL, Maldarelli F, Martin MA, Strebel K. Human immunodeficiency virus type 1 Vpu protein regulates the formation of intracellular GP160-CD4 complexes. Journal of Virology. 1992b;66:226-34.

Wittlich M, Koenig BW, Stoldt M, Schmidt H, Willbold D. NMR structural characterization of HIV-1 virus protein U cytoplasmic domain in the presence of dodecylphosphatidylcholine micelles. The FEBS Journal. 2009a;276:6560-75.

Wu B, Chien EY, Mol CD, Fenalti G, Liu W, Katritch V, et al. Structures of the CXCR4 chemokine GPCR with small-molecule and cyclic peptide antagonists. Science. 2010;330:1066-71.

Xu F, Liu W, Hanson MA, Stevens RC, Cherezov V. Development of an automated high throughput LCP-FRAP assay to guide membrane protein crystallization in lipid mesophases. Cryst Growth Des. 2011;11:1193-201.

Xu Y, Kong J, Kong W. Improved membrane protein expression in *Lactococcus lactis* by fusion to Mistic. 66621-0. Microbiology. 2013.

Yang SJ, Lopez LA, Hauser H, Exline CM, Haworth KG, Cannon PM. Anti-tetherin activities in Vpu-expressing primate lentiviruses. Retrovirology. 2010;7:13.

Zhang H, Lin EC, Das BB, Tian Y, Opella SJ. Structural determination of Virus protein U from HIV-1 by NMR in membrane environments. Biochim Biophys Acta. 2015;1848:3007-18.

Zhang Q, Mi Z, Huang Y, Ma L, Ding J, Wang J, et al. 2-thio-6-azauridine inhibits Vpu mediated BST-2 degradation. Retrovirology. 2016;13:13.

BIOGRAPHICAL SKETCH

Arpan Deb was born in Kamakhyanagar, India on December 26, 1984. He completed his secondary education at New Stewart School, Cuttack, India where he was initiated in to the world of science and also won awards for excellence in physics. Interest in science further solidified during high-school at Ravenshaw Junior College, Cuttack. He pursued Bachelor of Technology in Biotechnology at Haldia Institute of Technology, Haldia, India where he was exposed to different tracks of research in Life Sciences. During this time, he also worked in the lab of Dr. Mukesh Singh and Dr. Keya Sau at the Department of Biotechnology on projects in Molecular and Computational biology respectively and developed an appetitte for scientific research in these fields. He began his graduate study in Molecular and Cell biology at Arizona State University in the year 2009. He intiallly worked on the evolution of malarial parasites in the lab of Dr Ananias Escallante and then moved on to the lab of Prof. Tsafrir S. Mor in 2011 to pursue his Ph.D. thesis research on structural characterization of HIV-1 membrane protein, Vpu. He was supported by the School of Life Sciences, ASU and the Center of Membrane Proteins in Infectious Diseases during his doctoral studies at ASU. After earning his Ph.D., Arpan plans to pursue post-doctoral research in Molecular biophysics at the University of Montana. Following post-doc, he hopes to pursue a career in scientific research in the area of Molecular biophysics of biomolecules involved in infectious diseases.